Universidade Estadual Paulista “Júlio de Mesquita Filho”
Faculdade de Medicina Veterinária e Zootecnia

RADIOGRAPHIC INDIRECT LYMPHOGRAPHY USING LIPOSOLUBLE CONTRAST FOR SENTINEL LYMPH NODE MAPPING OF DOGS WITH CUTANEOUS MAST CELL TUMOR

VINICIUS GONZALEZ PERES ALBERNAZ

Botucatu, SP
JULY – 2022

Universidade Estadual Paulista “Júlio de Mesquita Filho”
Faculdade de Medicina Veterinária e Zootecnia

RADIOGRAPHIC INDIRECT LYMPHOGRAPHY USING LIPOSOLUBLE CONTRAST FOR SENTINEL LYMPH NODE MAPPING OF DOGS WITH CUTANEOUS MAST CELL TUMOR

Tese apresentada junto ao Programa de Pós-graduação em Biotecnologia Animal para obtenção do título de Doutor

Vinicius Gonzalez Peres Albernaz
Orientadora: Profª. Dra. Juliany Gomes Quitzan

Botucatu, SP
July – 2022

FICHA CATALOGRÁFICA ELABORADA PELA SEÇÃO TÉC. AQUIS. TRATAMENTO DA INFORM.
DIVISÃO TÉCNICA DE BIBLIOTECA E DOCUMENTAÇÃO - CÂMPUS DE BOTUCATU - UNESP
BIBLIOTECÁRIA RESPONSÁVEL: ROSEMEIRE APARECIDA VICENTE-CRB 8/5651

Albernaz, Vinicius Gonzalez Peres.
Radiographic indirect lymphography using liposoluble contrast for sentinel lymph node mapping of dogs with cutaneous mast cell tumor / Vinicius Gonzalez Peres Albernaz. - Botucatu, 2022

Tese (doutorado) - Universidade Estadual Paulista "Júlio de Mesquita Filho", Faculdade de Medicina Veterinária e Zootecnia
Orientador: Juliany Gomes Quitzan
Capes: 50501070

1. Neoplasias cutâneas. 2. Mastocitoma. 3. Sistema linfático. 4. Metastasis. 5. Óleo iodado.

Palavras-chave: Iodized oil; Lymphatic; Mastocytoma; Metastasis; Radiographic.

Author's Name: Vinicius Gonzalez Peres Albernaz

Title: Radiographic indirect lymphography using liposoluble contrast for sentinel lymph node mapping of dogs with cutaneous mast cell tumor

EXAMINATION BOARD

Profa. Dra. Juliany Gomes Quitzan
Presidente e Orientadora
Departamento de Cirurgia Veterinária e Reprodução Animal, FMVZ - UNESP - Botucatu/SP

Profa. Dra. Sabrina Marin Rodigheri
Membro Titular
Universidade Positivo – Curitiba/PR

Prof. Dr. Victor José Vieira Rossetto
Membro Titular
Pontifícia Universidade Católica de Minas Gerais – Poços de Caldas/MG

Prof. Dr. Carlos Eduardo Fonseca Alves
Membro Titular
Departamento de Cirurgia Veterinária e Reprodução Animal, FMVZ/UNESP – Botucatu/SP

Profa. Dra. Thais Andrade Costa Casagrande
Membro Titular
Universidade Positivo – Curitiba/PR

Date of Thesis Defense: July 4th, 2022.

ACKNOWLEDGMENT

Agradeço a Universidade Estadual Paulista “Júlio de Mesquita Filho” – Campus Botucatu e a FMVZ pelo suporte fornecido durante o Doutorado no Programa de Biotecnologia Animal.

Agradeço a Universidade Federal do Paraná e ao Hospital Veterinário da UFPR por ceder o espaço, pessoal e material para o desenvolvimento de grande parte dessa pesquisa.

Meu mais sincero obrigado aos grandes amigos e autores dessa pesquisa: Natalia Kano, Giovanna Bonatto e William Prieto pela imensurável ajuda no desenvolvimento da pesquisa. Sem vocês esse trabalho jamais teria sido possível. Um agradecimento especial ao Professor Renato Silva de Sousa pelo apoio nas avaliações histológicas e na condução da pesquisa dentro do hospital veterinário.

A Professora Juliany Quitzan, orientadora e amiga de longa data, por toda ajuda, discussões, orientações e por fazer crescer a semente da pesquisa e da docência dentro de mim ao longo de todos esses anos.

A família, Pai Jorge, Mãe Sonia, Irmão Daniel, Bianca e Gisele, que em todos os momentos estiveram ao meu lado, dando suporte incondicional e amor.

Aos amigos caninos Mulder (in memorian), Menina (in memorian), Puck (in memorian), Megan (in memorian), Poncho, Tibério, Bionça, Pilantroso e Björn por serem os pilares que fazem tudo valer a pena. Os companheiros caninos que representam os verdadeiramente beneficiados por essa pesquisa.

Á todos os proprietários de cães participantes deste estudo por valorizarem a pesquisa nacional e se prontificarem a doar um pouco do seu tempo para contribuir com a evolução da oncologia veterinária. Nossos futuros pacientes caninos agradecem imensamente.

e finalmente, aos cães pacientes do HV-UFPR e HV-UNESP que participaram do estudo, não há palavras humanas que possam agradecer a contribuição que fizeram a pesquisa e ao desenvolvimento da oncologia veterinária.

O presente trabalho foi realizado com apoio da Coordenação de Aperfeiçoamento de Pessoal de Nível Superior - Brasil (CAPES) - Código de Financiamento 001

“Passion is what gets you through the hardest times
that might otherwise make strong men weak, or
make you give up”
Neil deGrasse Tyson

RESUMO

ALBERNAZ, V.G.P. **Linfografia indireta utilizando contraste liposoluble para mapeamento de linfonodos sentinelas em cães com mastocitoma cutâneo** Botucatu – SP. 2022. 189p. Doutorado – Faculdade de Medicina Veterinária e Zootecnia, Campus Botucatu, Universidade Estadual Paulista.

O mastocitoma cutâneo (MCTc) é uma das neoplasias cutâneas mais comuns em cães. Metástase para o linfonodo (LN) drenante é a principal rota de disseminação sistêmica do MCTc. A detecção precoce de metástases em LNs é crucial no estadiamento e tratamento correto de cães com MCTc. O LN sentinela é amplamente variado entre indivíduos. O objetivo desta tese é realizar uma revisão descritiva do sistema linfático canino aplicado ao mapeamento de LNs sentinelas de cães com MCTc. Simultaneamente, foi conduzido um estudo clínico de cães com ocorrência natural de MCTc para avaliar se o papel da linfografia indireta (LI) com óleo iodado (OI) combinado com o método colorimétrico com azul patente (AP) na detecção do LN sentinela. A principal hipótese era que a LI ajudaria o cirurgião a detectar LNs intracavitários e mais LNs que a técnica do AP. Vinte e três cães fizeram parte do estudo prospectivo. LI OI detectou 29 LNs sentinelas em 19 cães, enquanto 4 não exibiram opacificação em LNs. O AP detectou 26 LNs em 19 cães, com 4 cães não demonstrando coloração azulada em LNs. Trinta e um LNs foram resseccionados, sendo que 10 estavam metastáticos. Laparotomia foi necessária para remover LNs ilíacos opacificados em 26% dos cães. A taxa de concordância entre a LI OI e LN regionais e AP e LNs regionais foi de 82,6%. A taxa foi de 78.2% quando comparando a LI com o AP. Somente um cão apresentou o LN sentinela drenante diferente do LN regional detectado pela LI. Em um contexto clínico, a LI com OI foi responsável por aumentar o número de LNs ressecionado em 41% (29% dos LNs removidos). Não houve diferença estatística quando comparando AP e a LI no cenário base do estudo ($p=0.01855$), contudo em um cenário clínico houve diferença significativa favorecendo a LI ($p=0.0081$). A opacificação desigual dos LNs sentinelas não teve associação significativa com a presença de metástase ($p=0.2264$). O mesmo ocorreu com a coloração azul clara do LN ($p=0.6673$). Contudo, o tamanho dos LNs metastáticos foi significativamente maior que os normais ($p=0.0456$). LNs aumentados de tamanho apresente 4.6 mais riscos de estarem metastáticos que os LNs não-palpáveis ou normais ($p=0.0374$). Locais de alto risco, limites de 3cm no tamanho, invasão profunda e sinal de Darier não estavam associados com metástase locorregional ($p>0.05$). Os resultados provenientes do mapeamento de LNs sentinelas foram responsáveis por 62,5% das indicações para quimioterapia adjuvante pós-operatória, mas somente um caso teve indicação alterada somente pela LI. Contudo, 60% dos cães com doença metastática apresentaram um LN sentinela metastático intracavitário que só pode ser detectado no pré-operatório pela LI. A LI com OI pré-operatória associada com o AP é um método eficiente de detectar LNs sentinelas em MCTc realizando cirurgia curativa. LI aumenta a taxa de detecção de LNs sentinelas em um contexto clínico. O padrão de opacificação do LN sentinela não deve ser utilizado para predizer metástases.

Palavras-chave: Linfático; Metástases; Mastocitoma; Óleo Iodado, Radiografia;

ABSTRACT

ALBERNAZ, V.G.P. **Indirect lymphography using lipossoluble contrast for sentinel lymph node mapping in dogs with cutaneous mast cell tumor**. Botucatu – SP. 2022. 189p. Doctorate Degree– Faculdade de Medicina Veterinária e Zootecnia, Campus Botucatu, Universidade Estadual Paulista.

Cutaneous mast cell tumor (cMCT) is one of the most common skin cancers in dogs. Metastasis to draining lymph nodes is the main route to systemic dissemination of cMCT. Early detection of lymph node metastasis is crucial to correctly stage and treat dogs with cMCT. The sentinel lymph node (SLN) is widely variable among individuals. The objective of this thesis was to make a descriptive review of the canine lymphatic system applied to SLN mapping of dogs bearing cMCT. Simultaneously a clinical study of dogs with naturally occurring cMCT was conducted to evaluate the role of iodized oil (IO) indirect lymphography (IL) combined with patent blue colorimetric method in detecting SLN. The main hypothesis was that IL would aid the surgeon to detect intracavitary or more lymph nodes than the patent blue technique. Twenty-three dogs were enrolled in the prospective study. IO IL detected 29 contrasted SLN in 19 dogs, while 4 dogs did not exhibit lymph node opacification. Patent blue detected 26 SLN in 19 dogs and 4 dogs did not have blue-colored nodes. Thirty-one lymph nodes were resected, of which 10 were metastatic. Laparotomy was necessary to remove opacified iliac lymph nodes in 26% of the dogs. The rate of agreement between IO IL and patent blue with regional lymph nodes was 82.6%. The rate was 78.2% when comparing IL and patent blue. Only one dog had a draining SLN different from the regional lymph node as detected by IL. In a clinical setting, IO IL was responsible to increase the number of resected lymph nodes by 41% (29% of the resected SLN). There was no difference in detected SLN by PB and IO IL in the base scenario (p=0.1855), however, in a clinical scenario, there was a significant difference favoring IL (p=0.0081). Unequally opacified SLN could not be significatively associated with metastasis (p=.2264). The same occurred with light-blue color SLN (p=.6673). However, tumor size was significatively higher in dogs with lymph node metastasis (p=.0456). Enlarged lymph nodes had 4.6-fold more risk of being metastatic than non-palpable/normal-sized nodes (p=.0374). High-risk sites, 3cm size cut-off, deep invasion, and Darier's sign could not be associated with locoregional metastasis (p>.05). The SLN mapping was responsible for 62.5% of the postoperative indications of adjuvant chemotherapy, however, only one case was indicated solely by the IL. However, 60% of dogs with metastatic disease had an intracavitary metastatic SLN that could only be detected preoperatively by IL. Preoperative IO IL associated with patent blue is an efficient method to detect SLN in cMCT undergoing curative surgery. IL increases the rate of SLN detected in a clinical setting. The pattern of SLN opacification should not be used to predict metastasis.

Keywords: Lymphatic; Metastasis; Mastocytoma; Iodized Oil, Radiographic

LIST OF FIGURES

LIST OF TABLES

LIST OF ABBREVIATIONS

PB: Patent Blue

IO: Iodized Oil

IL: Indirect Lymphography

cMCT: Cutaneous Mast Cell Tumor

MCT: Mast Cell Tumor

CT: Computer Tomography

SLN: Sentinel Lymph Node

RLN: Regional Lymph Node

LN: Lymph Node

SUMÁRIO

CHAPTER 1

1. INTRODUCTION

The lymphatic draining system is the main pathway for metastasis of canine cutaneous mast cell tumor (cMCT), which makes the histological evaluation of the lymph nodes (LN) one of the central aspects of MCT staging as a predictive of distant metastatic potential (Warland et al., 2014; Lejeune et al., 2015). The LN evaluation is a prognosis factor for survival time and can also be a determinant to decide whether to pursue adjuvant chemotherapy after surgical resection of the primary cMCT (Worley et al., 2014; Lejeune et al., 2015).

Metastatic disease of the LNs is often suspected on clinical examination and confirmed on fine needle aspirate biopsy (FNA) or histology after LN sampling or resection (Lejeune et al., 2013). However, both palpation and FNA have low sensitivity and specificity for MCT metastasis (Lejeune et al., 2015; Grimes et al., 2017; Fournier et al., 2018), and histology remains the gold-standard method for diagnosis of nodal metastasis (Liptak et al., 2019). Furthermore, detection of which LN must be sampled or removed, especially when these are normal-sized or could not be palpated, can be challenging as the anatomical location does not precisely reflect the LN that drains the tumor site (Mayer et al., 2013; Worley et al., 2014).

The non-selective dissection of LNs of women with breast cancer was associated with increased postoperative morbidity and complication without a real benefit on survival time (Ball et al., 2010; Abass et al., 2018). In these human patients, a sentinel lymph node (SLN) mapping approach is preferred as it allows the detection of the most probable LN to bear a metastasis while sparing the remaining nodes (Ball et al., 2010; Beek et al., 2015; Abass et al., 2018). Although extensive lymphatic dissection in dogs and cats may result in a lower complication rate compared to humans, there is a potential risk of not removing an affected LN thus missing a metastatic focus (Qiu et al., 2018; Liptak et al., 2019). In this context, techniques to detect SLNs have been considered an alternative to the non-selective dissection of LNs in both humans and animals (Liptak et al., 2019).

The SLN is the first draining LN of a lymphatic chain to drain the tumor site, and, therefore, is a representative sample of the remaining lymphatic chain.

The challenge for SLN detection is that lymphatic draining is anatomically unpredictable and variable, especially when a neoplasm is present, whose process of tumoral lymphangiogenesis can open inactivated lymphatic vessels, altering the normal lymphatic pattern (Werner 1995; Pereira et al., 2003; Liptak et al., 2019).

Among the techniques for the detection of SLN, the intraoperative peritumoral injection of methylene blue or patent blue is the most straightforward. However, the techniques depend on the active search of the LNs by the surgeon as there is no prior information on which LN is the sentinel and must be removed. Furthermore, deep LNs located inside the abdominal cavity cannot be accessed during superficial skin surgery, even when colored, requiring a laparotomy for visual confirmation. To overcome this limitation, other techniques were developed, such as contrast-enhanced ultrasound, lymphoscintigraphy, computed tomography lymphangiography, and indirect lymphography with hydrosoluble or liposoluble contrast (Masannat et al., 2006; Somasundaran et al., 2007; Giuliano et al., 2010; Gelb et al., 2010; Layfield et al., 2011; Morton, 2012; Zengel et al., 2013; Lyman et al., 2017; Van der Noordaa et al., 2017; Qiu et al., 2018). The techniques of indirect lymphography acts in complement to the intraoperative mapping as contrasted LNs retain their normal appearance which is often hard to locate when dissecting the subcutaneous fat (Liptak et al., 2019; Brissot et al., 2016).

This thesis aims to provide a throughout review of the current literature about mast cell tumor focusing on the lymphatic metastatic process and the sentinel lymph node mapping techniques. Finally, a scientific manuscript evaluating the indirect lymphography with liposoluble contrast for radiographic sentinel lymph node mapping of dogs bearing cutaneous mast cell tumor is presented.

2. DESCRIPTIVE REVIEW

2.1. Canine Cutaneous Mast Cell Tumor

Mast cells originate in the bone marrow but rapidly migrate to the peripheral tissues where it differentiates into mature mast cells. In healthy dogs, mast cells are present in most tissues, but mainly in those with environment contact, such as skin and mucosal surface. Mast cells can occasionally be found in the bone marrow but rarely in the systemic circulation (Scott et al., 2000). Among the main characteristics of the mast cells are the considerable number of cytoplasmatic granules containing histamine and heparin, both related to inflammatory and hypersensitivity reactions, such as allergy. (Scott et al., 2000; Castells, 2006).

cMCT is the neoplastic proliferation of mast cells located in the dermis or subcutaneous tissues (Blackwood et al., 2012). Two histological forms of skin MCT are usually described: The cutaneous or dermal and the subcutaneous MCT (Willmann et al., 2021). While the first are usually nodular or ulcerative lesions, the last has a clinical presentation like lipoma (Blackwood et al., 2012; Willmann et al., 2021). The cMCT is the most common skin tumor, with an overall prevalence of 0.27% and up to 21% of all canine skin cancer (Sledge et al., 2003; Govier et al., 2003; Thamm et al., 2007; Shoop et al., 2015).

Despite being most seen on the skin, MCT can also occur in hematopoietic organs, such as LNs, spleen, liver, bone marrow (i.e., extracutaneous/extramucosal MCT), and oral or gastrointestinal mucosa (mucosal MCT) (Willmann et al., 2021). In rare cases, MCT can progress to mast cell leukemia (O'Keefe et al., 1987; Moirano et al., 2018; Willmann et al., 2021).

2.1.1 Clinical Presentation

The classic and most frequently seen clinical presentation of cMCT are of a solitary nodule (London et al., 2003; Misdorp et al., 2004; Sledge et al., 2016; Kiupel et al., 2019). However, about 10-21% of the dogs develop multiple primary cMCT rather than solitary lesions (Seguin et al., 2001; Murphy et al., 2006; Thamm et al., 2007). Solitary cMCT with satellite lesions around the primary

tumor can also be found (Blackwood et al., 2012).

The gross appearance of cMCT can be correlated with histological grade and aggressiveness. While rapid growing, ulcerated, pruritic lesions with small satellite lesions are usually poorly differentiated while slow-growing hairless solitary cMCTs are frequently well-differentiated (Blackwood et al., 2012). However, a non-aggressive gross appearance should not be used alone to assume the tumor has a benign biological behavior (Blackwood et al., 2012).

Signs of aggressive clinical behavior include: (1) the rapid growth of the tumor; (2) local inflammation and hyperemia; (3) poorly delimitated borders and local infiltration; (4) ulceration; (5) satellite lesions; (6) signs of paraneoplastic syndrome; (7) and tumor spreading to LNs or visceral organs (London et al., 2003; Misdorp et al., 2004; Mullins et al., 2006; Weiss et al., 2006; Thamm et al., 2007; Sledge et al., 2016; Kiupel et al., 2019).

The anatomical location of the cMCT is also associated with variable clinical behavior and is considered an important clinical prognostic factor. Head and neck, inguinal, scrotum, digit, and axillar cMCT are usually more aggressive than those located at other sites (Misdorp et al., 2004; Blackwood et al., 2012; Smiech et al., 2018). MCT located in the inguinal or mucocutaneous regions has been associated with a worse prognosis (Cahalane et al., 2004; Sfiligoi et al., 2005). Similarly, visceral forms of MCT also have a poor prognosis (Iwata et al., 2000; Takahashi et al., 2000; Ozaki et al., 2002; Marconato et al., 2008).

2.1.2 Paraneoplastic Syndrome

The release of bioactive substances, such as histamine, heparin, and proteases, from the mast cell's granules, is the main cause of paraneoplastic syndromes seen on cMCT (O'keef, 1990; London et al., 2003; Mullins et al., 2006; Thamm et al., 2007). These substances cause pruritus, edema, bruising, ulceration, and swelling of the tumor site (London et al., 2003; Misdorp et al., 2004; Sledge et al., 2016; Kiupel et al., 2019). Mast cell degranulation during manipulation of a cMCT can cause the so-called Darier's sign, characterized by local edema, erythema, and itching of the lesion (London et al., 2003; Misdorp et al., 2004; Blackwood et al., 2012; Sledge et al., 2016; Kiupel et al., 2019). Frequent cycles of increase and decrease in tumor size can also occur (Blackwood et al., 2012). Dogs with cMCT may experience delayed wound

healing and abnormalities in coagulation when submitted to surgical resection (Blackwood et al., 2012). However, a recent controlled study found no increased risk for incisional complications after cMCT resection in comparison to soft tissue sarcomas (Iodence et al., 2021).

Systemically, gastrointestinal signs associated with gastric ulceration are often found due to histamine stimulation of H2 receptor (Fox et al., 1990; London et al., 2003; Misdorp et al., 2004; Sledge et al., 2016; Kiupel et al., 2019). Vomiting, gastrointestinal hemorrhage, anorexia, and abdominal pain are frequent findings. Iron deficiency anemia and peritonitis can also occur. Dogs with extensive disease are at an increased risk for a massive release of histamine from cMCT cells causing acute collapse and anaphylactic reaction (Blackwood et al., 2012).

The use of gastroprotectants such as omeprazole (1mg/kg once daily), ranitidine (2mg/kg twice daily), or famotidine (1mg/kg once daily) is usually prescribed to control the gastrointestinal signs from MCT histamine release (Stirborova et al., 2019). Diphenhydramine (2-4 mg/kg two to three times daily) or other H1-blocker are useful in preventing local and systemic allergic-like reactions caused by mast cell degranulation (Blackwood et al., 2012; Garret et al., 2014)

2.1.3 Diagnosis and Staging

Despite the suggestive clinical signs of cMCT, they may not be detected and, otherwise, cMCT is grossly like any other skin lesion (Blackwood et al., 2012; Willmann et al., 2021). For this reason, fine needle aspirate biopsy is indicated as a triage for cMCT suspected lesions. Cytology can diagnose MCT in about 92-96% of the cases (Baker-Gabb et al., 2003). Mast cells easily exfoliate from the tumor and can be readily identified on routine staining due to their intracytoplasmic granules (Blackwood et al., 2012). Poorly differentiated MCT can lack granules which can difficult making a diagnosis by routine cytology. However, cytology grading systems for cMCT usually over- or underdiagnose high-grade MCT (Camus et al., 2016; Scarpa et al., 2016). Thus, an adequate determination of biological behavior requires additional data from histological examination and the grade associated with the clinical staging (London et al., 2003; Misdorp et al., 2004; Sledge et al., 2016; Kiupel et al., 2019). Histology is

also required to differentiate cutaneous and subcutaneous MCT (London et al., 2003; Misdorp et al., 2004; Sledge et al., 2016; Kiupel et al., 2019).

Histology from an incisional or excisional biopsy is the mainstay method for diagnosis and grading of cMCT (Patnaik et al., 1984; Northrup et al., 2005; Northrup et al., 2005b; Kiupel et al., 2011; Blackwood et al., 2012; Stefanello et al., 2015). Preoperative incisional biopsy is useful for planning a definitive surgical approach, however, carries an increased risk of wound dehiscence and mast cell degranulation (Blackwood et al., 2012). On the other hand, excisional biopsies are only indicated if there is preoperative cytology confirming MCT and the tumor is amenable for wide surgical resection (Blackwood et al., 2012). The excision of a cMCT without wide margins may jeopardize further treatments and decrease the chances of cure (Blackwood et al., 2012).

Prednisone is commonly used before surgery to provide cytoreduction and decrease tumor volume, however, there is a concern that it may affect the histological features of a preoperative incisional biopsy. According to a recent blinded randomized placebo-controlled trial with 28 dogs, no significant difference was found in naïve histological samples and prednisone-treated samples regarding mitotic count, atypia, and tumor grade (Linde et al., 2021).

cMCT staging determines the extent of cancer spread and is critical to predict prognosis and guide the decision-making of both medical and surgical treatment. The World Health Organization (WHO) clinical staging system for cMCT (Table 1) in dogs (Owen et al., 1980) has been used so far, but it does not correlate well with prognosis, reason why it is not routinely used (London et al., 2003; Murphy et al., 2006; Dobson et al., 2007; Horta et al., 2018). MCT often metastasizes to locoregional LNs, liver, spleen, bone marrow, or even skin, but rarely to the lungs (Blackwood et al., 2012). Minimal cMCT staging should include LN examination and abdominal ultrasound (Blackwood et al., 2012). Full staging is recommended when extensive treatment is planned, when dealing with poorly differentiated cMCT, and in cases of nodal metastasis (Blackwood et al., 2012). Full staging should include a complete clinical examination, complete blood count, serum biochemistry, regional lymph node (RLN) examination, lung radiography, and abdominal ultrasound with or without spleen/liver aspiration (Patnaik et al., 1984; Finora et al., 2006; Book et al., 2011; Kiupel et al., 2011; Stephanello et al., 2015). Bone marrow aspiration is not usually beneficial as

most cMCT does not have bone marrow infiltration, however, if major blood abnormalities or visceral lesions occur, cytology and histology may be recommended (Valent et al., 2001; Thamm et al., 2007; Marconato et al., 2008; Cartagena-Albertus et al., 2019).

It is important to note that all current staging systems are suitable for cMCT only and are not established for other sites MCT (Allan et al., 1974; Owen et al., 1980; Patnaik et al., 1984; Hikasa et al., 2000; Iwata et al., 2000; Takahashi et al., 2000; Newman et al., 2007; Krick et al., 2009; Matsuda et al., 2009; Kiupel et al., 2011; Thompson et al., 2011; Thompson et al., 2011b; Willard et al., 2012; Shekell et al., 2018; Cartagena-Albertus et al., 2019).

Table 1. World Health Organization system for clinical staging of cutaneous mast cell tumor in dogs (Owen et al., 1980).

Stage	Description
0	One tumor incompletely excised from the dermis, identified histologically, without regional lymph node involvement. a. Without systemic signs b. With systemic signs
I	One tumor confined to the dermis without regional lymph node involvement a. Without systemic signs b. With systemic signs
II	One tumor confined to the dermis with regional lymph node involvement a. Without systemic signs b. With systemic signs
III	Multiple dermal tumors; large infiltrating tumors with or without lymph node involvement a. Without systemic signs b. With systemic signs
IV	Any tumor with distant metastasis, including involvement of blood and bone marrow

Skin MCT usually spread progressively, initially to the RLNs (stage 2) and then to the spleen and liver (stage 3) and, less commonly to other organs, such as kidney, heart, and bone marrow (stage 4) (Marconato et al., 2008; Valent et al., 2017; Cartagena-Albertus et al., 2019). Metastases in the lungs are exceedingly rare (Marconato et al., 2008; Valent et al., 2017; Cartagena-Albertus et al., 2019). Subcutaneous MCTs are rarely metastatic with a reported rate of only 4% (Thompson et al., 2011).

A recent consensus statement concluded that full staging of low-grade cMCT is not indicated after surgical resection due to the benign biological behavior (Willmann et al., 2021). However, organomegaly and signs of metastatic disease are indications that full staging should be performed. On the other hand, SLNs examined is recommended regardless of the grade (Willmann et al., 2021).

2.1.4 Lymph Node Metastasis

LN metastasis is a well-established predictor of negative prognosis in canine cMCT (Cahalane et al., 2004; Murphy et al., 2006; Thamm et al., 2006; Hayes et al., 2007; Krick et al., 2009; Hillman et al., 2010; Hume et al., 2011; Blackwood et al., 2012; Warland et al., 2014). The diagnosis of locoregional metastasis puts the dog at a higher risk for distant metastasis and often requires adjuvant chemotherapy despite the histological grade or other prognostic factors (Warland et al., 2014). A study found that dogs bearing LN metastasis had a median survival time of 0.8 years against 6.2 years for those without locoregional metastasis (Krick et al., 2009). For this reason, early detection of node metastasis at the time of diagnosis is crucial to establishing the correct treatment and prognostication (Ferrari et al., 2018; Lapsley et al., 2020). Recently, a study evaluating lymphadenectomy in low-grade canine cMCTs found that not performing immediate prophylactic lymphadenectomy was associated with a higher risk for disease progression but did not improved survival time (Sabattini, 2021). In a retrospective study evaluating dogs with cMCT and non-palpable or normal-sized LNs, the authors found 65% of pre-metastatic or metastatic locoregional disease (Ferrari et al., 2018). A case series found 12 out of 19 dogs with metastatic SLN using a combination of preoperative and intraoperative lymphoscintigraphy with methylene blue dyeing (Worley et al., 2014).

About 24% of normal dogs exhibit a low number of normal mast cells on LN cytology which may cause false-positive results (Bookbinder et al., 1992). Cytology often cannot tell morphological normal or reactive mast cells from neoplastic ones, which can impair its use in detecting cMCT LN metastasis (Blackwood et al., 2012). In general, cytologic examination of the LN has a limited value for cMCT (McManus et al., 1992).

Based on LN and extracutaneous organs status, cMCT can be classified as either localized, regional metastatic, and/or distant metastatic (Willmann et al.,

2021). A localized cMCT is that confined to the dermis and subcutis without LN or extracutaneous involvement and no signs of mast cell leukemia; regional metastatic cMCTs are those with regional or SLN metastasis, while distant metastatic cMCT has extracutaneous involvement (Willmann et al., 2021).

2.1.5 Surgical Treatment

Treating cMCT depends on several clinical characteristics, disease stage, and histological grade. Surgical resection of primary cMCT is the standard of care treatment in dogs (Weisse et al., 2002; Govier et al., 2003). Localized and nonmetastatic cMCT are the main indications for surgery (Weisse et al., 2002; Govier et al., 2003). Wide surgical resection with lateral margins of 1 to 3 cm and one fascial plane deep to the tumor are recommended to achieve complete resection (Thamm et al., 2001; London et al., 2003; Seguin et al., 2001; Govier et al., 2003; Simpson et al., 2004; Fulcher et al., 2006; Thamm et al., 2007). The choice of surgical margin wideness is based on the histological grade of the tumor. For most grade, I and II cMCT a lateral margin of 2 cm and a deep fascial plane is adequate (Seguin et al., 2001; Simpson et al., 2004; Fulcher et al., 2006). However, lateral margins proportional to the tumor size were also described as a good option for local control of small low-grade tumors (Fulcher et al., 2006). Panniculus muscle, underlying fascia, and the superficial muscular layer are adequate planes for deep margins if they were not affected by tumor invasion (Murphy et al., 2004; Simpson et al., 2004; Fulcher et al., 2006).

It is important to note that the abovementioned margin recommendation was not evaluated for tumors larger than 4 cm diameter, and may not be adequate for large cMCT(Blackwood et al., 2012). Wide resection of grade III cMCT, requires a 3 cm plus one deep fascial plane margin, but systemic adjuvant treatment is recommended regardless of margin status (Thamm et al., 2007).

Nonresectable tumors or those in difficult locations may receive neo-adjunctive chemotherapy or prednisolone therapy to obtain cytoreduction and make the tumor amenable to surgery (Stanclift et al., 2008). Incomplete or marginal resection is usually preferred over radical procedure when complete excision is impossible but must be followed by adjuvant radiotherapy (AlSarraf et al., 1996; Frimberger et al., 1997; LaDue et al., 1998; Poirier et al., 2006; Welle et al., 2008).

Surgical specimens should be submitted for histological evaluation of tumors and margins. Margin statuses are defined as: (1) complete resection when no tumor cells could be found within 1mm of the surgical borders; (2) complete but close (or narrow) when mast cells are seen within 1mm of the surgical margins; or (3) incomplete resection when there is sheets or clusters of malignant mast cells at the margin (Stanclift et al., 2008; Blackwood et al., 2012). The definition of completely resected and incompletely resected is not straightforward (Karbe et al., 2021). The current definition of narrow margins is widely variable from >1mm to 9mm (Thamm et al., 2009; Seguin et al., 2001; Weisse et al., 2002; Gieger et al., 2005; Fulcher et al., 2006; Seguin et al., 2006; Scarpa et al., 2012). Nonetheless, the presence of sparse mast cells on the periphery of the resected margin is a confounding factor as it is hard to tell whether they are normal tissue residents or malignant mast cells (Misdorp et al., 1987; McManus et al., 1999; Murphy et al., 2004; Fulcher et al., 2006; Marconato et al., 2008). The clinical significance of close or narrow margins remains unknown and discussion of whether it should be considered complete resection remains in debate with some authors suggesting the use of a residual tumor classification scheme (Seguin et al., 2006; Liptak, 2020; 50,51 – Table 2).

Table 2. The residual tumor classification system (adapted from Liptak 2020). HTFM = Histologic Tumor-Free Margin.

Status	Description
RX	**Residual tumor presence unassessed or unknown**
R0	**No residual tumor**
	Complete histologic excision (HTFM >0mm)
R1	**Microscopic residual tumor**
	Incomplete histological excision
	Satellite tumor cells distant to the tumor
	Lymphatic, venous, or perineural invasion
	Lymph node or microscopic distant metastasis
R2	**Macroscopic residual tumor**
	Gross residual disease
	Macroscopic distant metastasis

Incompletely resected tumors and local recurrence are negative prognostic factors (Thamm et al., 1999; Chaffin et al., 2002; Scarpa et al., 2012; Kry et al., 2014). When incompletely resected, about 18 to 38% of the cMCT recurs (5-9); while the rate of recurrence for completely excided cMCT was only

3 to 11% (Seguin et al., 2001; Michels et al., 2002; Weisse et al., 2002; Murphy et al., 2004). Incompletely resected cMCT often requires additional local treatment, mostly scar resection, to achieve a disease-free status (Kry et al., 2014; Karbe et al., 2021). High-grade tumors are significantly more prone to local recurrence when compared to low-grade tumors (Donnelly et al., 2015). A study found no recurrence in grade II cMCT with narrow histologic margins (Seguin et al., 2006). Remains unclear whether narrowly excised grade II requires additional therapy (Seguin et al., 2006).

A recent study evaluating incompletely resected cMCT submitted to scar revision surgery had only 4% of recurrence (Karbe et a., 2021). Previous studies found a 13% rate of recurrence (Kry et al., 2014) Also, dogs with incompletely excised cMCT submitted to scar revision lived longer than those without additional local therapy (Kry et al., 2014).

2.1.6 Histological Grade and Prognosis

Risk factors for disease progression, recurrence, and survival time include tumor grade, size, location, and surgical margin status (Patnaik et al., 1984; Turrel et al., 1988; Hahn et al., 2004; Seguin et al., 2006). However, the histological grade is the single most important prognostic factor for cMCT (Blackwood et al., 2012). Two systems are currently used to histologically grade cMCT: The three-tier Patnaik system (Patnaik et al., 1984; Table 2) and the two-tier Kiupel system (Kiupel et al., 2011). The Patnaik system differentiates in grade I (well-differentiated), II (intermediately-differentiated), and III (poorly-differentiated) cMCT according to cellularity, cell morphology and pleomorphism, mitotic index, and the reaction of the stroma to the degree of tissue infiltration, cell pleomorphism, (Patnaik et al., 1984)

Grade I cMCT is usually of benign behavior, growing slowly and persisting for years without increasing in size (Blackwood et al., 2012). Dogs are unlikely to die from grade I cMCT and metastasis occurs in less than 10% of the cases (Blackwood et al., 2012). On the other hand, grade III cMCT exhibit an aggressive clinical and biological behavior, growing fast, and a high rate of both metastasis (80%) and recurrence is reported (Welle et al., 2008; Blackwood et al., 2012). Grade II cMCT had a wide variable prognosis and behavior, with only 5-22% metastasizing (Séguin et al., 2001; Weisse et al., 2002; Séguin et al.,

2006; Blackwood et al., 2012). However, a subset of 17 to 56% of grade II dies of cMCT-related causes, such as local recurrence and metastatic dissemination (Blackwood et al., 2012). Other prognostic factors are necessary to indicate whether a grade II cMCT belongs to the high or low aggressive population of patients (Blackwood et al., 2012).

In the context of the variable and often unpredictable behavior of grade II cMCT along with the subjective histological criteria causing disagreement among pathologists analysis in 64-75% of the cases (Northrup et al., 2005; Kiupel et al., 2011), the Kiupel grading system emerged as an alternative (Kiupel et al., 2011). The two-tier grading system established that high-grade cMCT must have one of four criteria: (1) at least 7 mitotic figures in 10 high-power fields; (2) at least 3 multinucleated (3 or more nuclei) cells in 10 high-power fields; (3) at least 3 bizarre nuclei in 10 high-power fields; (4) karyomegaly (nuclear diameter at least two-fold in at least 10% of the neoplastic mast cells). Using Kiupel's grading system, all tumors that do not meet at least one of the abovementioned criteria are considered low-grade (Kiupel et al., 2011).

Kiupel high-grade cMCT had a shorter time to metastasis, a higher rate of new tumor formation, and a shorter survival time (Kiupel et al., 2011). However, about 15% of low-grade MCT still exhibit aggressive biological behavior (Kiupel et al., 2011; Stefanello et al., 2015). Both Patnaik and Kiupel grading systems are currently used for the prognostication of cMCT in dogs (Willmann et al., 2021).

Nevertheless, there was a subset of patients in high-grade cMCT that exhibit a better outcome. A study evaluating 49 dogs with stage I high-grade cMCT was evaluated after surgical excision and those with a smaller tumor diameter and lower mitotic count had a longer survival time. The median survival time was 1046 days with a 1-year survival of 79.3% and 2-year survival of 72.9% (Moore et al., 2020).

Immunohistochemical markers can aid in determining the behavior and prognostic of cMCT in complement to histological grade. The proliferative rate measured by the proliferative markers Ki67 and AgNOR is indicative of cMCT biological behavior, such as the likelihood of recurrence (Abadie et al., 1999; Scase et al., 2006; Webster et al., 2007; Vascellari et al., 2013; Willmann et al., 2021). Low-grade cMCT with a low Ki67/AgNOR proliferative index has a low recurrence rate even when incompletely resected (Séguin et al., 2006; Smith et

al., 2017).

The KIT expression (CD117) and mutational status are also prognoses (Willmann et al., 2021). KIT labeling pattern correlates with recurrence and survival of cMCT (Kiupel et al., 2004; Preziosi et al., 2004). The full KIT gene sequence is not routinely performed in a clinical setting, however, a clinically relevant mutation known to be recurrent in MCT (such, as in exons 8, 9, and 11) is recommended (Hahn et al., 2008; London et al., 2009; Hadzijusufovic et al., 2012; Marconato et al., 2014; Weishaar et al., 2018). The detection of phosphorylated KIT by immunohistochemical assay is associated with a shorter progression-free interval and overall survival time in dogs with cMCT (Thamm et al., 2020). Finally, the detection of c-Kit mutation seems to be more useful for identifying histological low-grade but biologically aggressive cMCT, while c-Kit expression is better to predict tumor with increased risk for disease progression (Thamm et al., 2019).

2.1.7 Adjuvant Chemotherapy

The decision to pursue adjuvant treatment after resection of the primary cMCT is usually based on margin status, histological grade, and presence of residual or gross disease: (1) Completely excised grade I and II cMCT without metastatic disease may be monitored only; while in the presence of metastasis adjuvant treatment is recommended; (2) Incompletely resected grade I and II without gross residue disease may be submitted to en bloc scar revision, adjuvant therapy or be monitored for recurrence. In the presence of gross disease, the patient must receive adjuvant treatment; (3) Grade I and II with nodal metastasis should receive adjuvant therapy such as radiotherapy or chemotherapy; and (4) Grade III cMCT must receive adjuvant chemotherapy regardless of margin or nodal status (Blackwood et al., 2012).

Chemotherapy is commonly used in dogs bearing cMCT when systemic therapy is necessary to treat, delay or prevent metastatic dissemination, such as in high-grade tumors, node metastasis, or to treat residual microscopic disease following surgery (Bostock et al., 1973; Patnaik et al., 1984; Bostock et al., 1989; Thamm et al., 2006; Blackwood et al., 2012). Chemotherapy may also be used in a neo-adjunctive setting before primary treatment for down-stage disease and improve the likelihood of adequate excision or to turn it safer to remove the tumor

(Blackwood et al., 2012).

Chemotherapy protocols for cMCT often include vinblastine and/or lomustine associated with prednisone or prednisolone (Blackwood et al., 2012; Néčová et al., 2021). Vinblastine is more often applied as first-line therapy while lomustine is frequently used as second-line treatment (Blackwood et al., 2012). Corticosteroids as a single agent have an effect against cMCT however, only 20% of the dogs exhibit complete or partial response (McCaw et al., 1994).

The vinblastine protocol usually consists of weekly administration of 2mg/m² for four treatments and then fortnightly for four more treatments (Thamm et al., 1999). Gradual dose escalation of vinblastine to 2.5mg/m² is also described (Serra Varela et al., 2016; Stirborova et al., 2019). Prednisone or prednisolone is given orally daily basis for the first two weeks in a 2mg/kg dose and then at 1mg/kg every other day for the remaining 10 weeks of the protocol. Corticosteroids should be discontinued thereafter (Stirborova et al., 2019).

Side effects of vinblastine protocols are reported to occur in 6 to 46% of the patients. Neutropenia is the most common side effect and occurs in about 20-23% of patients (Davies et al., 2004; Thamm et al., 2006; Hayes et al., 2007; Blackwood et al., 2012; Serra Varela et al., 2016; Stirborova et al., 2019). Vinblastine has been associated with radiotherapy for local control without a significant increase in adverse events (Stirborova et al., 2019).

The prednisone-vinblastine protocol showed a median response duration of 154 days and a median survival time of 331 days for grade III cMCT (Thamm et al., 1999). In an adjuvant scenario of high-grade cMCT, vinblastine plus prednisone resulted in a median survival time of 1374 days with 70% and 58% of 1-year and 2-year survival rates (Thamm et al., 2006).

Lomustine, also known as CCNU, is an alkylating agent and well-tolerated oral chemotherapy (London, 2020). The usual dose of lomustine is 90mg/m², however, dose reduction to 80 or 70mg/m² may be necessary if severe adverse events occur (Hay et al., 2019).

Most side effects of lomustine are related to dose-limiting myelosuppression, acute neutropenia, thrombocytopenia, and hepatic dysfunction (Hay et al., 2019; London, 2020). Neutropenia and elevated ALT is the predominant laboratorial abnormality found in animals submitted to lomustine treatment. Neutropenia occurred in 67% of the dogs with a median dose of

70mg/m², but no hospitalization was required (Hay et al., 2019). Liver toxicity with lomustine has been reported in 6.1% of the dogs treated, but the median time to hepatotoxicity was 11 weeks after the last lomustine administration (Kristal et al., 2004).

A study evaluating completely excised high-grade cMCT treated with lomustine found a median overall survival time of 904 days with a 1-year and 2-year survival rate of 60 and 40%, respectively (Hay et al., 2019). Other studies reported a median time to progression of only 77 days with single-agent lomustine (Rassnick et al., 1999). A combination of lomustine, vinblastine, and prednisolone provided only 141 days of median progression-free interval (Rassnick et al., 2010).

Prednisone as a single-agent neoadjuvant therapy demonstrated significative effect on decreasing tumor size in a randomized blinded placebo-controlled trial with 28 dogs (Linde et al., 2021). Other studies also found a reduction in tumor size with the use of glucocorticoids (McCaw et al., 1994; Standclift et al., 2008; Teng et al., 2012). This therapy is often administered to reduce peritumoral edema and downstage local disease to improve the likelihood of complete tumor resection (Linde et al., 2021). The decrease in tumor size is often quite short and does not typically last for more than a few weeks (Standclift et al., 2008;). A median of 81% reduction in 87% of grade II cMCT patients was reported (Standclift et al., 2008;).

Doses of 1 and 2.2 mg/kg of prednisone are sufficient to achieve a significant reduction in tumor volume, however, 1mg/kg is preferred due to the lower side effects of corticoid therapy (Standclift et al., 2008; Linde et al., 2021). Concerning treatment duration, effects on tumor size can be seen as early as 7 days, however, 70% of the response was reported within 9 days, and maximum tumor reduction was achieved within 21 days (Standclift et al., 2008; Teng et al., 2012; Linde et al., 2021). In summary, when aiming for cytoreduction, 1mg/kg of prednisone is usually recommended for 7 to 14 days before definitive surgical resection (Linde et al., 2021).

The suppression of MCT proliferation and response to treatment depends on the expression of glucocorticoid receptors by tumoral cells (Matsuda et al., 2011). Poorly differentiated or high-grade cMCT are less responsive to corticoid treatment (Takahashi et al., 1997).

2.1.8 Tyrosine Kinase Inhibitors

Tyrosine kinase inhibitors are inhibitors of small molecules that act by competitive inhibition of ATP binding, targeting and blocking the activity of tyrosine kinase cell-surface receptors (London et al., 2009). These receptors are present in normal cells and have a critical role in cell growth, differentiation, and proliferation, but in cancer cells the tyrosine kinase receptors are dysfunctional (London et al., 2009). Among the tyrosine kinase receptors, the most cited is the KIT (encoded by c-KIT proto-oncogene) (Webster et al., 2006). C-KIT mutation is present in about 15% of the cMCT, but prevalence increases to 30 to 50% in high-grade tumors (Downing et al., 2002). Interestingly, c-Kit mutation status cannot predict response to toceranib phosphate therapy in cMCT (Weishaar et al., 2018).

Tyrosine kinase inhibitors can also be used alone or associated with chemotherapy or radiotherapy in the treatment of cMCT (London et al., 2009; Blackwood et al., 2012; Todd et al., 2021;). Toceranib phosphate, masitinib mesylate, and imatinib have shown effective in treating canine cMCT (London et al., 2009; Grant et al., 2016; Todd et al., 2021). The toceranib phosphate was the first tyrosine kinase inhibitor to be studied for veterinary cMCT (London et al., 2009). The overall response rate of toceranib for treatment of cMCT is 42% with a median progression-free time of 18.1 weeks (London et al., 2009).

Toceranib can either be used as a single-agent treatment or in combination with other chemotherapy, such as vinblastine (Todd et al., 2021). Despite neutropenia being a dose-limiting toxicity in this combining protocol, the response rate of 71 to 90% has been described with a median survival time of 893 and 218 when in an adjuvant or gross disease scenario (Robat et al., 2011; Olsen et al., 2018). Another study found 310 days and 375 days for either progression-free interval and overall survival, respectively (Todd et al., 2021). The association of toceranib and lomustine is contraindicated due to severe adverse events that lead to the premature interruption of a clinical trial (Bavcar et al., 2017).

The dose of toceranib phosphate is widely variable in the literature. While the initial studies suggest an effective dose of 3.25 mg/kg every other day (London et al., 2009), further studies found that reducing the dose to 2.2-2.9

mg/kg every other day or allowing 1 or 2 weeks of drug interruption is equally effective and well tolerated (Bernabe et al., 2013).

Masitinib is also a potent tyrosine kinase inhibitor that also targets PDGF receptor, lyn, and FGF receptor 3 (Lyles et al., 2012). The first studies of Masitinib evaluated dogs with non-metastatic, recurrent, or nonresectable cMCT and found an improved progression-free time (118 vs 75 days), increased survival rates (1-year 62.1% vs 36%, and 2-years 39.8% vs 15%) (Hahn et al., 2008). An overall response rate of 50% and a median survival time of the dogs that respond to treatment of 630 was reported (Smrkovski et al., 2013). More recently, an 82% clinical response rate was reported with masitinib achieving complete remission in 38.5% and partial response in 43.6% of the dogs. The median time to progression was only 79 days, and 64% of the dogs experienced adverse effects, being vomiting and elevation on serum ALT the most reported (Grant et al., 2016).

Imatinib mesylate is also a tyrosine kinase inhibitor with antineoplastic effect due to its inhibition of ATP binding, phosphorylation, and downstream signal transduction pathways inhibiting cell growth (Isotani et al., 2008; Dubreuil et al., 2009). Dogs are usually treated with 10mg/kg once daily of Imatinib for 8 weeks (Macedo et al., 2022). Complete remission, partial response, and stable disease were reported to occur in 7.7%, 23.1 and 38.5% of the cMCT patients treated with imatinib a significant difference when compared to vinblastine/prednisone (Macedo et al., 2022).

2.2. Canine Lymphatic System and Lymph Nodes

The lymphatic system is a highly specialized drainage system present in every organ and tissue with a blood supply. It is composed of collecting lymphatic vessels, LNs, and lymphoid organs (Fujimoto et al., 2021). The spleen, thymus, bone marrow, and mucosa-associated lymphoid tissue such as the tonsils and Peyer’s patches are also part of the lymphatic system (Bezuidenhout, 2013).

The key role of the lymphatic system is the physiologic major drainage system that allows the return of interstitial fluid back to the systemic circulation through the lymph. The lymph carries not only water, but immune cells, cellular debris, proteins, pathogens, and toxins (Oliver et al., 2004; Moore et al., 2018). Along with the vascular system, these functions are essential to maintaining fluid

homeostasis and eliminating potentially harmful substances (Moore et al., 2018; Oliver et al., 2020; Petrova et al., 2020). The lymph is also responsible for transporting antigens and dendritic cells from the peripheral tissues to LNs and then to the systemic circulation via the thoracic duct (Oliver et al., 2020; Petrova et al., 2020; Figure 1). Antigen and antigen-presenting cells are exposed to naïve lymphocytes at the LNs triggering adaptive immune responses (Kitagawa et al., 2002; Loo et al., 2017).

Each anatomical region of the dog has a dedicated lymphatic draining system that flows out to chain arranged LNs (Suami et al., 2013; Greene et al., 2003). The lymphatic system is wide variable according to body organs in humans and internal viscera lymphatic drainage is far more complex than skin and breast drainage (Leong et al., 2022).

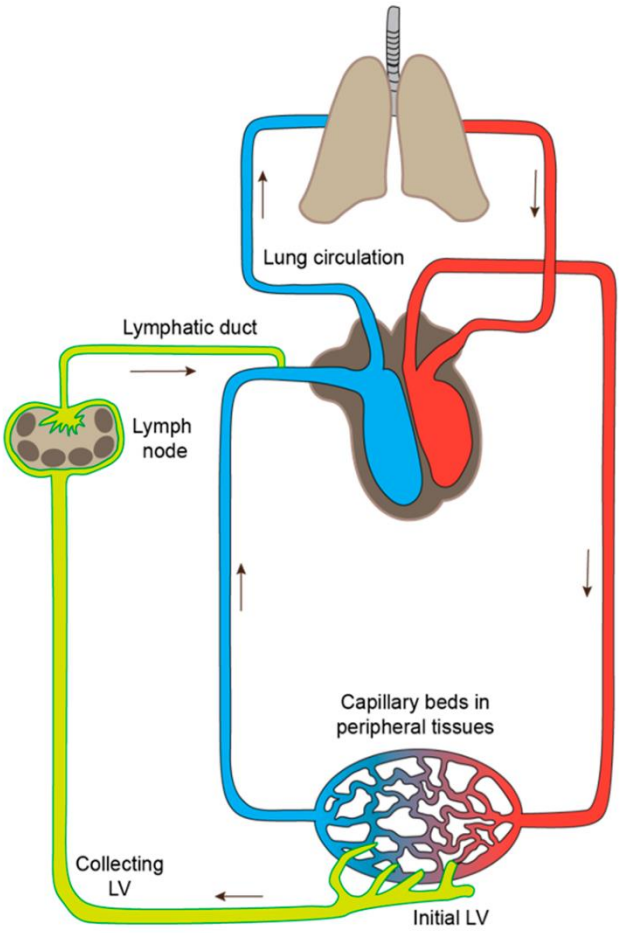

Figure 1. The lymphatic system and its interaction with the systemic circulation. The initial lymphatic vessels (LV) are responsible for uptaking fluids and other particles from the peripheral tissues and transporting them through the collecting LV to the lymph nodes and to the thoracic duct that debouches to the venous circulation at the vena cava. (Adapted from Fujimoto et al., 2021)

2.2.1 Lymph Vessels

Different from the blood vessels, which are composed of a basal membrane, pericytes, endothelial cells, and large vessels also have smooth muscle cells (Tucker et al., 2020), the lymphatic vessels are simpler, consisting of a single layer of endothelial cells without a basement membrane, pericytes or smooth muscle cells. The lymphatic vessels suffer anatomical adaptations according to the tasks it develops (Petrova et al., 2018).

The lymphatic vessels begin at the periphery of the tissues as blind-ended capillaries that once progress merging to form large vessels. The early type is called initial lymphatic vessels and the latter collecting lymphatic vessels (Forster et al., 2012). Moreover, lymphatic vessels that are traveling toward a LN are called afferent lymphatic vessels, and those coursing away from the LN are termed efferent lymphatic vessels.

Initial lymphatic vessels are blind-ended structures that uptake interstitial fluid, soluble molecules, particles, and cells of the peripheral non-lymphoid tissues (Fujimoto et al., 2021). The initial capillary lymphatic vessels consist of a single layer of leaf-shaped overlapping lymphatic endothelial cells and button-like junctions (Oliver et al., 2005; Baluk et al., 2007; Breslin et al., 2018; Figure 2). To avoid collapsing due to increased interstitial fluid pressure, these endothelial cells are loosely attached to a discontinuous basement membrane by anchoring filaments (Leak et al., 1968). The overlapping endothelial cells open in the presence of an increased interstitial pressure allowing the entry of fluid, other substances, and cells (Lutter et al., 2012). As mentioned before, these initial lymphatic vessels merge to form pre-collecting and intermediate vessels that share features of both initial and collecting vessels (Lutter et al., 2012).

Conversely, collecting lymphatic are responsible to transport the lymph from the initials toward the LNs. Collecting lymphatic vessels have regular elongated shaped and tightly adhered endothelial cells connected by continuous zipper-like junctions and a continuous basement membrane (Baluk et al., 2007; Pflick et al., 2009; Fujimoto et al., 2021; Figure 2). These characteristics aim to avoid the leakage of lymph back to the interstitium (Baluk et al., 2007; Pflick et

al., 2009). Moreover, collecting lymphatics have smooth muscle cells that contract and project the lymph forward, even if it is against a pressure gradient (Von der Weid et al., 2004; Scallan et al., 2016; Fujimoto et al., 2021). The presence of intraluminal semi-lunar valves throughout the collecting vessels divides it into segments termed lymphangions and ensures there will be only unidirectional lymph flow and prevent backflow (Lauweryns et al., 1973; Breslin et al., 2018; Fujimoto et al., 2021). The internal diameter of a lymphatic vessel is about 100 microns (Breslin et al., 2018).

Once on initial lymphatic vessels, the lymph courses through a mesh of afferent collecting vessels to the draining LN where it travels through a network of lymphatic sinuses. The lymph then leaves the LN through a single efferent collecting vessel that connects to secondary LNs (Fujimoto et al., 2021). Finally, the lymph flows according to the arterial pulse, contraction of the smooth muscle cells of the large collecting lymphatic vessels, and the action of surrounding skeletal muscles (Kawai et al., 2009).

As initial and collecting lymphatic vessels plays distinct roles, the lymphatic endothelial cells are heterogeneous and exhibit various molecular phenotypes according to the organ and bed (Petrova et al., 2018). In humans, for example, the lymphatic network of the lungs, intestine, heart, and central nervous system exhibit specific structures and functions (Bradham et al., 1970; Bernier-Latmani et al., 2015; Bernier-Latmani et al., 2017; Brakenhielm et al., 2019; Reed et al., 2019; Ma et al., 2019; Oliver et al., 2020; Petrova et al., 2020).

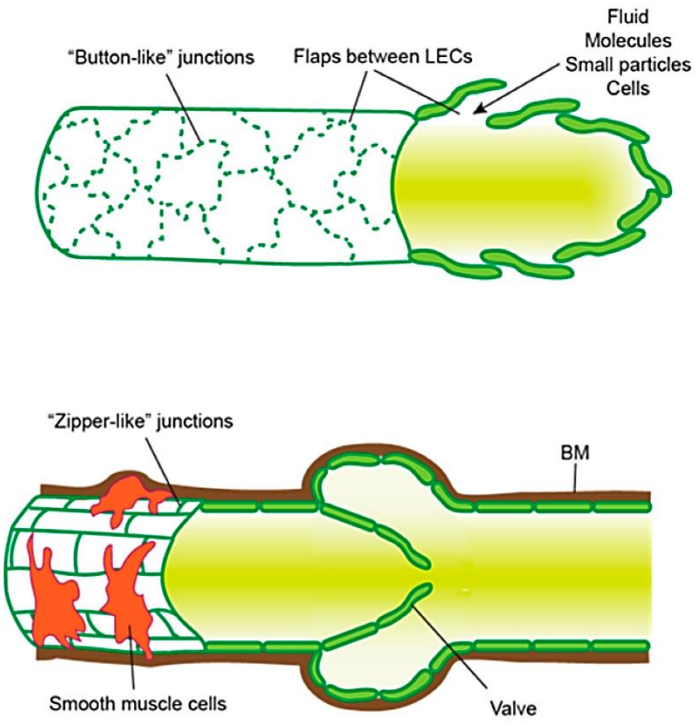

Figure 2. Types of Lymphatic Vessels. (A) The anatomical features of the initial lymphatic vessels. The lymphatic endothelial cells are irregular and overlap forming flaps that are associated with the discontinuous basement membrane and "button-like" junctions facilitate intravasation of fluids, molecules, and cells from the interstitial space. (B) The anatomical features of the collecting lymphatic vessels. The lymphatic endothelial cells are regular and have a continuous basement membrane, tight junctions, smooth muscle layer outlining, and a valve to allow unidirectional flow. (Adapted from Fujimoto et al., 2021).

2.2.2 Lymph Nodes

The LNs are responsible for initiating the adaptive immune response, continuous immunosurveillance, and propagation of immune tolerance. The LNs have a capsule, cortex, paracortex, and medulla (Schineis et al., 2019). The afferent lymphatic vessel reaches the subcapsular sinus located below the collagen-rich capsule forming the sinus system that surrounds the LN parenchyma. The subcapsular sinus is connected to cortical and medullary sinuses (Fujimoto et al., 2021). The LN cortex is the outer region of the LN parenchyma where B-cell follicles and interfollicular T-cell zones are located (Rezzola et al., 2022). The paracortex is located deep inside the LN parenchyma and harbors the T-cell zones and high endothelial venules, the gateway of T- and B cells entering the LN from blood circulation (Schwager et al., 2019).

The LNs also have a conduit system formed by extracellular matrix and fibroblastic reticular cells that transport low-molecular-weight macromolecules, antigens, and antibodies (IgM) between LN divisions (Sixt et al., 2005; Thierry et al., 2018; Reynoso et al., 2019). This system allows the contact of antigen-presenting cells, tissue-derived antigens, and soluble immune mediators with naïve B and T lymphocytes and recirculating central memory T cells (Leon et al., 2019). Once in contact with a cognate antigen on an antigen-presenting cell, the T cells become activated and then proliferate and differentiate on antigen-specific effector cells that ultimately will leave the LN through efferent lymphatic vessels (Girard et al., 2012; Qi et al., 2014; Breart et al., 2016; Benechet et al., 2016). If a cognate antigen cannot be found, T-cells leave the LN via efferent lymphatics (Girard et al., 2012; Qi et al., 2014; Breart et al., 2016; Benechet et al., 2016).

Lymphatic endothelial cells of the LN have different properties than those of the peripheral lymphatic vessels (Rezzola et al., 2022). Also, lymphatics endothelial cells resident on the LN and lining the outer and inner layer of the sinuses are phenotypically different. While the first is more tightly bound to avoid interaction with adjacent tissues, the second is permeable to facilitate the emigration of leukocytes between sinuses and parenchyma (Jalkanen et al., 2020). Five types of lymphatic endothelial cells have been described. The ceiling and floor lymphatic endothelial cells form the subcapsular sinus. These endothelial cells express chemokine receptors to guide the migration of dendritic cells across the subcapsular sinus and to enter the LN parenchyma (Ulvmar et al., 2014). The floor lymphatic endothelial cells also harbor macrophages, sinus-resident dendritic cells, and diaphragm-like filters that capture soluble antigens (Gray et al., 2012; Gerner et al., 2015) and control the transport of macromolecules (Rantakari et al., 2015). The medullary and cortical lymphatic endothelial cells express both histocompatibility complex class I and II (MHC-I and MHC-II; Cohen et al., 2010; Fletcher et al., 2010) and programmed death-ligand 1 (PD-L1; Fletcher et al., 2010; Tewalt et al., 2012). The expression of these receptors, along with evidence of deletion of CD8+ T cells, induction of CD4+ anergy, and induction of regulatory T cells suggest that lymphatic endothelial cells promote more immunotolerance reactions rather than immune-

stimulatory reactions when in a steady-state (Tewalt et al., 2012; Rouhani et al., 2015; Nadafi et al., 2020)

2.3. The Mechanisms of Lymphatic Cancer Metastasis

Metastatic disease is one of the major causes of cancer-related death (Warland et al., 2014; Elliot et al., 2016). The metastatic potential of a tumor is mainly determined by its genotype and phenotype (Friedl et al., 2011; Jung et al., 2015). Once initiated, the metastatic process involves the dissemination of malignant cells to distant organs by intravasation, systemic circulation, evading immune destruction, extravasation, and finally distant site growth (Lambert et al., 2017; Figure 3). The two major routes of metastatic spread are the hematogenous and lymphatic. Sarcomas usually metastasize by vascular invasion, while carcinomas and round cell tumors primarily infiltrate the lymphatic vessels and metastasize to RLNs before gaining access to the bloodstream (Friedl & Wolf, 2003; de Boer et al., 2010). Metastasis of primary canine mammary tumors to distant organs, for example, occurs mainly through lymphatic invasion and spread, and rarely by hematogenous dissemination (Klopfleishch et al., 2010; Soultani et al., 2017). In canine cMCT, the lymphatic system is the main initial route for metastatic spread, being the draining node the first site of metastatic disease (Conzo et al., 2014; Worley et al., 2014; Mendez et al., 2020).

As the main route for immune cells and pathogens to travel from peripheric tissues to other body sites, the lymphatic system can also be exploited by cancer cells to achieve systemic dissemination (Lambert et al., 2017). In this context, the lymphatic system acts as a conduit to allow the cancer cell to move from the primary tumor microenvironment to the draining LNs, then to other RLNs, and posteriorly to distant viscera (Leong et al., 2022).

Intravasation of interstitial content into lymphatic vessels is an essential process for immunosurveillance and fluid balance (Fujimoto et al., 2021). However, tumor cells also intravasate to lymph vessels to metastasize. Breaching through the basement membrane in an invasive growth pattern on vascularized tissue is required. Pre-existing vessels can be enslaved by the tumor, or new vessel formation can be inducted by the tumor angiogenesis and

lymphangiogenesis (Fujimoto et al., 2021). Cancer cells are usually just a few microns larger (~20 microns) than an average lymphocyte (~15 microns) making the internal lumen of the lymphatics suitable for cancer cell dissemination (Leong et al., 2022). Also, cancer lymphangiogenesis frequently results in dilated lymphatic vessels (He et al., 2005).

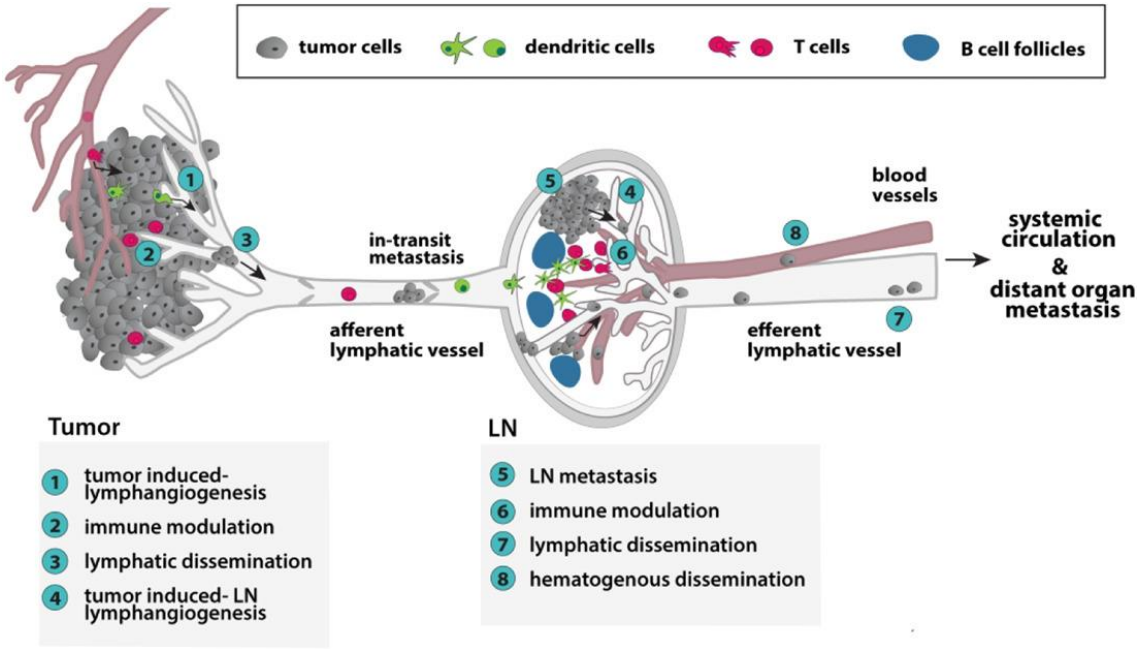

Figure 3. Scheme of the main routes of lymphatic dissemination of metastatic tumor cells. The steps of lymphatic metastasis are illustrated: The primary tumor induces the formation of new lymphatic vessels through the lymphangiogenesis process (1). This process increased the area of interaction between the tumor cell and lymphatic endothelial cells inducing intravasation of tumor cells to lymphatic vessels (2 and 3). Once metastatic foci travels through the lymphatic vessels they can stuck at the lymphatic vessel – forming in-transit metastasis – or drain to the LN (5 and 6). At the lymph node, antigen-presenting dendritic cells, T cells, leukocytes, and lymphatic endothelial cells induce antitumor immunity and, conversely, immune modulation reducing antitumor immunity. At this point, metastasis can access the systemic circulation through the nodal blood vessels (8) or continue to travel via efferent lymphatic vessels (7). The subsequent draining lymph node can be affected by metastasis, or it can eventually get access to the systemic circulation. (Adapted from Rezzola et al., 2022).

2.3.1 Lymphangiogenesis Process

The tumor microenvironment is highly metabolic tissue, requiring an adequate blood supply to provide nutrients, waste removal, immune and stromal cells, and, once invaded, acts as a conduit for metastatic spread (Joyce et al., 2009; Liotta et al., 2001; Jayson et al., 2014). To sustain this high metabolic state,

solid malignant tumors are known for their ability to form new blood vessels through angiogenesis and stimulate the formation of new tumoral lymphatic vessels from pre-existing ones by lymphangiogenesis (Joyce et al., 2009; Fujimoto et al. 2021). The latter process is a multistep sequence of activated lymphatic endothelial cells that proliferate and migrate in response to specific signaling (Rezzola et al., 2022). The extracellular matrix, cancer cells, and host-derived cells residents of the tumor microenvironment (i.e., stromal, and immune cells) are responsible for the release of lymphangiogenic factors, such as chemokines and growth factors, that stimulates new lymphatic formation (Liotta et al., 2001; Joyce et al., 2009; Fujimoto et al., 2021). The vascular endothelial growth factor (VEGF) C, D and A stimulated both angiogenesis and lymphangiogenesis while angiopoietin-2, hepatocyte growth factor (HGF), and fibroblast growth factor (FGF) are also involved (Dieterich et al., 2016). The activation and inactivation of genes involved in lymphangiogenesis by microenvironmental signaling are also part of the complex nature of the metastatic process (Jung et al., 2015).

Beyond causing an effect on the tumor microenvironment, these growth factors drain to the collecting lymphatic vessels and the draining LN stimulating preexisting lymphatic vessels and causing lymphangiogenesis (Halin et al., 2007). The LN lymphangiogenesis can be detected on tumor-draining LN even before the onset of an overt metastatic niche (Hirakawa et al., 2005). In human cancer such as malignant melanoma and breast cancer, this pre-metastatic changes in the LN precede a metastatic stage as patients fatally develop a metastatic lesion further in the course of the disease (Qian et al., 2006; Van den Eynden et al., 2007; Kerjaschki et al., 2011; Olmeda et al., 2017).). These still incompletely understood concept is seen clinically as increased lymph flow, dilatated lymph vessels, and enlarged LNs (He et al., 2005; Hoshida et al. 2006; Proulx et al., 2010). Once the metastatic cells reaches the LN, they are responsible for the continuous release of stimulating growth factors that sustain the lymphangiogenesis process (Kerjaschki et al., 2011).

2.3.2 Changes in Microenvironment Lymphatic Vasculature

Despite the ability to create new lymphatic vessels, most malignant epithelial tumors are also surrounded by lymphatic vessels (Jain et al., 2002). In the early stages of progression, the lymphatic vasculature suffers active modification as the lymphangiogenesis process occurs both surrounding and inside the tumor and causes the dilation of the lymphatic vessel lumen (Tacconi et al., 2015; Jalkanen et all., 2020). This lymphatic remodeling results in an increased flow rate and favors cancer spreading through the lymphatics (Proulx et al., 2010; Karnezis et al 2012; Stacker et al., 2014; Figure 4).

As the tumor grows, the intra-tumoral interstitial pressure increases pushing the lymph flow towards the peritumoral lymphatic vessels and increasing the volume of interstitial fluid (Christiansen et al., 2011; Karaman et al., 2014). Most of the intratumoral vessels collapse due to the high interstitial fluid pressure and the pressure exerted by tumor cells, which compromises their normal function (Padera et al., 2002; Stanczyk et al., 2010; Olszewski et al., 2012). On the other hand, the peritumoral lymphatic vessels are thought to represent the main route for cancer cell dissemination as it does not suffer from these microenvironmental conditions (Cochran et al., 2004; Wong et al., 2006; Dihge et al., 2019). Prostaglandins released by the upregulation of COX2, VEGF stimulation, or secreted by lymphatic endothelial cells were associated with an increased capacity of peritumoral lymphatic capillaries and collecting vessels (Karnezis et al., 2012; Karnezis et al., 2012b; Le et al., 2016). In summary, tumor interstitial fluid tends to be direct to the periphery creating a gradient of pressure that promotes cancer cell invasion and migration toward the dilated lymphatic vessels (Huang et al., 2015; Cornelison et al., 2018).

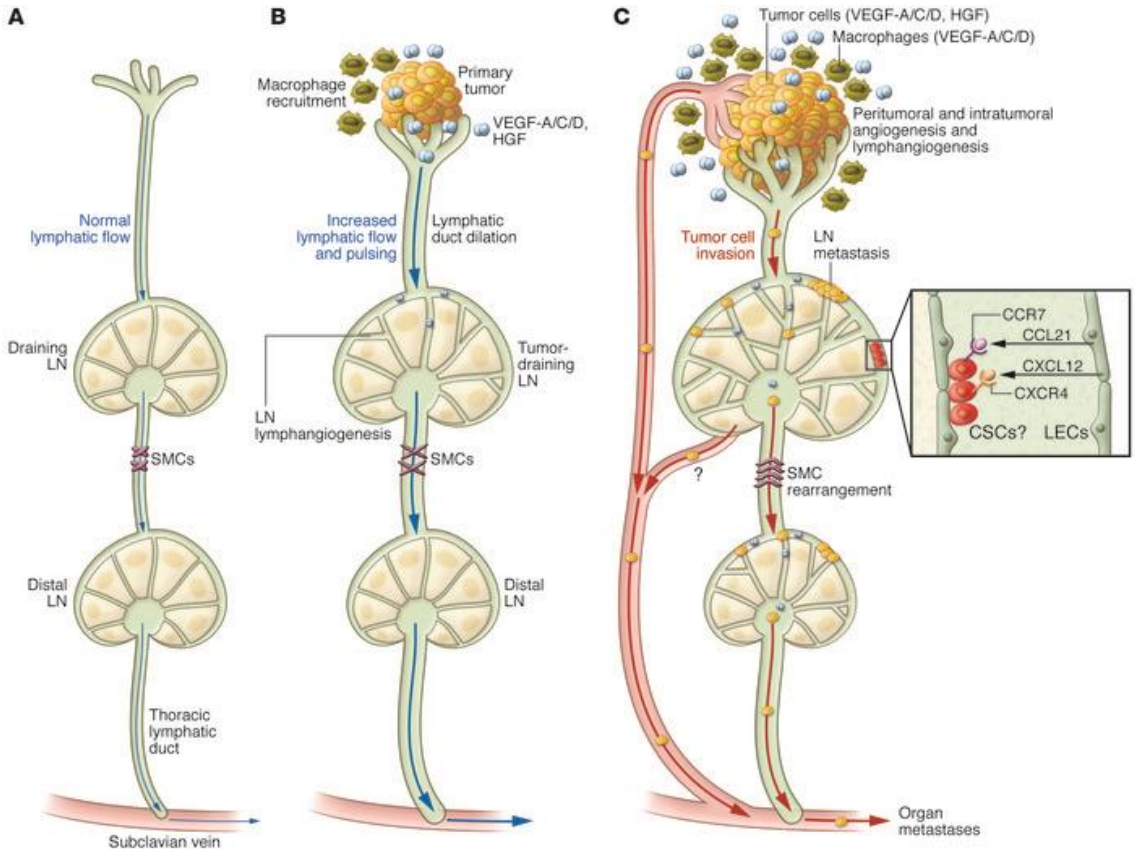

Figure 4. Changes in the lymph node, afferent, and efferent vessels in the presence of a malignant tumor. (A) Normal lymphatic drainage of a peripheral tissue showing the normal lymph flow from the capillaries, collecting lymphatic vessels and the chain-organized lymph node. (B) The release of lymphangiogenic factors produced by cancer cells causes lymphatic vessel dilatation, increased lymph flow, and lymph node lymphangiogenesis from preexisting lymphatic vessels preparing the tissue for further metastatic spread. (C) Metastatic spread through the lymphatic vessels to the draining lymph node causing remodeling and rearrangement of efferent lymphatic vessels and further lymphangiogeneses in secondary lymph nodes of the basin. Systemic spread occurs after drainage to the thoracic duct or through direct drainage from the tumor or lymph node blood vessels. At the right detail, cancer stem cells forming a niche of cancer cells expressing specific receptors. (Source: Adapted from Karaman et al., 2014).

2.3.3 Cancer Invasion and Lymphatic Intravasation

The secretion of proteolytic enzymes, expression of adhesion proteins and chemokines, are also responsible for driving tumor cell invasion, motility on extracellular matrix, movement to lymphatic vessels, and intravasation (Liotta et al., 2001). Human studies evaluating the clinical impact of lymphatic vessels surrounding or inside tumors found a correlation with a poor prognosis (Stacker et al., 2014; Dieterich et al., 2016; Ma, 2018). Furthermore, the cancer cells

located at the tumor-vessel interface often exhibit an invasive behavior different from the rest, which contributes to gaining access to the vessel's lumen (Fujimoto et al., 2021).

The epithelial-to-mesenchymal transition (EMT) occurs physiologically to allow cell mobility in wound healing and tissue repair. On the other hand, carcinoma cells often take advantage of this maneuver to downregulate their epithelial features, such as cell polarity and cell-cell binding enabling them to invade surrounding tissues. The vascular or lymphatic invasion often occurs on cell clusters of emboli rather than a single cell infiltration (Bronsert et al., 2014; Saxena et al., 2020; Sinha et al., 2020). In humans, the EMT is rarely completed, with most tumor cells being able to invade surrounding tissues with a partial EMT (Saxena et al., 2020; Sinha et al., 2020). Another factor influencing cancer cell invasion is the frequent tumor-induced remodeling of the extracellular matrix caused by cancer-associated fibroblasts and macrophages located in the tumor microenvironment (Belhabib et al., 2021; Cox et al., 2021; Ray et al., 2021).

The following step on cancer dissemination in the vascular invasion through a stepwise sequence of infiltrating the perivascular region, the basement membrane, and the endothelial layer. Four key mechanisms are reported to occur: (1) Mechanical disruption of the endothelial cells; (2) Mimicry of leukocytes; (3) Destabilization of lymphatic junctions; (4) Formation of entry portals into lymphatic vessels (Fujimoto et a., 2021).

Tumors cells can invade de lymphatic vessels by pushing growth disrupting the lymphatic endothelial barrier. This mechanical lymphatic invasion is reported to be a passive process in humans (Figure 5). The passive nature is explained by the mechanical stress and changes caused by the physical presence of the malignancy causing stretching forces on nearby cells, including the endothelial barrier; however, the real nature of this process remains unclear (Chen et al., 1999; Niimi et al., 2001; Fujimoto et al., 2021).

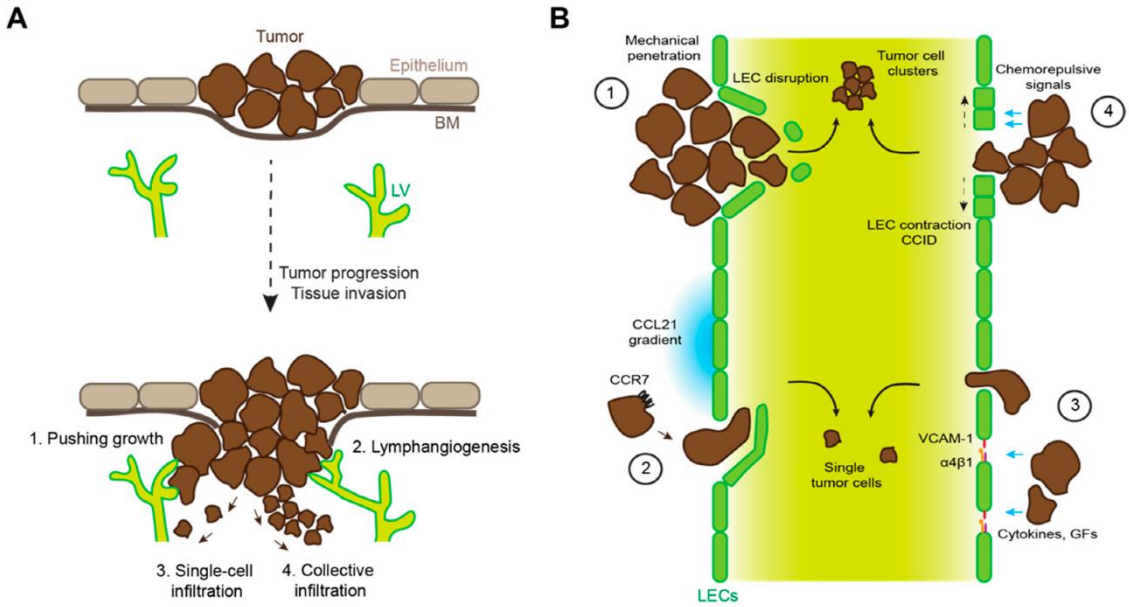

Figure 5. The mechanisms of lymphatic invasion by neoplastic cells. (A) Tumors progress from an in-situ stage, breaching the basement membrane, to invasive an invasive stage and promote lymphangiogenesis. Once in an invasive phenotype, the tumor get gets into the lymphatic vessels and both single cell or cluster infiltration. (B) Invasion of the lymphatic vessels occurs either by mechanical Disruption of the endothelial wall, intravasation through endothelial flap junction, inducing lymphatic permeability mediated by cytokine and growth factors, and release of chemorepulsive agents (Adapted from Fujimoto et al., 2021).

Tumor cells also mimic the signaling of normal immune cells to allow intravasation. In humans, tumor cells can express CCR7 a protein that promotes migration toward lymphatic vessels (Mashino et al., 2002; Emmett et al., 2011; Sperveslage et al., 2012). Furthermore, CCR7 expression has been correlated with lymphatic invasion and LN metastasis in several types of human cancers (Mashino et al., 2002; Emmett et al., 2011; Sperveslage et al., 2012). The CCR7 expression can be triggered by TGF-β induced during EMT (Pang et al., 2016). The lymphatic junctions can be destabilized by signals released by tumor cells or the tumor microenvironment causing an increase in lymphatic permeability (Fujimoto et al., 2021). Several mechanisms including the expression of VCAM-1, and VEGF-C resulting in reduced VE-cadherin expression have been investigated in several human cancers (Garmy-Susini et al., 2010; Dieterich et al., 2019; Tacconi et al., 2015; Chen et al., 2019).

Finally, the fourth mechanism of tumor cell lymphatic intravasation is the formation of a large entry portal in the endothelial lining. Entire clusters of tumor

cells can reach the lymphatic vessel through this mechanism. These portals result from the tumor-derived signal that is chemorepulsive for the lymphatic endothelial cells. The release of the enzyme Alox15 that catalyze the production of bioactive lipid mediator 12(S)-HETE is proposed as the mechanism underlying the formation of gates on lymphatic endothelium (Keriaschki et al., 2011; Rigby et al., 2015; Nakayama et al., 2019).

2.3.4 Moving Inside the Lymphatic Vessel

Once inside the lumen of the lymphatic vessels, the smooth muscle of the wall pumps the lymph towards the valves preventing the backflow and embolizing the cancer cells in clusters (Yancopoulos et al., 2000; Karaman et al., 2014). Human studies have shown that cancer causes direct changing in LN and lymphatic vessels. The lymphatic endothelial cells lining the LN that drain tumors proliferate causing expansion of sinuses (Commerford et al., 2018). In the presence of cancer, collecting vessels dilatated and increases the pumping rate improving lymph moving (Kamezis et al., 2012; Bachmann et al., 2019). However, circulating cancer cells are exposed to mechanical stress and biological adversity (Rezzola et al., 2021).

The mechanical stress to which a cancer cell is subjected is well known in vascular circulation, however, the low lymph flow results in lower fluid shear stress (Moore et al., 2018; Follain et al., 2020). On the other hand, cancer cells must adapt to an inhospitable environment inside the lymphatic system due to the presence of a huge number of immune cells. However, the lymphatic vessels act actively to induce and sustain an immunosuppressive tumor microenvironment (Rezzola et al., 2022). The counterintuitive issue of this fact enters in conflict with evidence that peritumoral lymphatic vessels are responsible for providing active immune cells to initiate anti-immune responses and modulate the tumor microenvironment (Kataru et al., 2019; Song et al., 2020). Conversely, other studies found a negative association with lymphatic vessels as cancer cells can “hijack” the lymphatic system by expressing receptors to escape from the immune system and cause the expression of immune-inhibitory molecules (Rezzola et al., 2022). The upregulation of PD-L1 and other nitric oxide derivates

can damper CD8+ T-cell response, inhibit T-cell proliferation, and affect Treg differentiation (Lukacs-Kornek et al., 2011; Bordry et al., 2018; Hornyák et al., 2018; Lane et al., 2018). The tolerogenic phenotype of the lymphatic endothelial cells and lymphocytes increases the risk of lymphatic colonization and further dissemination of cancer cells (Rezzola et al., 2022).

2.3.5 “In Transit” Metastasis

In human literature, the possibility of a cluster of cancer cells getting stuck on a lymphatic valve has been hypothesized (Karpanen et al., 2001). These cells may grow and colonize the inner wall of the lymphatic vessel and result in an “in-transit metastasis” (Karpanen et al., 2001). This kind of metastasis develops in the lymphatic vessel somewhere between the primary tumor and the draining LN (Meier et al., 2002). This process may be regulated by a specific receptor that remains unclear (Leong et al., 2022). Some experimental evidence found that human breast cancer cells may initially get access to the lymphatic system as a single cell, but further aggregate forming cell clusters (Dadiani et al., 2006; Giampieri et al., 2009). Once a blockage of the lymphatic flow occurs, the stagnation favors further accumulation and growth of tumor cells at the lymph vessel junctions and in-transit metastasis (Luzzi et al., 1998; Alitalo et al., 2012). The lymphatic endothelial cells and the lymph itself can act as a protective microenvironment that can sustain the long-term survival of tumor cells (Meier et al., 2002).

2.3.6 Lymph Node Pre-Metastatic Stage

After reaching a LN, the cancer cells pass through the subcapsular sinus and can either gain access to the vascular system by the lymphatic-venous connections or bypass the node and progress to the next LN of the basin by the efferent lymphatic vessel (Fisher et al., 1966; Weiss et al., 1989; Weiss et al., 1996). However, at the LN, the cancer cell can interact with the stroma to induce a microenvironment where cancer stem cells can colonize and form a niche and further progress, resist, and grow as metastasis (Li et al., 2015). Pro-lymphangiogenic factors (i.e., VEGF family, Erythropoietin, COX-2 prostaglandin)

are an important mechanism of the cancer cell to induce the creation of new lymphatic vessels inside the LN and favor metastatic dissemination (Lee et al., 2011; Ogawa et al., 2014; Rezzola et al., 2022).

The systemic spread of a small number of tumor cells that cannot be routinely detected on screening tests is known as micrometastasis (Tuohy et al., 2009). The presence of micrometastasis is hypothesized as one of the main reasons for the development of metastatic disease in individuals with previous negative LNs (Tuohy et al., 2009). In this scenario, the lymphatic endothelial cells also play a role in recruiting and maintaining cancer stem cells at the lymphatics (Kim et al., 2010). Genes responsible for cell division, immune modulation, and cell-cell and cell-matrix adhesion were found to be upregulated and altered on lymphatic endothelial cells when a neoplastic lymphangiogenic process is underway (Commerford et al., 2018).

2.3.7 Immune Evasion at the Lymph Node

Interestingly, despite contributing to tumor progression and dissemination, the lymphatic system is also responsible to transport tumor antigen toward LN allowing activation of T-cell response (Kimura et al., 2015; Lund et al., 2016). However, tumors cell also induces immune tolerance at the draining LN in a similar fashion as occurs in the lymphatic vessels (Rezzola et al., 2022). The main mechanisms of immune evasion are: (1) the low antigenicity of the tumor cells compared to other pathogens; (2) the loss of MHC receptors avoiding being detected by antigen-specific cytotoxic T lymphocytes (Rezzola et al., 2022); (3) incapacity of activating innate immunity (Beatty et al., 2015; Spranger et al., 2018); (4) induction of Treg or T cell dysfunction such as anergy and exhaustion; (5) immunosuppressive environment induced by lymphatic endothelial cells in non-inflammatory LN conditions (275); (6) release of immunosuppressive molecules (immune checkpoints) such as PD-L1 that induce Tregs and inhibit naïve T-cell proliferation and response against tumor cells (Niedbala et al, 2007; Lukacs-Kornek et al., 2011; Dieterich et al., 2017; Lane et al., 2018; Knoblich et al., 2018; Nadafi et al., 2020, Cousin et al., 2021).

2.3.8 Systemic Dissemination Following Lymphatic Metastasis

Metastasis from the primary tumor site to the LN is not the final stage of the metastatic dissemination but just a step until systemic dissemination and further colonization. Distant metastasis is one of the most life-threatening aspects of cancer. This type of metastasis requires systemic dissemination of cancer cells from the blood circulation to organs distant from the primary tumor site. In most human solid tumors, the systemic dissemination through blood vessels is preceded by lymphatic metastasis (Rezzola et al., 2022). In summary, the LNs act as a source of cancer cells that give rise to distant metastasis (Rezzola et al., 2022).

Once at the first draining LNs, cancer cells can colonize other distal nodes and gain access to the bloodstream after draining to the thoracic duct or access directly from the node to blood vessels via the blood vasculature present at the LN (Brown et al., 2018; Pereira et al., 2018; Rezzola et al., 2022). The lymph-to-blood vessel has been demonstrated in animal models and includes the passage of tumor cells that occurs by the invasion of node blood vessels after infiltration on LN parenchyma and results in systemic dissemination for the lungs without drainage to the thoracic duct (Brown et al., 2018). In a human melanoma study, about 70% of the cancer cells at a lung metastasis originated from metastatic LNs (Pereira et al., 2018).

Also, metastasis can contribute to further dissemination of tumor cells as lymphangiogenesis also occurs at metastatic sites giving rise to intra-metastasis spreading (Gundem et al., 2015; Ma et al., 2018). This mechanism can explain why LN resection has no impact on the survival rate in some types of cancer while representing an important factor in terms of prognosis (Rezzola et al., 2022). In this scenario, the metastatic cells at the LN at the time of surgical resection are not the only niche of tumor dissemination throughout the body, as distant nodes, blood vessels, and distant organs may harbor micrometastasis that might become apparent later in the course of the disease (Rezzola et al., 2022).

In humans, the presence of lymphatic vessel invasion can be detected on hematoxylin-eosin-stained sections, but this approach significantly underestimates its diagnosis. The introduction of lymphatic-specific antibodies,

such as anti-LYVE-1 and D2-40, allowed better detection of lymphatic invasion in a clinical setting (Moy et al., 2017; Fujimoto et al., 2021). Also in humans, the diagnosis of lymphatic vessel invasion has prognostic value in diverse types of cancer (Bosch et al., 2013; Pastushenko et al., 2014; Zhang et al., 2017).

Lymphatic vessel invasion has been associated with local or locoregional recurrence (Borgstein et al., 1999; Merchant et al., 1999; Fujita et al., 2008; Matsuura et al., 2019). However, a causative association between lymphatic invasion and distant metastasis remains unclear in humans as at least two clinical trials of patients with melanoma and breast cancer found no association between LN metastasis and poorer prognosis (Leiter et al., 2016; Farier et al., 2017; Giuliano et al., 2017). The LN may function as a filter barrier to avoid tumor cells from entering the systemic circulation by exposing the neoplastic cells to the adaptive immune system (Molodtsov et al., 2021). Conversely, LN draining a neoplasm can seed tumor cells to distant sites using two main routes: blood vessels associated with the LN or the conventional efferent lymphatic vessel (Fujimoto et al., 2021).

A receptive microenvironment is required to allow tumor growth at the metastatic site after extravasation. The “Seed and Soil” theory is the most accepted explanation to affirm that metastatic dissemination to viscera is not random (Paget et al., 1989). This theory is based on the concept that tumor cells act like seeds that can only establish and grow in a selected organ microenvironment, the soil, that is suitable to that specific cell (Greene et al., 1965; Schackert et al., 1988).

2.4. Sentinel Lymph Node Mapping

The LN is usually the first site of metastatic spread of cMCT, the reason why LN evaluation possesses a highlight position on staging algorithms (Blackwood et al., 2012; Warland et al., 2014; Horta et al., 2018; Fournier et al., 2020; London et al., 2020).

The concept of SLN was first described in the early sixties in people with a neoplastic disease of the parotid glands (Gould et al., 1960). Further studies on people used different methods to detect the first LN to drain a malignancy

(Cabanas et al., 1977; Morton et al., 1992; Alex et al., 1993; Krag et al., 1993). All studies had similar results: It was very unlikely to find metastatic LNs further on a lymphatic chain if the first draining LN, now called sentinel, were negative. This concept was a milestone in surgical oncology that is currently the standard of care for most neoplastic diseases.

In theory, metastasis through a lymphatic pathway is an orderly process in which tumor cells drain from the tumor to the first draining RLN and then progress to the other nodes in the lymphatic field (Zeidman & Buss, 1954; Somasundaram et al., 2007; Ball et al., 2010; Balasubramanian et al., 2011). This concept makes the first draining LN a barrier to the dissemination of tumor cells to second echelon LNs, the systemic circulation, and, ultimately, distant organs (Wong et al., 1991; Giuliano et al., 1994; Morton et al., 2005; Somasundaram et al., 2007; Cochran et al., 2008; Balasubramanian et al., 2011; Figure 6).

The first LN to drain a tumor in a specific region or basin is known as the SLN (Figure 6). The SLN is not specific to a neoplasm germline or anatomic location, being highly variable among animals, tumor location, and affected structures (Liptak et al., 2019).

In the concept of SLN, distant metastasis should not occur without evidence of SLN metastasis. Hence, because of its position in the lymphatic draining system, the SLN status reflects the status of all the regional lymphatic basin. In other words, a metastatic SLN increases the probability of other metastatic LNs on the bed and, consequently, of distant metastasis (Liptak et al., 2019). In human patients with malignant thyroid and breast cancer, the rate of distant metastasis when there were negative SLN was less than 0.1% (Turner et al., 1997; Balasubramanian et al., 2011). The early detection of metastasis to the SLN also allows for the addition of adjuvant treatment, such as the extension of surgical resection, chemotherapy, radiotherapy, or other systemic therapy, and consequently a better prognosis (Newman, 2004; Somasundaram et al., 2007).

Detection of the SLN is not a straightforward procedure, as the RLN that naturally drains a specific region is not always the SLN (Herring et al., 2002; Smith, 2002; Lurie et al., 2006; Gelb et al., 2010; Suami et al., 2013; Worley, 2014; Liptak et al., 2019). The so-called “zones of ambiguity” are regions of the

body, described in humans, where lymphatic drainage is particularly unpredictable (Goldfarb et al., 1998; Uren et al., 2003) These zones are responsible for the aberrant lymphatic drainage that causes, for example, the skin tumor to drain to deeply located LN far for the original site (Bezuidenbut, 2013). Metastasis of cMCT, for example, has been described to drain to colic, medial iliac, and accessory axillary LN (Fournier et al., 2020). The identification of unexpected SLN is strongly associated with this phenomenon in humans (Uren et al., 2003; Saha et al., 2013).

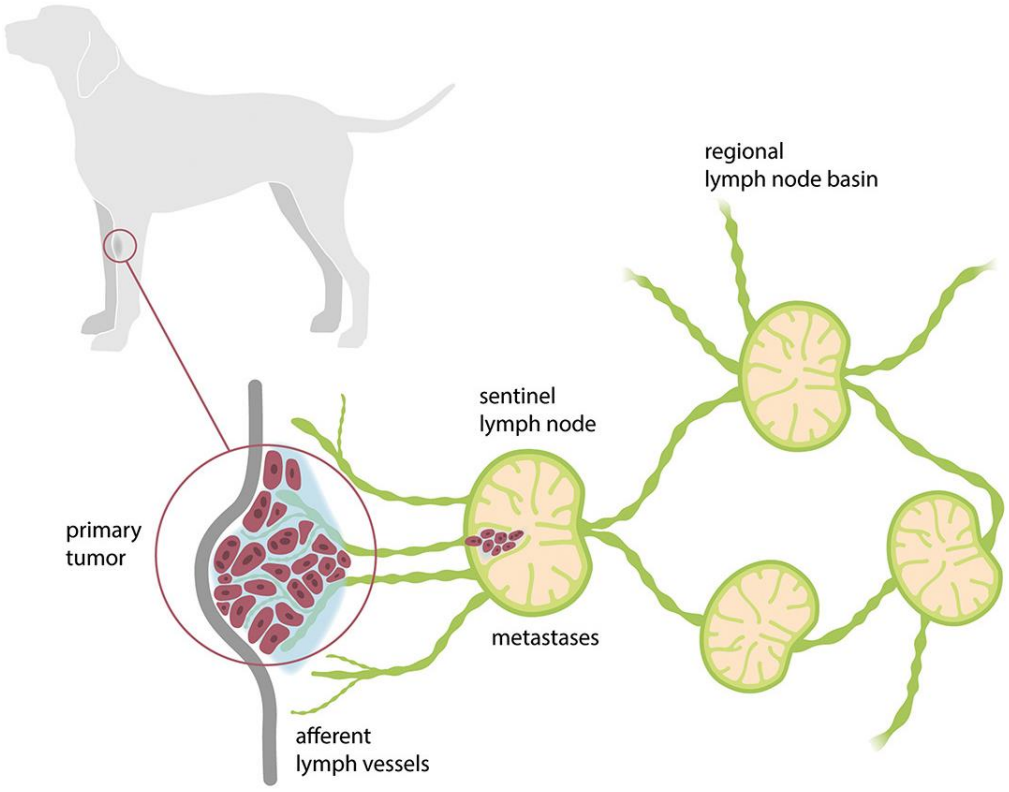

Figure 6. The hypothetical scheme of a lymphatic chain. Afferent lymph vessels draining the primary tumor site flow directly to the sentinel lymph nodes, where foci of metastatic cells are present. The sentinel lymph node also has afferent lymph vessels to the second echelon lymph nodes. (Adapted from Beer et al., 2018).

The unevenness and unpredictability of the lymphatic drainage were evident when a study detected that one or multiple lymphatic vessels can drain from a tumor for a single, but also several LNs (Thompson et al., 1999). A study evaluating lymphoscintigraphy for SLN mapping found that 42% of the dogs with

MCT, had a SLN other than that regularly draining the tumor site and these dogs received adjuvant treatment that otherwise would not be indicated (Worley et al., 2014). A study evaluating CT IL found about 25% of SLN different from the RLN (Lapsley et al., 2020). Other studies found up to 60% disagreement between SLN and RLN in cMCT (Ferrari et al., 2020). The unpredictable lymphatic drainage is also evident in dogs with mammary tumors, where the normal drainage pattern is altered when there is a neoplasm (Patsikas et al., 2006; Pereira et al., 2003; Veikkola et al., 2000). However, even normal mammary glands can have communication between LNs in approximately 44% of dogs (Pereira et al., 2008).

In a study evaluating canine patients submitted to lymphatic obstruction due to regional surgical procedures, the lymphatic drainage deviated from the ipsilateral to the contralateral LN as demonstrated by indocyanine green mapping (Suami et al., 2013). A CT lymphangiographic study also found that 26% of the dogs had afferent lymphatic vessels from the popliteal LN deviating from the medial iliac LN directly to the sacral and internal iliac LN (Mayer et al., 2017). In dogs with lateralized head and neck tumors, 62% had contralateral metastatic disease to the mandibular or retropharyngeal LN, against 92% of the patient that had ipsilateral metastatic disease (Skinner et al., 2017). The evidence supporting contralateral lymphatic anastomosis in head and neck cancer led to an important change in the previously indicated lateral incision to a ventral midline cervical surgical approach that allowed to remove the LNs bilaterally (Belz et al., 1995; Green et al., 2015; Wainberg et al., 2018).

To minimize extensive, mutilating dissection when performing lymphadenectomy of the entire lymphatic bed (i.e., non-selective LN dissection), a sample analysis of the SLN was advocated. If the SLN results positive for metastatic disease, the remaining lymphatic bed is finally removed. This approach spared human patients to be overtreated with extensive useless procedures (Wong et al., 1991; Morton et al., 2005; Cochran et al., 2008; Morton et al., 2012). Despite being widely used in oncologic human patients, several SLN mapping techniques are currently under investigation in small animals (Liptak et al., 2019).

In this context, using a technique to intraoperative guide the surgeon toward the SLN is essential to improve the detection of SLN, and decrease anesthesia time, surgical trauma, and postoperative morbidity (Beer et al., 2018).

2.4.1 Clinical Examination of Lymph Nodes

During tumor staging, palpation, and sampling of the RLNs are recommended for cMCT (Blackwood et al., 2012; Figure 7). However, only peripheral LNs can be clinically evaluated due to their superficial location. Peripheral RLNs should be evaluated looking for enlargement, asymmetry, and fixation to surrounding tissues (Wright & Oblak 2016). Normal LNs should be firm, smooth, and have an ovoid or bean shape (Beer et al., 2018).

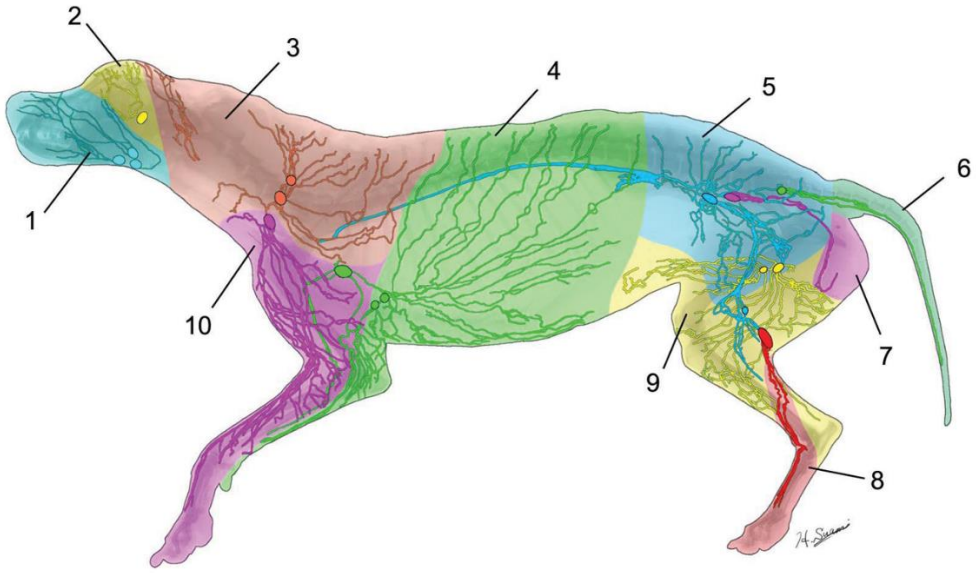

Figure 7. Lymphatic territories and the respective lymphatic vessels and corresponding lymph nodes. 1 – mandibular; 2 – parotid; 3 – dorsal superficial cervical; 4 – axillary; 5 – medial iliac; 6 – lateral sacral; 7 – hypogastric; 8 – popliteal; 9 – superficial inguinal; 10, ventral superficial cervical. (Source: Suami et al., 2013)

Palpation of the LNs may help raise suspicion for locoregional metastatic disease; however, palpation alone is a poor predictor of metastasis (Langenback et al., 2001; Herring et al., 2002; Williams et al., 2003). Also, RLN may not be clinically evaluated or aspirated due to size and anatomical location (Gieger et al., 2003; Worley et al., 2014; El et al., 2017). Metastatic disease of the LNs may be missed in more than 85% of the cases when palpation is used as the sole

method (Brissot et al., 2017). A multicentric retrospective study evaluating non-palpable or normal-size LNs found that 50% to 65% of the dogs with cMCT had metastatic RLN (either HN2 or HN3 according to Weishaar et al., 2014 classification) regardless of the histological grade (Ferrari et al., 2018). Tumors larger than 3 cm were associated with locoregional metastatic disease (Ferrari et al., 2018). The population of this study was comprised mainly of low-grade cMCTs (Ferrari et al., 2018). The sensitivity and specificity of palpation to detect metastasis in normal to mildly enlarged LNs were 60 to 72%, respectively (Langenbach et al., 2001). Clinicians were able to correctly identify all SLN in about half (54.2%) of the cMCTs in a study (Fournier et al., 2020).

2.4.2 Lymph Node Cytology

Fine needle aspiration biopsy followed by cytological examination of the LNs is an easy, quick, and non-invasive complement to clinical examination (Krick et al., 2009; Worley et al., 2014; Fournier et al., 2018). High sensitivity and specificity to detect metastasis of solid tumors to LNs have been described (Langenbach et al., 2001; Herring et al., 2002). A study found an 18.1% rate of metastasis in canine cMCT diagnosed by FNA and cytology (Stefanello et al., 2015). Nevertheless, when cytologically negative, biopsy and further histology are warranted as fine needle aspirate of the LNs can miss a focal metastatic lesion within the LN leading to a false-negative result (Wright & Oblak, 2016). FNA cytology can also result in nondiagnostic samples, even when ultrasound-guided is performed by an experienced professional (Lapsley et al., 2020). Furthermore, FNA can detect a normal number of mast cells within the LN that cannot be differentiated from metastatic disease causing false positives (Blackwood et al., 2012). Generally, a cluster of sheets of mast cells in LN FNA is highly suggestive of metastatic disease (Blackwood et al., 2012). FNA and Histology core biopsies have a sensitivity and specificity of 100% and 96% and 64% and 94% for LN metastasis, respectively (Langenbach et al., 2001). However, other studies reported only 68 to 75% sensitivity for detecting nodal MCT metastasis (Ku et al., 2007; Fournier et al., 2018). FNA cytology failure to result in diagnosed samples ranges from 25 to 68% (Weishaar et al., 2014; Fournier et al., 2018; Lapsley et al., 2020). A recent consensus proposal

suggested cytologic examination of all enlarged LNs and the SLN regardless of size (Willmann et al., 2021).

It is a challenge to differentiate reactive or metastatic LNs with the cytologic examination (Krick et al., 2009). The lack of standard criteria to define LN infiltration of neoplastic mast cells lead to a highly variable description of methods in the literature (Gieger et al., 2003; Cahalane et al., 2004; Thamm et al., 2006;). A cytological criterion was proposed to establish a standard approach to MCT LN metastasis (Krick et al., 2009). Krick's cytological criteria (Krick et al., 2009) use a similar classification that was further applied by Weishaar et al. (2014) to the histological diagnosis of MCT metastasis (Sabattini et al, 2021). LNs were classified as normal, reactive lymphoid hyperplasia, possible metastasis, probable metastasis, and certain metastasis (Krick et al., 2009; Table 3). However, the study that proposed the cytologic criteria for MCT LN metastasis did not compare with histopathology, so sensitivity, specificity, and predictive values were not described (Krick et al., 2009). A prospective study of SLN mapping detected that 7 out of 14 (50%) of the dogs had histologically detected metastasis that could not be diagnosed on cytology, changing adjuvant chemotherapy recommendation (Lapsley et al., 2020). Another study found >25% of false-negative cytology of LN when compared to histology (Fournier et al., 2018). Recently, a study reported only 5% of false-negative cytologic samples, but almost 37% were pre-metastatic histologically that could not be identified by cytology (Sabattini et al., 2021). The clinical influence of LN pre-metastatic stages is still uncertain (Sabattini et al., 2021).

Clinical examination and consequently cytology are limited to evaluating deep located peripheral LNs, such as retropharyngeal, or abdominal and thoracic LNs, such as iliac or mediastinal. An ultrasound-guided biopsy can be required to obtain samples of these LNs. Despite being useful for clinical tumor staging, palpation and ultrasound-guided FNA are unable to assess LNs in up to 60% of the cases (Gelb et al., 2016).

Table 3. Krick's Cytological criteria for mast cell tumor lymph node metastasis (Krick et al., 2009).

Interpretation	Description
Normal	No mast cell on cytologic smear
Reactive Lymphoid Hyperplasia	Greater than 50% of small lymphocytes associated with a mixed population of prolymphocytes, lymphoblasts, plasma cells, and/or a few to moderate numbers of macrophage, neutrophils, and eosinophils and/or rare individual mast cells
Possible Metastasis	Two to three aggregates of two or three mast cells on at least one slide.
Probable Metastasis	Greater than three foci of aggregated of two to three cells and /or two to five foci of more than three aggregated mast cells on at least one slide.
Certain Metastasis	Obliteration of the lymphoid tissue by mast cells and/or the presence of aggregates, poorly differentiated mast cells with pleomorphism, anisocytosis, anisokayosis, and/or decreased or variable granulation, and/or more than five aggregated of three or more mast cells.

2.4.3 Lymph Node Histology

Finally, it is well-known that normal-size LNs are still at risk of being metastatic and the proportion of cytologically negative, but histologically positive for metastasis may range from 10 to 50% (Ku et al., 2017; Ferrari et al., 2018; Fournier et al., 2018). The high risk of false-negative results of LN cytology makes lymphadenectomy and further histology the gold standard to diagnose LN metastasis (Langenbach et al., 2001; Ku et al., 2017; Ferrari et al., 2018).

Overall, it is well-established that suspected or confirmed metastatic LN must be surgically resected regardless of the histological grade of the primary tumor (Marconato et al., 2018; Grimes et al., 2020).

Weishaar et al. (2014) proposed a classification system to address degrees of histological diagnosis of LN metastasis. Metastatic states (HN2 and HN3) were associated with a poorer prognosis than pre-metastatic LNs (HN1) and non-metastatic LNs (HN0). Table 4 summarizes the histological criteria for Weishaar's LN metastasis classification.

The addition of toluidine blue staining on routine histologic evaluation of LN samples may improve the detection rate of cMCT metastasis (Fournier et al., 2020). However, regardless of the technique, a standardized trimming approach to the LN sample is warranted as it can also influence false-positive/false-

negative rates (Weaver et al., 2010; Weishaar et al., 2014; Kiupel et al., 2019). There are currently no guidelines on how and how many sections should be made for histological evaluation of LN. Studies that describe the section technique are rare. One study performed sections along the long axis at the level of the hilus (Sabattini et al., 2021).

Table 4. Weishaar et al. (2014) classification system for histopathological evaluation of mast cell tumor lymph node metastasis.

Classification	Histopathological Criteria	Interpretation
HN0	None to rare (0-3), scattered, individualized (isolated) mast cells in sinuses (subcapsular, paracortical, or medullary) and/or parenchyma per x400 field (0-3 mast cells per x400 field), or does not meet criteria for any other classification below	Non-metastatic
HN1	Greater than 3 individualized (isolated) mast cells in sinuses or medullary) and/or parenchyma in a minimum of 4 x400 fields (unless otherwise stated, at least 4 x400 fields each, which contain more than 3 mast cells)	Pre-metastatic
HN2	Aggregates (clusters) of mast cells (≥ associated cells) in sinuses (subcapsular, paracortical, or medullary) and/or parenchymal, or sinusoidal sheets of mast cells.	Early metastasis
HN3	Disruption or effacement of normal nodal architecture by discrete foci, nodules, sheets, or overt masses composed of mast cells	Overt metastasis

2.4.4 Non-Selective Lymph Node Dissection

While lymphadenectomy is highly recommended for suspected or confirmed metastatic LN regardless of the histological grade of the cMCT, the role of prophylactic regional LN resection remains unclear (Marconato et al., 2018; Bae et al., 2020; Grimes et al., 2020; Sabattini et al., 2021). As a result of this dilemma, the conflicting results across studies, and the absence of current evidence-based guidelines, a personalized approach based on balancing the risk-benefit considering clinical stage and risk of metastatic spread is frequently recommended (Sabattini et al., 2021).

Historically, the non-selective LN dissection is the surgical sample of the regional anatomic LN to determine whether there is a locoregional metastatic disease in an individual bearing cancer (Liptak et al., 2019). Choosing the RLN for sampling is currently the most used method during the stage and treatment phase of a cMCT (Suami et al., 2013; Figure 8).

Figure 8. The drainage pattern of the lymphatic territories according to the dog's anatomy. (Source: Suomi et al., 2013)

However, modern evidence demonstrated that the locoregional anatomic LN is not necessarily the SLN for that specific anatomic region (Liptak et al., 2019). The possibility of aberrant lymphatic drainage from the tumor and the risk of missing the SLN and consequently misdiagnosing tumor-free LN is the main reason why non-selective LN dissection is not indicated while searching for SLN (Liptak et al., 2019). Other factors affecting non-selective LN effectiveness are the individual variations, the variable number of LN, and the possibility of multiple nodal metastases (Patsikas et al., 2006; Suami et al., 2012; Suami et al., 2013; Bezuidenbut et al., 2013; Skinner et al., 2017). Simultaneous metastasis for several LN has been described for head and neck tumors, with some patients submitted to resection of 4 to 6 LN (Herring et al., 2002; Green et al., 2017).

Lymphadenectomy is an invasive surgical procedure requiring additional intraoperative time, increasing morbidity, and costs (Fournier et al., 2020). For these reasons non-selective LN dissection and radical regional lymphadenectomy have gradually been replaced by new refined methods for imaging and detecting SLN in both humans and animals (Tardelli et al., 2016). Finding and sampling SLN is a less invasive approach, that minimizes anesthesia time, tissue trauma, and postoperative morbidity in humans (Schrenk et al., 2000; Ashikaga et al., 2010). In human oncology, SLN mapping was established as the gold standard in certain malignancies (Worley et al., 2014; Tardelli et al., 2016).

Several techniques have been described for SLN mapping in humans: radiographic lymphography (Cabanas, 1977), computed tomography lymphography (Hayashi et al., 2006), magnetic resonance lymphography (Motomura et al., 2013), contrast-enhanced ultrasound or Lymphosonography (Sever et al., 2009; Moody et al., 2017), single-photon emission computed tomography (Naaman et al., 2016), positron emission tomography (Heusner et al., 2009; Chang et al., 2012), lymphoscintigraphy and intraoperative direct visualization using blue dyes (Niebling et al., 2016) or fluorescent dyes with near-infrared imaging (Wishart et al., 2012). These techniques are efficient for SLN mapping in dogs as well (Worley et al., 2014; Liptak et al., 2019; Randal et al., 2020; Grimes et al., 2020; Ferrari et al., 2021; Fournier et al., 2021; Lapsley et al., 2021).

Most of the current modalities of SLN mapping rely on the injection of a marker drug or substance at the tumor site and tracking the marker to the SLN (Lapsley et al., 2020). Tracking can be performed intraoperatively or preoperatively (Lapsley et al., 2020). The unpredictable pattern of SLN puts the preoperative methods of SLN mapping at an advantage. These methods are usually based on image examinations such as radiographic, CT, or scintigraphy (Lapsley et al., 2020).

Current human recommendations established regional lymphoscintigraphy combined with blue dyes and intraoperative lymphoscintigraphy as the gold-standard method for SLN mapping in human oncologic procedures (Worley et al., 2014; Ferrari et al., 2020).

2.4.5 Intraoperative Blue Dye Mapping

The peritumoral injection of blue dyes is the simplest and most widely used technique for SLN mapping in dogs. The colorimetric nature of the technique allows visualization of the marked SLN without any detection equipment (Beer et al., 2018). Methylene blue, patent blue, and isosulfan blue are the most used blue dye for SLN mapping (Beer et al., 2018). All dyes have in common a weak affinity to albumin, allowing a fast absorption by the lymph vessel (Newman, 2004; Somasundaram et al., 2007; Qiu et al., 2018). As the dye progress, it allows the intraoperative visualization of the blue-colored afferent vessels coursing from the tumor site to the SLN (Liptak et al., 2019). Drainage from the injection site to LN occurs within 5 to 10 minutes (Worley et al., 2014). Finally, both lymphatic vessels and SLN assumes a blue-colored appearance that facilitates tracking its site through the skin or surgically exposed and further removal by the surgeon (Worley et al., 2014; Beer et al., 2018; Figure 9).

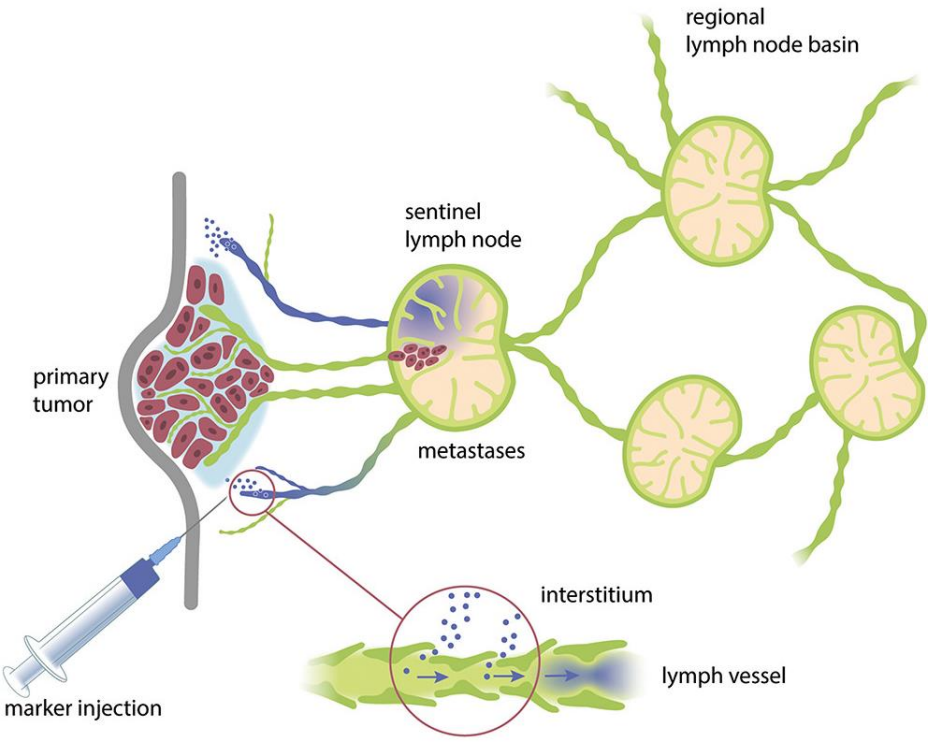

Figure 9. Schematic drawing of a hypothetic lymphatic chain after peritumoral injection of blue dyes. The blue dye drains through the interstitial tissue until reaches the lymphatics and further drains to the sentinel LN. (Adapted from Beer et al., 2018).

Despite the rapid absorption and efficient demarcation of the lymphatic pathways, the identification of the SLN can be difficult and require a wide surgical exposure to track back the afferent lymph vessels leaving the tumor to the LN (Somasundaram et al., 2007). For this reason, there is about 86% of false-negative when using blue dyes as the sole method of SLN mapping (Qiu et al., 2018).

Due to the difficulties to detect the SLN, the blue dye is frequently associated with other techniques, such as radioisotopes (Somasundaram et al., 2007) lymphoscintigraphy, or near-infrared imaging. In humans, SLN detection only by colorimetric methods is inferior (83-85% detection rate) when compared to radio-guides techniques (89.2-94%) or a combination of methods (92-99%) (Kim et al., 2006; Niebling et al., 2016). This combination led to 89% of LNs detected by pre-operative lymphoscintigraphy, 97% by intraoperative gamma probe, and only 77% with intraoperative blue dye (Balogh et al., 2002). Despite, the blue dye colorimetric method having a lower detection rate than radioactive tracers, the combination is still recommended because double-marked SLN are more likely to be the first tier LN than if only radiolabeled (Kang et al., 2010; Niebling et al., 2016).

The use of blue dyes for SLN mapping is cost-effective and simple to implement by an early trained surgeon. The learning curve to getting familiar with the blue dye technique was 22 procedures in women with breast cancer, for example (East et al., 2009).

The main disadvantages of using a blue dye for intraoperative SLN mapping include the difficulty to evaluate surgical margins during the procedure due to the diffuse alteration of the peritumoral tissue to a strong blue color, the systemic absorption of the blue dye that could color tissues distant from the site and interfere with pulse oximetry and the blue color of the skin and mucosa that can persist for months after injection (Newman, 2004; Somasundaram et al., 2007; Qiu et al., 2018). After injection, the blue dye is renal excreted, which can alter the urine color to a greenish-blue (Somasundaram et al., 2007). The discoloration of the tissues is often self-limiting and does not reflect on any harm to the animal. However, despite not being reported in dogs, approximately 0.4% of human patients experience allergic reactions, such as erythema, urticaria,

signs of necrosis, and in very rare cases, local skin necrosis (Hunting et al., 2010; Kang et al., 2010).

Alternatively, a study evaluated the application of hemosiderin derived from autologous blood to stain SLN in 6 dogs. The SLN exhibit a brown color instead of blue color and aided in LN detection and resection without adverse reactions (Pinheiro et al., 2009). Unfortunately, this technique was not evaluated further.

2.4.6 Radiographic Indirect Lymphography

Radiographic lymphography is usually performed in animals for detection and delineation of the thoracic duct before ligation (Radlinsky et al., 2002; Naganobu et al., 2006). In a research context, radiographic lymphography has been used in both dogs and cats to evaluate the local pattern of lymphatic drainage using plain radiographs (Patsikas et al., 1996; Patsikas et al., 1996b; Patsikas et al., 2006; Papadopoulou et al., 2009; Patsikas et al., 2010; Mayer et al., 2013; Brissot et al., 2017). Limitations in veterinary medicine impair the routine application of SLN mapping with nuclear medicine which turns the CT and radiographic indirect lymphography into the main techniques currently studied for SLN mapping in dogs and cats (Liptak et al., 2019).

Radiographic lymphography can be performed either directly or indirectly (Beer et al., 2018). Direct lymphography is the intralymphatic administration of the contrast and is usually performed to assist thoracic duct identification (Skelley et al., 1964; Radlinsky et al., 2002; Naganobu et al., 2006). On the other hand, indirect lymphography allows the evaluation of locoregional lymphatic drainage through absorption of contrast mean injected in the tissues of the periphery of the lymphatics (Patsikas et al., 1996; Patsikas et al., 2006; Brissot et al., 2017). Indirect lymphography is especially useful to the cancer patient since the peritumoral absorption of contrast drains through the afferent lymphatic vessels to the SLN (Wisner et al., 1996; Beer et al., 2018). The intratumoral injection of contrast for indirect lymphography was described, but the risk of cancer cell seeding due to capsular damage is a concern (Brissot et al., 2017).

Both direct and indirect lymphography requires serial radiographs to be taken within minutes to demarcate the lymphatic vessels (Brissot et al., 2017; Mayer et al., 2013). However, the type of contrast agent used may require further radiographs within a day or more to complete LN uptake.

Indirect lymphography can be performed using a hydrosoluble or liposoluble contrast means (Patsikas et al., 1996a; Suga et al., 2003; Suga et al., 2004; Patsikas et al., 2006; Cochran et al., 2008; Tuohy et al., 2009). The indirect lymphography with hydrosoluble contrast is indicated to evaluate the lymphatic drainage through CT scans (Suga et al., 2004; Cabanas, 2000; Soultani et al., 2017; Majeski et al., 2017; Grimes et al., 2017). This technique was studied in a cohort of bitches with mammary tumors. Patients underwent CT scans 1 and 3 minutes after peritumoral injection of 1 ml of iopamidol. Three LN contrast patterns were found: (1) homogeneous with a uniform distribution of contrast; (2) heterogeneous with an unequal distribution of contrast; (3) absence of contrast mean. Bitches whose LNs were homogeneously contrasted did not have metastatic disease (Soultani et al., 2017). A study of indirect lymphography and CT scan in dogs with apocrine gland anal sac adenocarcinoma could find the SLN in 92% of the cases, being 66% ipsilateral and 34% contralateral to the primary tumor (Makeski et al., 2017). The same method was able to detect the SLN in 89% of the dogs with oral cancer (Grimes et al., 2017).

The hydrosoluble contrasts are rarely used for lymphatic evaluation by radiographs, as the contrast is rapidly absorbed into the blood vessels (Pereira et al., 2003). Also, radiographs are unable to detect a small amount of contrast diluted in the tissues (Patsikas et al., 2006). On the other hand, using a liposoluble contrast for indirect lymphography allows the use of radiographs to detect the lymphatic contrast (Cabanas, 2000; Brissot et al., 2017). The techniques involve the peritumoral injection of up to 2.5 ml of lipiodol 24 hours before radiographs. This method is often performed on the day before surgery and radiographs are taken immediately before definitive surgical procedure (Brissot et al., 2017; Liptak et al., 2019). Lipiodol is an injectable, liposoluble iodinate radiographic contrast composed of ethyl esters of fatty acids of poppyseed oil. The contrast remains withheld on the LNs for several weeks to

months, which allows for serial radiographic evaluations (Liebner, 1977; Mayer et al., 2013).

The indirect lymphography with lipiodol can be associated with the injection of blue dyes for intraoperative SLN mapping (Brissot et al., 2017; Liptak et al., 2019). This combination of preoperative and intraoperative SLN mapping was studied in 30 dogs with solid tumors, and there was an 84.6% rate of agreement between them. Indirect lymphography with lipiodol detected the SLN in 96.6% of the dogs (Brissot et al., 2017). Preoperative radiographic indirect lymphography also found more SLN than previously. In a study evaluating the role of indirect lymphography with lipiodol in bitches with mammary tumors, preoperative SLN mapping was able to locate more than one LN in several cases (Patsikas et al., 2006).

Complications of the radiographic lymphography are uncommon and mild. One out of 30 dogs in a study with lipiodol indirect lymphography had mild blepharitis that resolved after topical treatment (Brissot et al., 2017). However, another reported complication was insufficient uptake of contrast by the LN preventing adequate identification of the SLN. The contrast was reinjected due to insufficient uptake in 4 out of 25 dogs in a study (Brissot et al., 2017). Another study using subcutaneous injection of lipiodol in healthy dogs reported a 50% rate of injection-site erythema and a 30% rate of LN swelling (Mayer et al., 2013). These minor complications were reported 14 to 38 days after lipiodol injection, but resolution occurred in 7 to 10 days in all dogs following symptomatic treatment only (Mayer et al., 2013). Asymptomatic pulmonary oil embolization has been reported once (Mayer et al., 2013). A 90.3% rate of minor temporary swelling of healthy feline mammary glands and a 9.7% rate of inflammation was reported after intramammary and subareolar injection of lipiodol (Patsikas et al., 2010). Allergic reactions, pulmonary embolism, or other severe complications have been reported in people but not in small animals so far.

The combined use of preoperative SLN mapping with lipiodol and radiographs with the intraoperative mapping with blue dye is an attractive alternative to other complex SLN mapping techniques, as the application is simple, radiographs are inexpensive, and equipment is widely available in most veterinary facilities (Patsikas et al., 2006; Blackwood et al., 2012; Brissot et al.,

2017; Liptak et al., 2019). Also, the procedure is considered non-invasive and usually does not require sedation or anesthesia (Brissot et al., 2017; Patsikas et al., 2006) The main disadvantage is the 24-hour time interval between contrast injection, lymphatic drainage, and radiographs which require two-stage procedures (Liptak et al., 2019). Also, the high rate of mild complications must be considered.

2.4.7 Computed Tomography Indirect Lymphography

Computed Tomography lymphography (CTL) was made to accurately display the anatomical location of the SLN and surrounding tissues (Suga et al., 2003; Suga et al., 2003b; Papadopoulou et al., 2009; Patsikas et al., 2010; Lee et al., 2013; Grimes et al., 2017). CTL allows the visualization of SLN afferent lymphatic vessels and thus differentiates between SLN and other distant LNs without radiographic superimposition (Hayashi et al., 2006; Kim et al., 2015)

The main characteristics of the technique are similar to radiographic lymphography (Suga et al., 2003; Suga et al., 2004; Hayashi et al., 2006; Papadopoulou et al., 2009; Patsikas et al., 2010; Lim et al., 2012). The contrast, however, is hydrosoluble and is rapidly absorbed from the tissue to the lymph vessel within minutes after peritumoral injection. Advantages of CTL over radiographic IL are the ability to visualize an entire area at the same time and the ability to do 3D-reconstructions (Mayer et al., 2013). On the other hand, CTL requires deep sedation or anesthesia, increased cost, and the possible adverse reaction to iodinated contrast agents (Mayer et al., 2013; Rossi et al., 2018).

In people with gastric and breast cancer CTL had a 100% and 95.8% rate of SLN detection when used as the sole SLN mapping strategy (Motomura et al., 2013; Lee et al., 2013; Mokhtar et al., 2016). Only a few studies in dogs successfully applied CTL in a clinical setting. Mammary cancer (Soultani et al., 2016), apocrine gland anal sac adenocarcinoma (Majeski et al., 2017), and several site tumors (Rossi et al., 2007; Grimes et al., 2017) have been investigated. All studies used pre-contrast scanning followed by sequential post-contrasted images. Scanning started 1 minute after contrast agent injection. Visualization of the SLN was made at the soft tissue windows. The contrasted lymphatic vessels could be visualized and followed to 1 or more SLN (Rossi et

al., 2007; Soultani et al., 2016; Majeski et al., 2017; Grimes et al., 2017). A pilot study evaluating CTL in 18 dogs with head tumors identified the SLN in 16 patients (89%). Two dogs (13%) had more than 1 SLN (Grimes et al., 2017).

A study evaluating CTL established three different patterns of SLN opacification: (1) The uniform uptake of contrast agent within the SLN leading to a homogeneous enhancement pattern; (2) Unequal opacification, including a single area or only the periphery of the SLN leading to a heterogeneous contrast pattern; (3) the absence of contrast uptake by the SLN (Soultani et al., 2016). These patterns of SLN contrast were associated with the presence or absence of metastasis. The homogeneous pattern was associated with the absence of metastasis while the heterogeneous contrasted SLN was usually metastatic (Soultani et al., 2016).

The absence of contrast uptake by the SLN does not mean there is no SLN or no metastatic disease in progress. Two out of 33 dogs in a CTL study had no contrasted SLN, but afferent lymph vessels were contrasted and both LNs were histologically metastatic. The authors hypothesized that a metastatic disease caused the interruption of continuous lymph flow (Soultani et al., 2016). Also, a low Houndsfield unit in the center of the SLN had high sensitivity and specificity to detect metastatic SLN (Soultani et al., 2016).

The CTL has been used to access the lymphatic drainage of several tumors and locations, such as breast (Suga et al., 2003; Papadopoulou et al., 2009; Patsikas et al., 2010), gastric (Lim et al., 2012; Kim et al., 2015;), esophageal (Hayashi et al., 2006), lung (Suga et al., 2004) in people with excellent results. In dogs and cats, there are studies evaluating normal lymphatic drainage of mammary glands (Papadopoulou et al., 2009; Patsikas et al., 2010) and a wide study evaluating several cancer types (Brissot et al., 2017).

Finally, the main advantages of CTL are the reliable detection of SLN and the ability to predict nodal metastatic disease (Soultani et al., 2016). The CTL is also safe and sensitive in the detection of SLN in several tumors (Beer et al., 2018). The main disadvantage of the CTL is the absence of intraoperative assistance to locate de SLN, which often requires the association with intraoperative blue dyes or lymphoscintigraphic mapping (Lee et al., 2013; Beer et al., 2018). The use of skin marks with a pen or needles was suggested as a

simple technique to surpass this difficulty in dogs (Suga et al., 2003; Suga et al., 2003b).

2.4.8 Other Techniques for Sentinel Lymph Node Mapping

The most common technique for intraoperative SLN mapping in humans is the peritumoral injection of radioactive isotopes and blue dye (Beer et al., 2018, Qiu et al., 2018). The use of radioisotopes is rarely available for veterinary patients, as the technique demands adequate facilities and specialized equipment for nuclear medicine with a high cost and generating radioactive waste (Liptak et al., 2019).

Magnetic resonance lymphography (MRL) uses the same principle of indirect lymphography either by radiographs or CT scans (Beet et al., 2017). A 3D reconstruction of the contrasted SLN and respective afferent lymphatics can provide detailed anatomic images of the draining lymphatics (Suga et al., 2004; Mayer et al., 2012; Turkbey et al., 2015). Superparamagnetic iron oxide particles, a contrast agent specific for MR use, had high sensitivity and specificity in predicting metastasis of the SLN in humans (Motomura et al., 2011). Despite some experimental MRL in dogs (Suga et al., 2004; Mayer et al., 2012; Turkbey et al., 2015), there is no current investigation on the use of MRL in a clinical setting.

Contrast-enhanced ultrasound (CEUS) has been suggested as an interesting method to detect SLN in both humans and animals (Beer et al., 2018; Fournier et al., 2020). The lymphosonography is a non-ionizing and non-invasive technique with a safe and rapid clearance of contrast associated with a low cost and does not require anesthesia (Wang et al., 2010; Seiler et al., 2013; Moody et al., 2017; Fournier et al., 2020). The diffusion of ultrasound contrast is real-time and allows a detailed view of lymphatic vessels and LN with minimal spillage to second-tier LN (Wisner et al., 2003; Goldberg et al., 2005; Wang et al., 2010; Xie et al., 2015; Liu et al., 2019). Microbubbles for CEUS seem to have restricted drainage to the first SLN of the basin, with a minimal to no spill-over of contrast to second-tier LN (Wisner et al., 2003; Gelb et al., 2010; Wang et al., 2010). The pattern of SLN enhancement has been recently associated with metastasis status, however, with low sensitivity and specificity (Fournier et al., 2020).

To allow visualization of the afferent lymphatic vessels, small gas-filled microbubbles in a lipid shell are injected into the peritumoral tumor (Goldberg et al., 2005; Lurie et al., 2006; Wang et al., 2010). As the lipidic contrast mean has a strong affinity to the lymphatics it enters the vessel in seconds (Goldberg et al., 2005) and rapidly drains to the SLN within minutes (Lurie et al., 2006; Goldberg et al., 2005; Gelb et al., 2010). Using a doppler or grey-scale ultrasound, the contrast starts oscillating reflecting a signal several times higher than that of body tissue (Blomley et al., 2001). The use of CEUS allowed the detection of small SLN that initially were not visible in standard B-mode ultrasound in a study (Fournier et al., 2020).

The CEUS has been used solely in preclinical research in pigs (Goldberg et al., 2004; Goldberg et al., 2005), dogs (Wisner et al., 2003; Goldberg et al., 2005; Lurie et al., 2006; Gelb et al., 2010; Wang et al., 2010) and rabbits (Goldberg et al., 2005). In humans, CEUS studies reported a rate of SLN detection of 87% to 97% (Sever et al., 2009; Sever et al., 2011; Cox et al., 2013; Esfehani et al., 2015; Xie et al., 2015) when comparing with blue dye and lymphoscintigraphy. In healthy dogs, a 91.3% detection rate was found when comparing blue dye (Wang et al., 2010). Dogs with cMCT subjected to CEUS SLN mapping had a 95.2% of detection rate (Fournier et al., 2020). CEUS could detect SLN in 8 out of 10 dogs bearing head and neck tumors when compared with lymphoscintigraphy (Lurie et al., 2006). The main challenge of using CEUS for SLN mapping is the necessity of selecting the lymphatic basins to be evaluated before scanning and the operator-dependent variables (Stefanello et al., 2009; Book et al., 2011; Horta et al., 2018; Pecceu et al., 2019).

The standard of care for SLN mapping in humans is the use of radioactive tracers (Niebling et al., 2016). Technetium-99m (Tc-99m) labeled colloids are the most used radiotracer (Wawroschek et al., 2003; Nwogu et al., 2002; Pereira et al., 2008; Worley et al., 2014). SLN mapping is obtained through a preoperative scan that detects the accumulation of radioactivity on LN after draining from the peritumoral injection site (Mariani et al., 2001). A hand-held gamma probe can be used intraoperatively to find radiolabeled SLN. However, lymphoscintigraphy cannot predict metastasis (Beer et al., 2018).

A preliminary study evaluating scintigraphy SLN mapping allowed to find 35 SLN in which 34 were detected both pre and intraoperative while only 27 were

identified by the blue dye technique (Balogh et al., 2002). A combination of radioisotopes and methylene blue detected 19 SLN in 19 dogs, but a gamma probe could detect an additional SLN than preoperative lymphoscintigraphy and blue dye (Worley et al., 2014). Scintigraphy could also detect SLN in studies evaluating prostate, mammary, pulmonary, and thoracic drainage in healthy dogs (Wawroschek et al., 2003; Nwogu et al., 2002; Pereira et al., 2008; Tuohy et al., 2014).

The main barrier to the widespread use of radio-guided SLN mapping is the restricted use of radioactive materials and environmental issues related to radiopharmaceuticals disposal (Mariani et al., 2001; Worley et al., 2014; Beer et al., 2018; Liptak et al., 2019).

Near-infrared imaging uses optical image-guided surgery to provide real-time detection of lymphatic vessels and SLN (Troyan et al., 2009; Wishart et al., 2012). The wavelength of the near-infrared light spectrum is 700 to 900 nm and invisible to human eyes (Schaafsma et al., 2011). The near-infrared system emits an infrared spectrum light that is absorbed by a fluorescent agent. The light is detected by a near-infrared camera that shows a real-time video on a screen (Schaafsma et al., 2011; Sevick-Muraca et al., 2012). The near-infrared imaging is useful for transcutaneous detection of SLN as the light of the near-infrared spectrum can penetrate a few centimeters but is not adequately absorbed by the tissue (Troyan et al., 2009; Hirche et al., 2010; Schaafsma et al., 2011; Sevick-Muraca et al., 2012). The most often fluorescent agent is the Indocyanine Green (Schaafsma et al., 2011).

In humans, near-infrared imaging with indocyanine green is usually used to detect SLN in breast cancer and melanoma (Hirche et al. 2010; Fujisawa et al., 2012; Wishart et al., 2012; Sugie et al., 2016). The detection rate seems to be comparable to that of lymphoscintigraphy, however, the faster drainage of indocyanine green to second-tier LNs is hypothesized as a cause of a slightly higher rate (Fujisawa et al., 2012; Wishart et al., 2012; Sugie et al., 2016). On the other hand, as near-infrared imaging allows visualization of afferent lymphatic vessels it can easily identify the first tier SLN of the basin (Troyan et al., 2009; Wishart et al., 2012). The near-infrared imaging system can also be applied in minimally invasive and robotic surgery (Holloway et al., 2012; Liss et al., 2014).

Tumor-specific targeting dyes have been developed for intravenous injection. These dyes aid in en bloc curative-intent resection as it demarcates tumor margins (Eward et al., 2013; Holt et al., 2015; Fidel et al., 2015; Mohs et al., 2015; Cabon et al., 2016). The transcutaneous visualization of fluorescent dye can make a massive wide surgical resection unnecessary in cases of cutaneous superficial tumors (Hirche et al., 2010). The technique has been tested in dogs with naturally occurring cancer as a model for human trials. Intradermal (Wells et al., 2006), submucosal gastric (Kim et al., 2015; Kong et al., 2015) and intraprostatic injection (Liss et al., 2014) of indocyanine green have been tested for SLN mapping in dogs.

Experimental studies of safe and feasibility of near-infrared in dogs bearing soft tissue sarcomas (Eward et al., 2013; Holt et al., 2015; Fidel et al., 2015; Cabon et al., 2016; Bartholf et al., 2016), MCT (Fidel et al., 2015; Bartholf et al., 2016), bladder carcinoma (Knapp et al., 2007; Mohs et al., 2015), and others types of cancer (Fidel et al., 2015) has been done. These studies aimed at SLN mapping (Knapp et al., 2007; Liss et al., 2014; Kim et al., 2015; Kong et al., 2015) and differentiating malignant tissues from benign ones (Eward et al., 2013; Holt et al., 2015; Fidel et al., 2015; Mohs et al., 2015; Bartholf et al., 2016; Cabon et al., 2016;). In cats, a study with intraoperative near-infrared finds it useful for en bloc tumor resection (Wenk et al., 2013). Veterinary studies of intravenous application of indocyanine green for detection of SLN and mammary tumors (Reynolds et al., 1999) and hepatocellular carcinoma (Iida et al., 2013).

Limitations of the near-infrared techniques include the low-depth penetration of the light, the short time of tracer uptake in the lymphatics, and the requirement of specific equipment (Schaafsma et al., 2011; Kim et al., 2015; Beer et al., 2018). In both humans (Hirche et al., 2010; Wishart et al., 2012; Jewell et al., 2014; 91) and dogs (Wenk et al., 2013; Cabon et al., 2016) there were no complications associated with the techniques.

2.4.9 Problems in Sentinel Lymph Node Mapping

In addition to the previously mentioned problems on detecting the SLN and the limitations of the several techniques available for mapping, the pathophysiology of the lymphatic metastasis may also be responsible for false negatives. After reaching the lymphatic vessels and LNs, the cancer cells can

form niches of metastatic disease that once reaching a certain size can obstruct the already abnormal lymph flow. The blockage of the lymph flow causes a deviation through the formation of collateral new lymphatic vessels draining to different LNs (Proulx et al., 2013).

The development of newly formed lymphatics is caused by the increased intranodal pressure in the blocked LN that stimulates drainage to LNs with low intranodal pressure (Nathanson et al., 2011). In humans, this concept is seen clinically when there is a rerouting of the lymph flow to other LNs in the presence of SLN metastasis (Leijte et al., 2009; Nathanson et al., 2011). Previously surgery or LN resection can also cause these changes (Blum et al., 2013).

The phenomenon of lymphatic rerouting is important clinically as it can mislead the results of SLN mapping techniques, causing false-negative results (Figure 10). In other words, LNs with metastatic niches does not receive draining dye or contrast agents because there are obstructed by metastasis while a normal LN that received the rerouted lymphatic vessel may be falsely considered the sentinel (Proulx et al., 2012b). Later in the course of the disease the LN that drained the rerouted flow may be colonized by metastatic cells as well (Karaman et al., 2014).

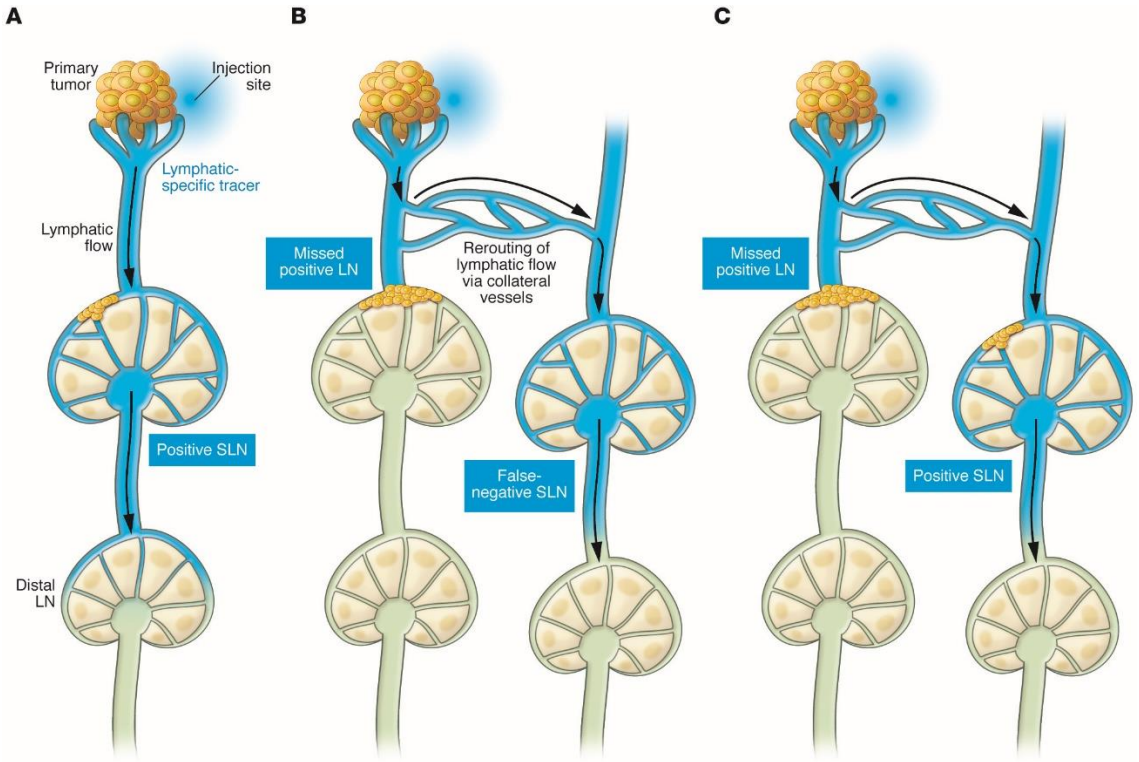

Figure 10. Possible results after peritumoral injection of a tracer that is taken by the lymphatic vessels. (A) The tracer enters the lymphatic vessels and is transported by the collecting lymphatic vessels to the lymph node that is correctly identified as the sentinel lymph node (SLN) and may or may not harbor metastatic cancer cells (i.e., a true SLN/true-positive for metastasis). (B) The tracer enters the lymphatic vessels and is transported but cannot mark the lymph node due to a large metastatic lesion causing an obstruction. In this scenario, the SLN was missed but is positive for metastasis (i.e., a true SLN/false-negative for metastasis). Newly formed lymphatic vessels cause a reroute pathway that led to lymph draining to another lymph node that was falsely identified as SLN (i.e., a false SLN/false-negative for metastasis). (C) The previously negative lymph node that received the rerouted lymph flow may also contain metastatic disease as well (i.e., True positive SLN was missed [false-negative] but alternative SLN was also positive [true-positive]). (Source: Adapted from Karaman et al., 2014).

2.5. Lymphadenectomy

In addition to diagnosis and prognosis, the surgical resection of metastatic SLN is also therapeutical, as it may decrease tumor burden before adjuvant therapy (Wright & Oblak 2016; Hume et al., 2011). LN resection and histological status have been associated with an increased progression-free survival time (Hume et al., 2011).

Lymphadenectomy of LN excisional biopsy is the gold-standard method to detect locoregional metastatic disease (Wright & Oblak 2016; Marconato et al.,

2018; Grimes et al., 2020). Lymphadenectomy can either be prophylactic, when there is no evidence of nodal involvement or therapeutic to treat a known malignancy (Conzo et al., 2014; Marconato et al., 2018; Gambardella et al., 2019; Mendez et al., 2020; Sabattini et al., 2021). Prophylactic lymphadenectomy remains controversial in grade 1 or low-grade cMCT without clinical features of aggressiveness or cytologic negative LN (Sabattini et al., 2021). A watch-and-wait strategy has been proposed, but the concern around a possible higher rate of undetected or late nodal metastasis and the fact that LN is the main metastatic site of cMCT make prophylactic lymphadenectomy a more reasonable option (Ferrari et al., 2018; Sabattini et al., 2021).

2.5.1 Surgical Technique for Lymph Node Resection

Most available literature about lymphadenectomy in dogs and cats is superficial and a standard surgical approach to specific LNs is rarely found. Furthermore, anatomical descriptions of the LN location and sites are resumed to the books or antique cadaveric reports.

The indications for lymphadenectomy are based on the lymphatic territories (Figure 11) and the results of SLN techniques. The surgical technique to remove LNs includes blunt and sharp dissection of the surrounding connective tissue outside the LN capsule. The capsule should be left intact. Small or delicate LNs can be dissected using cotton tip swabs. To avoid losing LN location and aid on dissection, thumb forceps, Allis tissue forceps, or even stay sutures can be used to grip the perinodal tissue. The vascular hilus of the LN should be ligated using 4-0 or 3-0 absorbable monofilament suture or coagulated using electrocautery (Wright & Oblak et al., 2016).

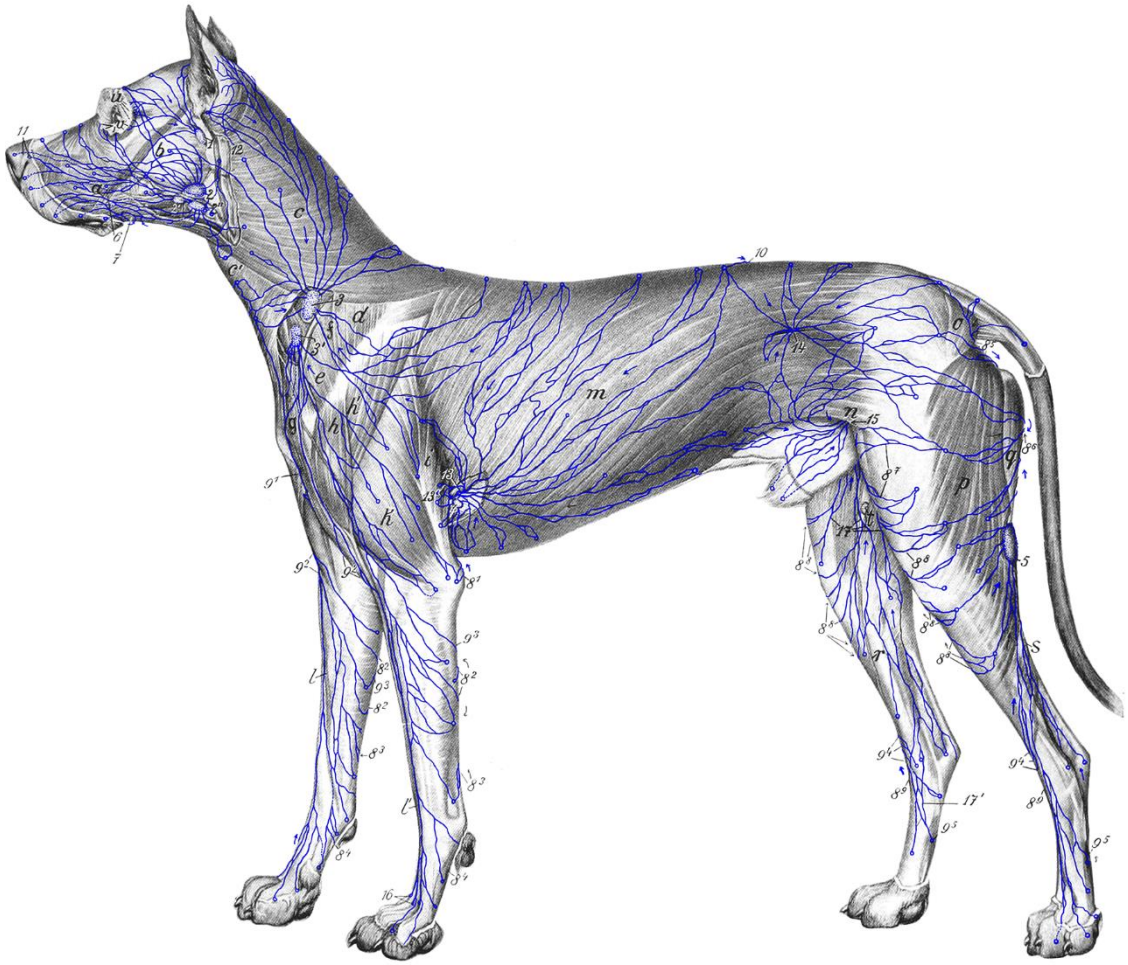

Figure 11. Lymphocenters and lymphatic vessels of canine skin *1* parotid lymph node; *2*, *2′*, *2″* mandibular lymph nodes; *3*, *3′* superficial cervical lymph nodes; *4* accessory axillary lymph node; *5* popliteal lymph node; *6* lymph vessels from the buccal gingiva of the maxillary teeth; *7* lymph vessels from the buccal gingiva of the mandibular teeth; 8^1-8^9 lymph vessels that go to the medial side of the leg (8^5-8^8 are lymph vessels that run to the superficial inguinal lymph nodes; 8^2 and 8^2, 8^3 and 8^3, 8^4 and 8^4 are the same lymph vessels); 9^1 lymph vessels from the skin of the ventral chest; 9^2-9^5 lymph vessels that go to the lateral side of the leg; 9^2 and 9^2, 9^3 and 9^3, 9^4 and 9^4, 9^5 and 9^5 are the same lymph vessels; *10* lymph vessel that crosses the median plane; *11* lymph vessels of the external nose; *12* lymph vessel that runs deep to the medial retropharyngeal lymph node; *13*, *13′* lymph vessels running to the axillary lymph node; *14* lymph vessels running to the medial iliac lymph node; *15* lymph vessels opening into the superficial inguinal lymph nodes; *16* lymph vessels passing from the palmar to the dorsal side; *17*, *17′* lymph vessels running to the superficial inguinal lymph nodes. (Adapted from the translated version of Dr. Hermann Baum's article of 1918 by Dr. Monique Mayer and colleagues)

2.5.2 Mammary Lymphatic Basin

The mammary glands harbor a wide variable lymphatic drainage, with several studies reporting drainage to LNs other than the superficial inguinal or

the axillary LN. The cranial and caudal thoracic glands usually drain to the ipsilateral axillary LN, but simultaneous drainage to the sternal LN is rarely reported (Graham et al., 1999). The third mammary gland often drains to the ipsilateral axillary and superficial inguinal LN at the same time, however, in some cases it can drain only to the axillary or, rarely, only to the inguinal (Graham et al., 1999; Collivignarelli et al., 2021; Figure 12). Drainage from the third mammary gland to the medial iliac LN has been reported as well (Graham et al., 1999). One study reported the drainage of the third mammary gland to the contralateral axillary LN (Collivignarelli et al., 2021). The fourth and fifth mammary glands drain to the ipsilateral superficial inguinal LN. Simultaneous drainage of the fourth gland to the ipsilateral axillary LN is rarely seen. Drainage of the fifth gland to the popliteal LN or those located at the medial aspect of the thigh is rarely seen (Graham et al., 1999). Both fourth and fifth glands can drain to the medial iliac LN when neoplastic (Collivignarelli et al., 2021).

Abnormal drainage to the contralateral axillary LN has been reported in the presence of neoplasms (Pereira et al., 2003; Pereira et al., 2008; Collivignarelli et al., 2021). According to a recent consensus, the axillary LN must be resected in the presence of a malignant mammary tumor at the first, second, and third mammary glands (Cassali et al., 2020). The inguinal LN must be extirpated when the tumor is located at the third, fourth, and fifth mammary glands (Cassali et al., 2020).

A single superficial inguinal LN is the most seen distribution of this basin, however, two or more may be seen in a few cases (Mayer et al., 2010; Bezuidenhout, 2013). The inguinal LN is frequently found deep at the fifth mammary gland in the female and at the level of the penile bulb in the male (Bezuidenhout, 2013).

The inguinal LN is usually removed along with the fifth mammary gland due to its intimate location close to the gland (Cassali et al., 2020). However, when a mastectomy is not planned, uni- or bilateral inguinal LN can be removed through a single midline incision or unilaterally by a lateral incision but may require an extensive dissection if not enlarged (Pierini et al., 2020).

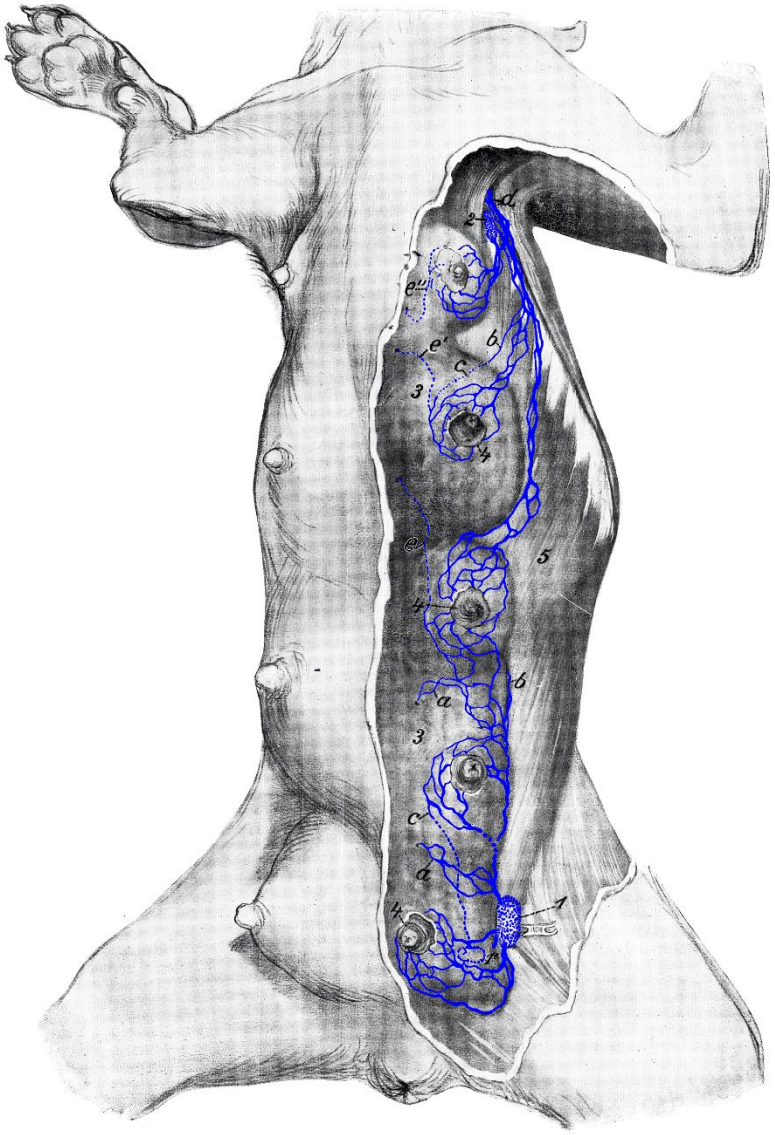

Figure 12. Lymphocenter and lymphatic vessels of the mammary gland. (Adapted from the translated version of Dr. Hermann Baum's article of 1918 by Dr. Monique Mayer and colleagues).

2.5.3 Head and Neck Lymphatic Basin

The mandibular LNs are the easiest peripheral LN to palpate and remove (Wright & Oblak et al., 2016). It receives drainage from the eyelids, skin of the calvarium, tongue, pharynx, oral cavity, and temporomandibular joint (Dyce et al., 2009; Evans et al., 2013).

On the other hand, retropharyngeal LNs cannot be readily palpated and are one of the most challenging RLNs to identify and remove during surgery (Wright & Oblak et al., 2016). The retropharyngeal LNs drain the tongue, oral

cavity walls, the nasal and pharyngeal tissues, salivary glands, external ear, larynx, esophagus, and deep nasal cavity (Dyce et al., 2009; Evans et al., 2013). The medial retropharyngeal LN is also the collecting center for the head as it also receives drainage from the lateral retropharyngeal, parotid, and mandibular LNs as well (Dyce et al., 2009; Evans et al., 2013). This central location on the lymphatic pathway increases the importance of staging the retropharyngeal LN in patients with head and neck malignancies (Wainbert et al., 2018; Figures 13 and 14).

The parotid LN receives drainage from the dorsal head, including the skin, the bones of the dorsal aspect of the skull, orbital content, and masticatory muscles (Smith et al., 2002). The parotid LN is not usually affected by metastatic disease in dogs (Smith et al., 2002).

Buccal lymph was described to be present in about 9% of the dogs in a cadaveric study. Furthermore, its location was widely variable: rostral, medial, or caudodorsal to the facial vein at the lateral aspect of the maxilla just dorsal to the zygomatic muscle and rostral to the masseter muscle at the level where the superior labial vein drains to the facial vein. The buccal node was bilaterally in about half of the cases where it was present (Casteleyn et al., 2008).

The head and neck drainage is known to have a lymphatic crossover in the oropharynx that makes the lymphatic drainage and consequently metastasis patterns unpredictable (Lurie et al., 2006; Tuohy et al., 2009). Removal of a single LN can easily underestimate the actual LN status of a patient (Lurie et al., 2006; Tuohy et al., 2009).

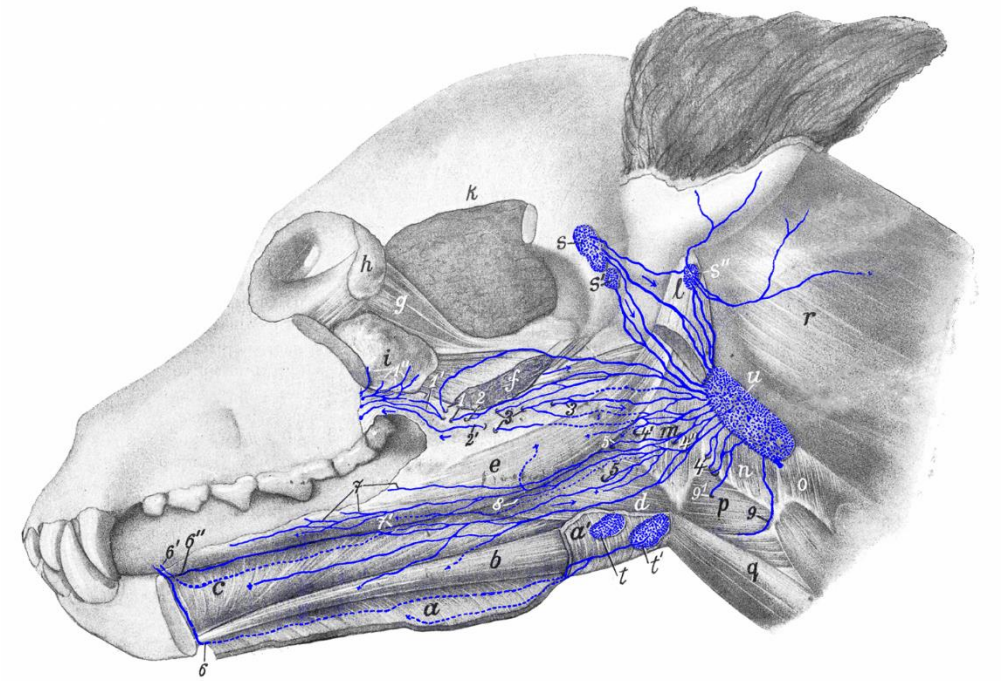

Figure 13. Lymphosomes and lymphatic vessels of the head and cranial neck. *Legend: s*, *s'* parotid lymph nodes; *s"* lateral retropharyngeal lymph node; *t, t'* mandibular lymph nodes; *u* medial retropharyngeal lymph node. *1*, *1'* lymph vessels from hard palate and soft palate; *1"* lymph vessels of the zygomatic gland; *2*, *2'* lymph vessels from the soft palate or *2'* lymph vessel from the fold surrounding the tonsillar sinus; *3*, *3* lymph vessels from the tonsil; *4*, *4'*, *4"* lymph vessels from the soft palate, the tonsil, the base of the tongue and from the mucous membrane of the cavity of the pharynx; *5*, *5* lymph vessels from the tongue; *6*, *6'*, *6"* lymph vessels of the tip of the tongue; *7*, *7'* and *8* lymph vessels of the body of the tongue; *9*, *9'* lymph vessels from the larynx. (Adapted from the translated version of Dr. Hermann Baum's article of 1918 by Dr. Monique Mayer and colleagues).

The resection of the LN of the cranial aspect of the neck is usually performed through a unilateral approach or a single ventral midline incision (Green et al., 2017). A unilateral approach was described first and required an incision extending from the rostral aspect of the vertical ear canal to the external jugular vein bifurcation (Smith et al., 2002). The unilateral technique allows dissection of multiple LNs but requires extensive dissection and does not allow resection of the contralateral nodes (Smith et al., 2002). Furthermore, the location and possible bilateral incisions certainly interfere with surgical planes for tumor resection and the possibilities for surgical reconstruction of the primary defect (Smith et al., 2002; Green et al., 2017).

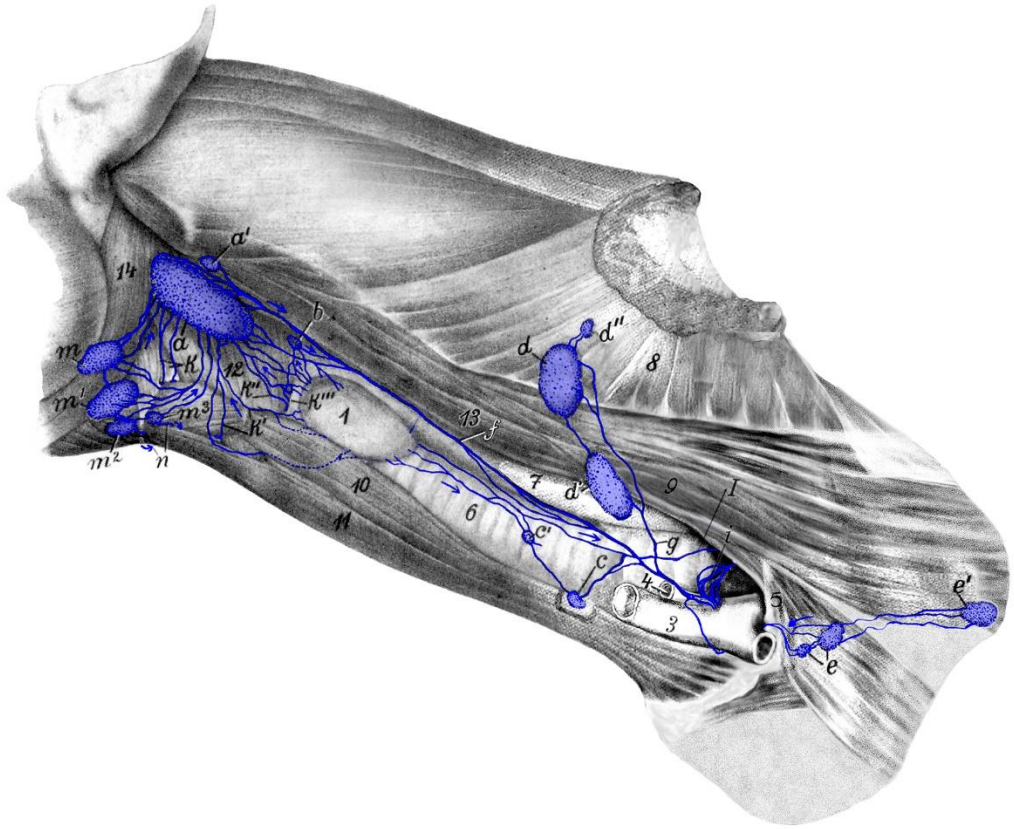

Figure 14. Lymphossomes and lymphatic vessels of the neck. *a*, *a'* medial retropharyngeal lymph nodes; *b* cranial cervical lymph node; *c*, *c'* caudal cervical lymph nodes; *d*, *d'*, *d"* superficial cervical lymph nodes; *e* axillary lymph node; *e'* accessory axillary lymph node; *f* left tracheal duct; *i* thoracic duct with its terminal branches; *k*, *k'*, *k"*, *k"'* lymph vessels from the larynx; *l* lymph vessel opening into a cranial mediastinal lymph node; *m*, m^1, m^2, m^3 mandibular lymph nodes (Adapted from the translated version of Dr. Hermann Baum's article of 1983 by Dr. Monique Mayer and colleagues).

On the other hand, a single ventral midline incision is described as suitable for accessing both mandibular and retropharyngeal LNs bilaterally with considerably less dissection (Green et al., 2017). For this approach, the patient is positioned in dorsal recumbency, and the head is extended to expose the area ventral to the mandible to the thoracic inlet. After surgically preparing the skin to provide an adequate area, an incision is performed through the skin and platysma muscle at the level of the caudal third of the mandible and the larynx. The mandibular LN can be palpated along the caudal aspect of the mandible while the retropharyngeal LN requires retracting the mandibular salivary gland laterally to be visible. Blunt dissection with eventual electrocautery is adequate for isolating and resecting both LNs. The same procedure can be performed

bilaterally through the same skin incision if required Care must be taken to avoid damaging the facial vein and the structures adjacent to the retropharyngeal node especially with an extensive dissection is performed (Green et al., 2017). The parotid LN cannot be accessed by this single midline incision (Green et al., 2017). A Rummel tourniquet can be applied to the carotid arteries through this approach before primary tumor resection to reduce bleeding if required (Green et al., 2017).

A prospective randomized ex vivo trial concluded that the single midline incision was preferred for veterinarians with advanced surgical training for retropharyngeal LN dissection and allowed a significantly smaller incision than the lateral approach performed bilaterally (Wainberg et al., 2018).

2.5.4 Thoracic Lymphatic Basin

In normal dogs, the cranial mediastinal LNs can be found between the right jugular vein and the cranial vena cava, between the brachiocephalic artery and the cranial vena cava, and between the brachiocephalic artery and left subclavian artery (Kayanuma et al., 2020; Figure 15). Normal mediastinal LN size usually ranges from less than 1 mm to 3 mm and may vary in number from 1 to 9 being 3, 4, and 5 the most found in dogs. Like most thoracic LNs, the mediastinal LN can only be seen if the overlying fat and the pleural tissue were removed from covering the great vessels (Bezuidenhout, 2013).

The sternal LNs are part of the ventral thoracic lymphatic basin (Figure 15). There is a right and left sternal LN, but variable numbers are described. The nodes are located at the dorsal aspect of the sternum, medial to the second costal cartilage, and cranioventral to the internal thoracic vessels (Smith et al., 2012; Bezuidenhout, 2013; Iwasaki et al., 2016; Stehlík et al., 2020). The ventral thoracic lymphatic center drains the sternum, ribs, the thymus, and other viscera such as the muscles, peritoneal and pelvic cavity, and the mammary glands (Patsikas et al., 2006; Bezuidenhout, 2013; Iwasaki et al., 2016; Iwasaki et al., 2018; Stehlík et al., 2020).

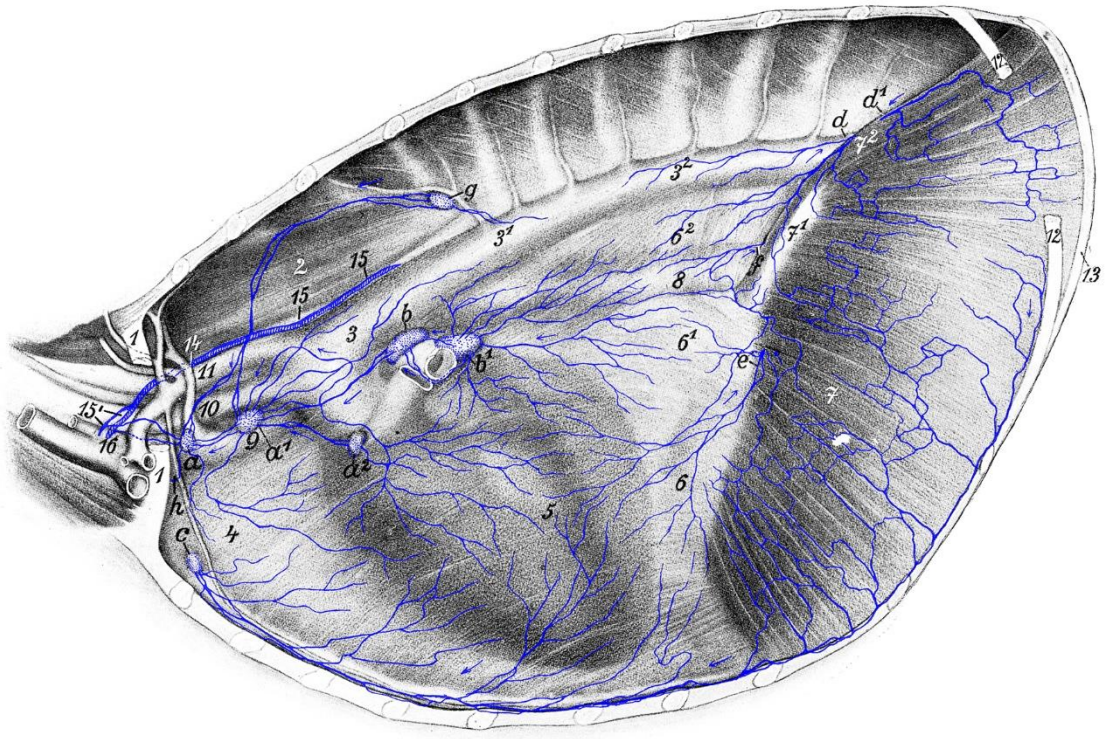

Figure 15. Lymphatic vessels e lymph nodes of the thoracic cavity. *a*, *a*[1], *a*[2] cranial mediastinal lymph nodes; *b* left tracheobronchial lymph node; *b'* middle tracheobronchial lymph node; *c* sternal lymph node; *d*, *d*[1] lymph vessels that run to the cranial lumbar aortic lymph node; *e* lymph vessels that enter the abdominal cavity through the diaphragm and open into splenic lymph nodes, gastric lymph node, left hepatic lymph node or the cranial lumbar aortic lymph node; *f* lymph vessel entering the abdominal cavity with the esophagus; *g* intercostal lymph node; *h* one efferent vessel running to the right side. (Adapted from the translated version of Dr. Hermann Baum's article of 1918 by Dr. Monique Mayer and colleagues)

The tracheobronchial LNs are usually triple and named right, left, and middle nodes (Kayanuma et al., 2020; Figures 16 and 17). Despite most dogs most commonly having all three tracheobronchial nodes, some dogs may have only two, one, or none (Kayanuma et al., 2020). The left and the right tracheobronchial LN are located at the dorsal left and cranial right side of the trachea respectively, while the middle node is located immediately at the tracheal bifurcation (Kayanuma et al., 2020).

The aortic thoracic LN is not commonly found in dogs, with only 12 out of 100 dogs having this LN found in a CT study (Kayanuma et al., 2020). When present, the aortic thoracic LN is located at the end of the fourth to seventh

intercostal space close to the vertebra and can be unilateral or less commonly bilateral (Kayanuma et al., 2020).

In a canine ex vivo study using SLN mapping techniques, there was no lobar, segmental, or subsegmental LN in the lung (Tuohy et al, 2014). Hilar and pulmonary LNs are not consistently present in dogs, and, when present, frequently occur unilaterally only (Bezuidenhout, 2013).

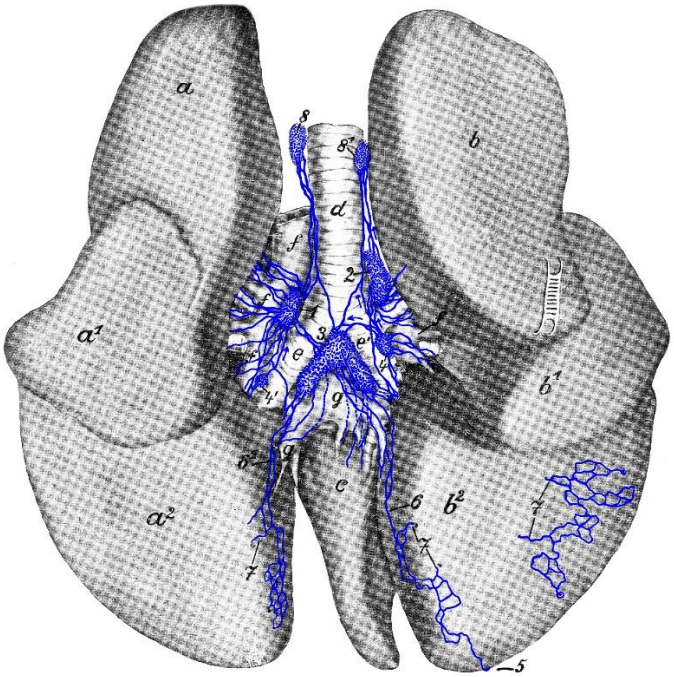

Figure 16. Lymph nodes and lymphatic vessels of the lungs and bronchial tree. Dorsal View. *1* left tracheobronchial lymph node; *2* right tracheobronchial lymph node; *3* middle tracheobronchial lymph node; *4, 4′* pulmonary lymph nodes; *5* subserous lymph vessel; *6, 6¹* subserous lymph vessels running in the first part of the pulmonary ligament; *7, 7, 7* subserous lymph vessels, which start to run deep at this location; *8* left and *8¹* right mediastinal lymph node. (Adapted from the translated version of Dr. Hermann Baum's article of 1918 by Dr. Monique Mayer and colleagues).

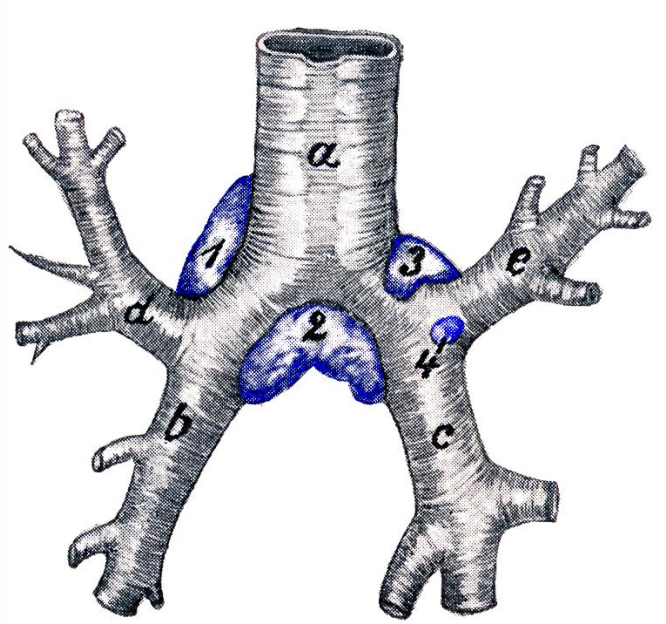

Figure 17. Lymph nodes of the bronchi. *a* end of the trachea; *b* *l*eft and *c* right main bronchus; *d* left and *e* right cranial bronchus. *1* left tracheobronchial lymph node; *2* middle tracheobronchial lymph node; *3* right tracheobronchial lymph node; *4* pulmonary lymph node. (Adapted from the translated version of Dr. Hermann Baum's article of 1918 by Dr. Monique Mayer and colleagues)

2.5.5 Forelimb Lymphatic Basin

The axillary LN drains the thoracic and abdominal mammary gland, the thoracic wall, the cranial aspect of the abdominal wall, and the median aspect of the forelimb (Patsikas et al., 1996; Patsikas, 1996b; Patsikas et al., 2006; Bezuidenhout, 2013). An accessory axillary LN may be present in some dogs, but it is considerably smaller than the actual axillary node (Bezuidenhout 2013; Figure 18A). Unless considerably enlarged, the axillary LN is difficult to palpate due to its location deep in the axilla and surrounded by the bulky muscles of the thoracic limb (Rehnblom et al., 2022; Figure 18B).

The axillary LN can be surgically excised through an incision at the axillary region with the animal in dorsal recumbency. The forelimb can be retracted cranially to improve visualization. The depression at the intersection of the pectoralis profundus and the latissimus dorsi muscle can be palpated and an incision made at this region in a cranial-caudal orientation. The caudal border of the humerus and the second rib are the landmarks for the cranial and caudal end of the incision, respectively. The subcutaneous is sharp and/or blunt dissected further through the pectoralis profundus and latissimus dorsi border. Dissection

can continue cranio-dorsal at the caudal axillary region taking care to identify and avoid inadvertent damage to nerves and vascular structures. At this point, an axillary LN should be seen, but the brachial vein can be used as a landmark as the node is located immediately caudal to it. If an accessory axillary LN is present, it can be dissected following the lymphatic trunk located at the caudal aspect of the axillary node (Rehnblom et al., 2022). For both nodes, blunt and sharp dissection with or without the use of electrocautery can be performed for lymphadenectomy. Damage to the lateral thoracic, thoracodorsal, and intercostobrachial nerves is the most concern during axillary lymphadenectomy as they are located close to the LNs (Rehnblom et al., 2022).

The ventral superficial cervical LN (previously known as the prescapular node) is bilaterally and comprised of a single node, or, in some dogs, 2 or 3 nodes. It is located cranial to the shoulder joint at the subcutaneous tissues under the superficial muscles of the neck (Wright et al., 2016; Figure 18A). The superficial cervical artery and vein can be found at the caudal portion of the LN (Wright et al., 2016). If not enlarged, this LN is seldom palpated externally. The ventral cervical LN is the dominant pathway draining the forelimb along with the axillary LN (Suami et al., 2013).

For lymphadenectomy of the ventral superficial cervical node, the patient is positioned in dorsal or dorsolateral recumbency with the forelimb reflected caudally to improve prescapular visualization. An incision is made cranial to the shoulder and extended cranially toward the omotransversarius muscle at the point medial to the scapula and lateral to the ribs. The LN is located medial to the superficial muscles of the neck, the omotransversarius, and the supraspinatus muscle (Wright et al., 2016).

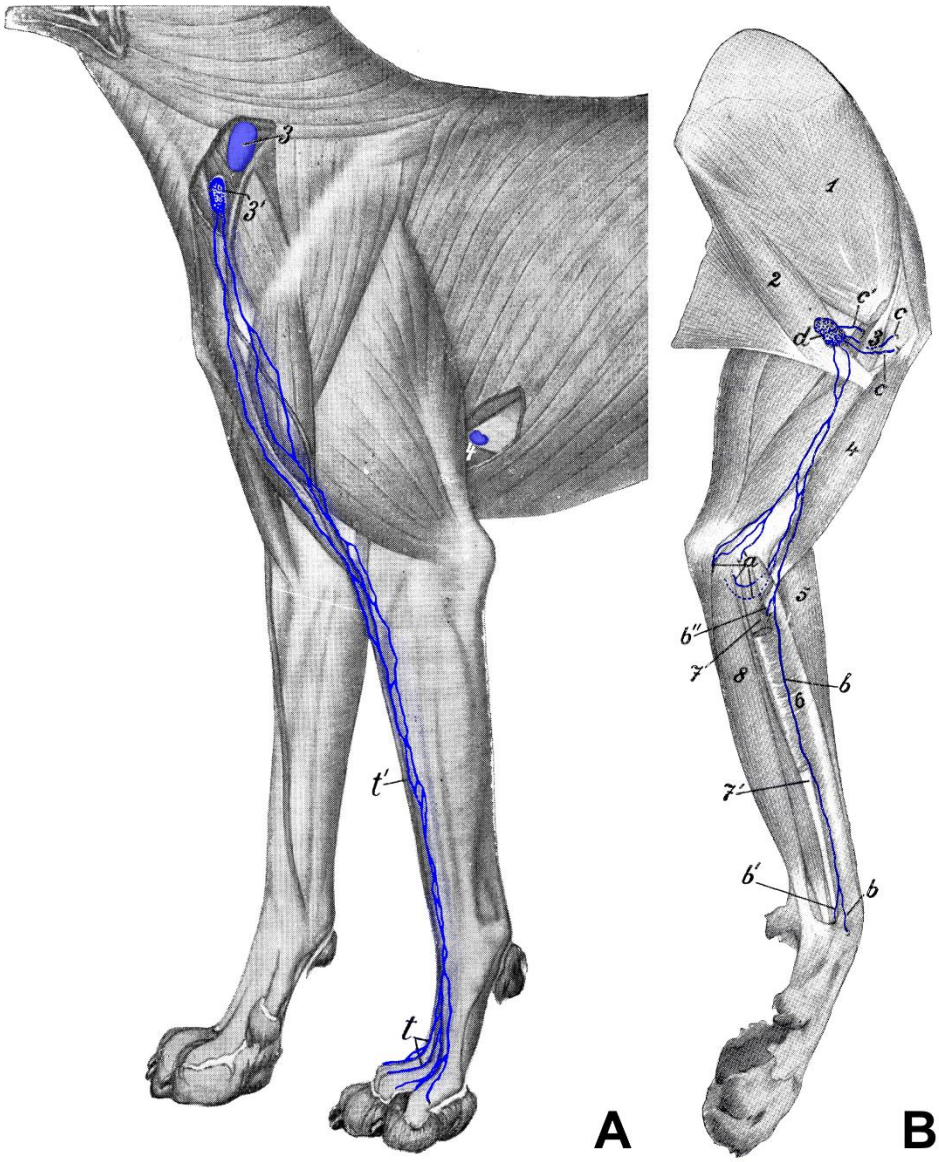

Figure 18. Lymph nodes and lymph vessels of the canine forelimb. (A) Lateral view of the forelimb showing the lymph vessels draining the cranial aspect toward the superficial cervical lymph nodes (3 and 3') and the accessory axillary lymph node (4). (B) Medial view of the forelimb showing the lymph vessels draining the carpal (b and b'), elbow (a), and shoulder (c and c') regions towards the axillary lymph node (d) (Adapted from the translated version of Dr. Hermann Baum's article of 1918 by Dr. Monique Mayer and colleagues)

2.5.6 Iliosacral Lymphatic Basin

The iliosacral lymph center, also known as sublumbar LNs, includes the paired medial iliac and internal iliac (also known as hypogastric) and the sacral LN (Ganesan et al., 2016; Sutton et al., 2021; Figure 19). The sublumbar nodes drain the cutaneous and muscle tissues of the caudal abdomen, perineal and pelvic region including the pelvic limb and organs such as the colon, rectum,

anus, vagina, prostate, ureter, bladder, and urethra (Bezuidenhout, 2013; Ganesan et al., 2016). Most LNs of the iliosacral basin are paired, but anatomical variations can occur (Pugh et al., 1994; Bezuidenhout et al., 2013). Furthermore, unless considerably enlarged, iliosacral LNs cannot be evaluated through rectal palpation or externally by abdominal palpation and therefore imaging examinations are necessary to adequately assess this basin (Mayer et al., 2010). Several image techniques have been described to evaluate the sublumbar LNs, including CT, ultrasonography, and radiography (Turek et al., 2003; Llabrés-Díaz, 2004; Palladino et al., 2016; Pollard et al., 2017; Murphy et al., 2020).

The medial iliac LN is the largest sublumbar node, and it is located between the deep circumflex iliac and external iliac arteries at the level of the 5th and 6th lumbar vertebra where the aorta, caudal vena casa, and the psoas muscle forms a ruck (Evans and Lahunta, 2012; Bezuidenhout, 2013; Anderson et al., 2015). It is most often located as a single paired LN, but two separate structures can be seen at one or both sides of the arteries in some animals. The medial iliac LN is the most evaluated RLN when regional metastasis of a perineal tumor is suspected (Chaffin et al., 2002; Williams et al., 2005; Llabrés-Díaz, 2004; Sutton et al., 2022).

The internal iliac LN is located caudal to the medial iliac nodes at the level of the 6th and 7th lumbar vertebrae between the median sacral and internal iliac arteries (Evans and Lahunta, 2012; Anderson et al., 2015). It is often single nodes, but some animals can have more than one (Evans and Lahunta, 2012).

The sacral LNs can be found caudal to internal iliac node just ventral to the sacrum and caudal vertebra close to the median sacral artery (Evans and Lahunta, 2012; Bezuidenhout, 2013). It is important to note that around 50% of dogs do not have the sacral LN (Evans and Lahunta, 2012).

The anatomical location close to important large blood vessels (i.e., aorta, caudal vena cava, and external iliac arteries) of the medial iliac LN makes diagnostic techniques challenging due to the risk of hemorrhage (Steffey et al., 2015; Lim et al., 2017).

Resection of the medial iliac LN has been described through a conventional celiotomy or by laparoscopy (Steffey et al., 2015; Lim et al., 2017).

Exploration of the internal iliac and sacral LNs by laparoscopy is limited due to the generally small size of the nodes and difficulties to visualize caused by the abdominal fat and lack of adequate angle for laparoscopy camera and instruments (Lim et al., 2017).

Despite the deep location close to important vascular structures, hemorrhage or other intraoperative or postoperative complications associated with the lymphadenectomy of the sublumbar LNs are uncommon and usually mild to moderate (Barnes et al., 2017; Tanis et al., 2022). However, dissection must be performed with caution as severe life-threatening bleeding can occur (Tanis et al., 2022).

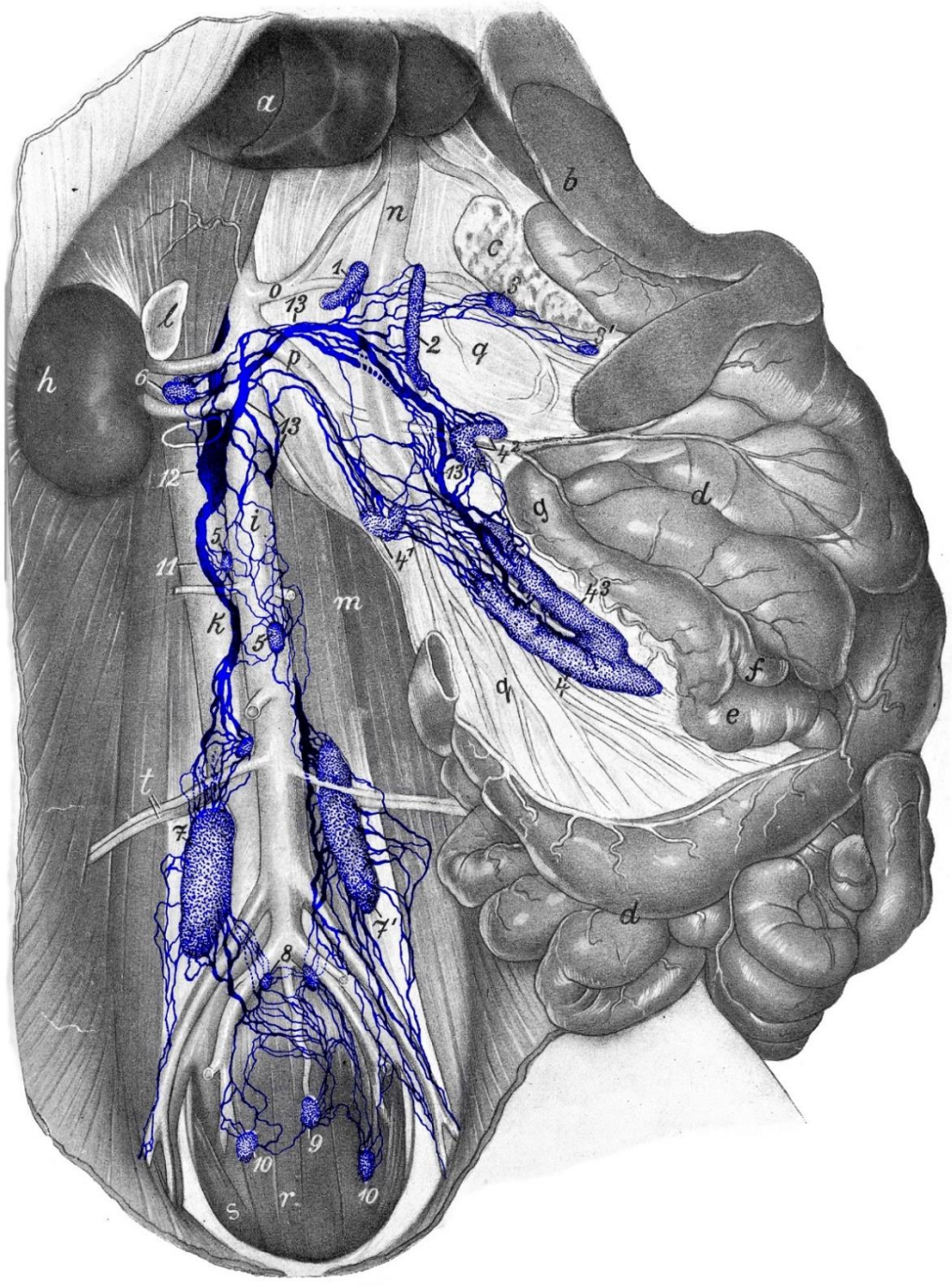

Figure 19. Lymph nodes and lymphatic vessels of the abdominal cavity, pelvic region, and mesentery. a liver; b spleen; c pancreas; d jejunum; e ileum; f cecum; g colon; h right kidney; i aorta; k vena cava; l right adrenal gland; m lumbar musculature; n portal vein; o celiac artery; p cranial mesenteric artery; q mesentery with blood vessels; r depressor and s curvator muscles of tail; t deep circumflex iliac artery and vein. 1 right hepatic lymph node; 2 left hepatic lymph node; 3, 3^1 splenic lymph nodes; 4, 4^1, 4^2, 4^3 jejunal lymph nodes; 5 lumbar aortic lymph nodes; 6 right cranial lumbar aortic lymph node; 7, 7^1 medial iliac lymph nodes; 8 internal iliac lymph nodes (originally termed as hypogastric lymph nodes); 9 medial sacral lymph nodes; 10 lateral sacral lymph nodes; 11 lumbar trunk; 12 cisterna chyli; 13, 13, 13 lymphatic trunks from the viscera. (Adapted from the translated version of Dr. Hermann Baum's article of 1918 by Dr. Monique Mayer and colleagues)

2.5.7 Hindlimb Lymphatic Basin

The popliteal LN is a single superficial node located at the subcutaneous fat between the medial aspect of the biceps femoris and the lateral of the semitendinosus muscle (Bezuidenhout et al., 2013; Figure 20A). At this point, both muscles diverge forming a depression where the LN lies (Wright et al., 2016). The popliteal LN drains most of the hindlimb located distal to it, including the caudal half of the lateral stifle, lateral, cranial, and caudal tarsus, metatarsus, and phalanges (Bezuidenhout et al., 2013). In addition to the skin, the popliteal node also drains from the bones, such as the tibia, fibula, tarsal, metatarsal, phalanges, joints, and muscles (Bezuidenhout et al., 2013). Efferent lymphatic vessel from the popliteal LN usually drains to the medial iliac, superficial inguinal, internal iliac LN and, when present, to the femoral and external iliac (Pflug et al., 1969; Schacher et al., 1972; Schacher et al., 1973; Smaropoulos et al., 2005; Bezuidenhout et al., 2013; Mayer et al., 2018). However, while drainage to the medial iliac LN seems to occur in all cases through medial thigh efferent vessels, the drainage to the superficial inguinal LN is less likely and controversial among studies (Pflug et al., 1969; Schacher et al., 1972; Mayer et al., 2018).

Surgical access to the popliteal LN is performed with the animal in dorsal or lateral recumbency. An incision is made at the popliteal fossa between the muscles and just caudal to the stifle joint. The LN is usually palpated due to its superficial location and extensive dissection is generally unnecessary. The perinodal fat can be blunt and sharp dissected to allow proper visualization and the LN resected routinely (Wright et al., 2016).

The distal femoral LN is not always present in dogs, but, when present, it is located at the level of the femoral vein between the sartorius and the gracilis muscles (Pflug et al., 1969; Schacher et al., 1972; Figure 20B). On the other hand, the external iliac artery is located at the ventral surface of the tendon of the psoas minor muscle (Pflug et al., 1969; Schacher et al., 1972) Both distal femoral and external iliac LN drains to the medial iliac LN (Mayer et al., 2018).

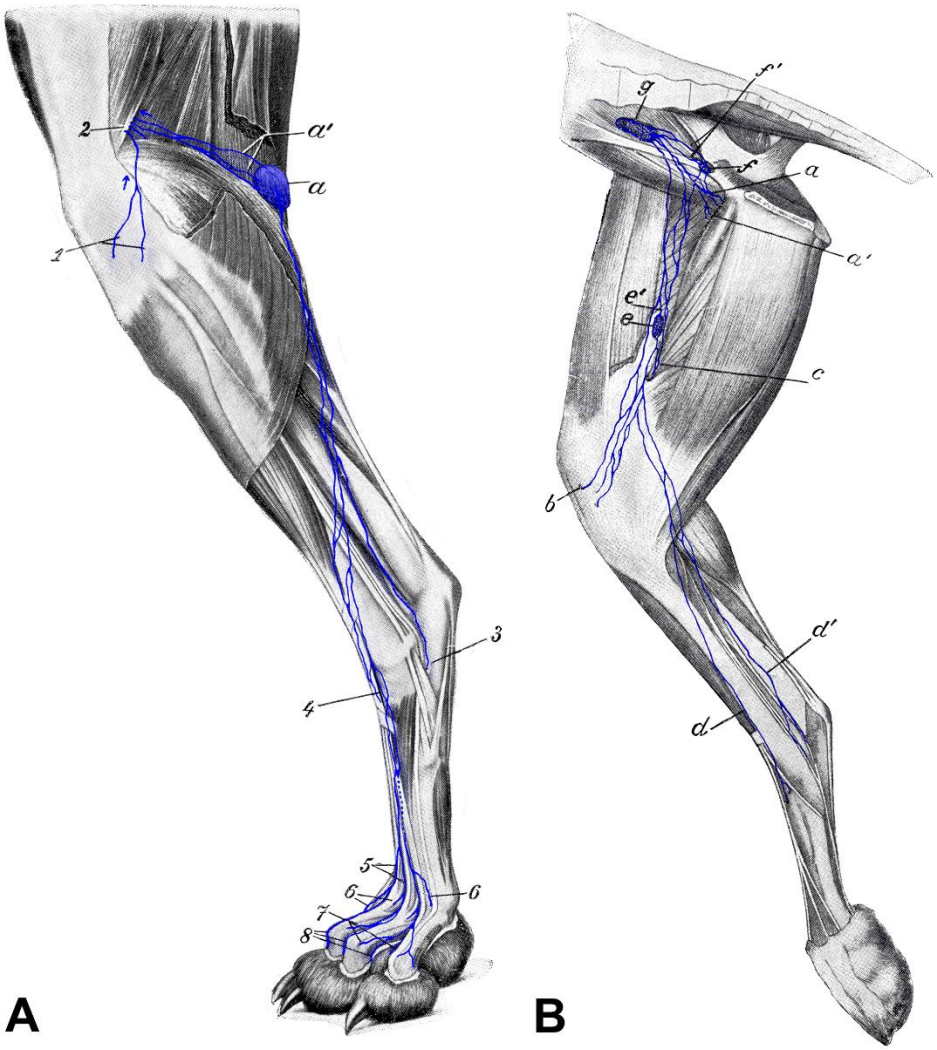

Figure 20. Lymph nodes and lymph vessels of the hindlimb. (A) Lateral view showing the lymphatic vessels of the dorsal-lateral aspect draining the metatarsal, tarsal and tibial region to the popliteal lymph node. (B) Medial view showing the lymphatic drainage of the medial aspect of the tibia and thigh to the femoral and inguinal lymph nodes. (Adapted from the translated version of Dr. Hermann Baum's article of 1918 by Dr. Monique Mayer and colleagues)

2.5.8 Complications of Lymph Node Resection

Lymphadenectomy is not a simple procedure, and postoperative morbidity is expected. The main complications following lymphadenectomy are the increased risk for lymphedema, wound healing impairment and dehiscence, and still theoretical tampering of the immune response against the metastatic spread when an unaffected regional LN is resected (Bodenham et al., 1969; Baum et al., 1973). Infection and seroma can also occur at the surgical site (Wright et al., 2016).

Other specific complications include the inadvertent resection of the salivary glands during head and neck lymphadenectomy; damaging of major blood vessels when dissecting head and neck or sublumbar LNs and nerve lesions when accessing the axillary node (Wright et al., 2016).

The lack of evidence of a clear benefit on the outcome is the main reason to contraindicate prophylactic lymphadenectomy for low-grade unaggressive cMCT (Bodenham et al., 1969; Baum et al., 1973; Sabattini et al., 2021). However, despite being highly relevant in human patients, complications of lymphadenectomy in dogs are usually mild and uncommon, which frequently encourages the surgeon to resection one or multiple LN even prophylactically (Sabattini et al., 2021)

3. CURRENT GAPS IN KNOWLEDGE

It is well-established that lymphatic metastasis is an important prognostic factor for canine cMCT, however, the role of detecting SLN and consequently removing metastatic LNs remains unclear. The filter barrier effect of the LN is well described in humans, however, despite some weak evidence that early lymphadenectomy may be beneficial, the role of extensive LN removal remains unknown.

There is a series of techniques described for SLN mapping in dogs. Some of them, such as the use of blue dyes, are currently used in routine practice for detecting SLN and aid surgeons during the intraoperative search. However, there are only a few studies evaluating other techniques that may improve precision and consequently staging, treatment and prognosis. Remains unclear whether these techniques are equivalent or superior to previous mapping ways.

There is also a concern about how metastasis is diagnosed after a LN sample has been collected. The Weishaar classification system still requires further validation regarding its clinical significance. Furthermore, the technique of slide cutting and processing also requires standardization.

4. HYPOTHESIS AND OBJECTIVES

4.1. Hypothesis

Considering that the use of intraoperative blue dye may miss the detection of other SLNs, such as those located in deeper tissues or the intracavitary ones. We hypothesized that radiographic indirect lymphography can be useful to aid the surgeon in precisely detecting SLNs before surgical procedure and thus removing SLNs, improving the accuracy of the number of LNs at risk of metastatic disease. Consequently, dogs bearing cMCT would be better staged and may experience a longer disease-free interval.

4.2. General Objectives

This thesis must achieve two main objectives: (1) Writing a descriptive review of the main aspects of the canine cMCT, lymphatic system, the mechanisms leading to lymphatic dissemination of cancer cells, a summary of the anatomy of the mains lymphatic basins, and the evidence available that supports the use of indirect lymphography in a clinical setting. (2) Conduct a prospective non-randomized clinical trial of dogs with cMCT that underwent both radiographic indirect lymphography and intraoperative patent blue SLN mapping followed by lymphadenectomy and histological evaluation.

4.3. Specific Objectives

Specifics objectives of this thesis include:

- Determination of the agreement rate between preoperative iodized oil (IO) Indirect lymphography (IL) and Intraoperative patent blue (PB) SLN mapping in dogs with cMCT.
- Determine whether IL is superior to IPB in detecting multiple SLNs at risk
- Find a correlation between enlarged LN x contrast-enhanced LN pattern and/or PB dyeing pattern.
- Define if the SLNs detected would be in an area distant from the surgical site of the primary tumor resection and would need a separate surgical approach to be accessed.
- and finally, to determine if there are benefits of adding the IO IL to the staging protocol of dogs with cMCT.

5. REFERENCES

1. Abadie JJ, Amardeilh MA, Delverdier ME. Immunohistochemical detection of proliferating cell nuclear antigen and Ki-67 in mast cell tumors from dogs. J Am Vet Med Assoc. 1999; 215:1629–34.
2. Abass MO, Gismalla MDA, Alsheikh AA, Elhassan MMA. Axillary Lymph Node Dissection for Breast Cancer: Efficacy and Complication in Developing Countries. J Glob Oncol 2018; 4:1-8.
3. Alex JC, Krag DN. Gamma-probe guided localization of lymph nodes. Surg Oncol. 1993; 2(3):137–143.
4. Alitalo A, Detmar M. Interaction of tumor cells and lymphatic vessels in cancer progression. Oncogene. 2012; 31(42):4499-4508.
5. Allan GS, Watson AD, Duff BC, Howlett CR. Disseminated mastocytoma and mastocytemia in a dog. J Am Vet Med Assoc. 1974; 165:346–9.
6. AlSarraf R, Mauldin GN, Patnaik AK and Meleo KA. A prospective study of radiation therapy for the treatment of grade 2 mast cell tumours in 32 dogs. Journal of Veterinary Internal Medicine 1996; 10:376–378.
7. Anderson CL, Mackay CS, Roberts GD, Fidel J. Comparison of abdominal ultrasound and magnetic resonance imaging for detection of abdominal lymphadenopathy in dogs with metastatic apocrine gland adenocarcinoma of the anal sac. Vet Comp Oncol 2015; 13:98–105.
8. Bachmann SB, Gsponer D, Montoya-Zegarra JA, Schneider M, Scholkmann F, et al. A Distinct Role of the Autonomic Nervous System in Modulating the Function of Lymphatic Vessels under Physiological and Tumor-Draining Conditions. Cell Rep 2019; 27:3305–3314.
9. Bae S, Milovancev M, Bartels C, Irvin VL Tuohy JL, et al. Histologically low-grade, yet biologically high-grade, canine cutaneous mast cell tumours: a systematic review and meta-analysis of individual participant data. Vet Comp Oncol. 2020; 18(4):580–9.
10. Baginski H, Davis G, Bastian RP, The prognostic value of lymph node metastasis with grade 2 MCTs in dogs: 55 cases (2001-2010). J Am Vet Hosp Assoc 2014; 50(2):89-95.
11. Baker-Gabb M, Hunt GB, France MP. Soft tissue sarcomas and mast cell tumours in dogs; clinical behaviour and response to surgery. Australian Veterinary Journal 2003; 81:732–780.

12. Balasubramanian SP, Harrison BJ. Systematic review and meta-analysis of sentinel node biopsy in thyroid cancer. Brit J of Surg 2011; 98:334-44.
13. Ball CG, Sutherland F, Kirkpatrick AW, Dixon E, Maclean AR, et al.. Dramatic innovations in modern surgical subspecialties. Can J of Surg 2010; 53:335-41
14. Balogh L, Thuróczy J, Andócs G, Máthé D, Chaudhari P, et al. Sentinel lymph node detection in canine oncological patients. Nucl Med Rev. 2002;5(2):139–144.
15. Baluk P, Fuxe J, Hashizume H, Romano T, Lashnits E, et al. Functionally specialized junctions between endothelial cells of lymphatic vessels. J Exp Med. 2007; 204(10):2349-2362.
16. Barnes DC, Demetriou JL. Surgical management of primary, meta-static and recurrent anal sac adenocarcinoma in the dog: 52 cases.J Small Anim Pract. 2017; 58:263-268.
17. Bartholf DeWitt S, Eward WC, Eward CA, Lazarides AL, Whitley SB, et al. A novel imaging system distinguishes neoplastic from normal tissue during resection of soft tissue sarcomas and mast cell tumors in dogs. Vet Surg. 2016; 45(6):715–722.
18. Bavcar S, de Vos J, Kessler M, de Fornel P, Buracco P, et al. Combination toceranib and lomustine shows frequent high grade toxicities when used for treatment of non-resectable or recurrent mast cell tumours in dogs: A European multicentre study. Vet J. 2017; 224:1-6.
19. Beatty GL, Gladney WL. Immune escape mechanisms as a guide for cancer immunotherapy. Clin Cancer Res Off J Am Assoc Cancer Res. 2015; 21(4):687-692.
20. Beek MA, Verheuvel NC, Luiten EJ, Klompenhouwer EG, Rutten HJ, et al. Two decades of axillary management in breast cancer. Brit J Surg 2015; 102:1658-64
21. Beer P, Pozzi A, Rohrer Bley C, Bacon N, Pfammatter NS, et al.The role of sentinel lymph node mapping in small animal veterinary medicine: A comparison with current approaches in human medicine. Vet Comp Oncol 2018; 16:178-187.

22. Belhabib I, Zaghdoudi S, Lac C, Bousquet C, Jean C. Extracellular Matrices and Cancer-Associated Fibroblasts: Targets for Cancer Diagnosis and Therapy? Cancers 2021; 13:3466.
23. Belz GT, Heath TJ. Lymph pathways of the medial retropharyngeal lymph node in dogs. J Anat 1995; 186:517-26.
24. Benechet AP, Menon M, Xu D, Samji T, Maher L, et al. T cell-intrinsic S1PR1 regulates endogenous effector T-cell egress dynamics from lymph nodes during infection. Proc Natl Acad Sci USA. 2016;113(8):2182-2187.
25. Bernabe LF, Portela R, Nguyen S, Kisseberth WC, Pennell M, et al. Evaluation of the adverse event profile and pharmacodynamics of toceranib phosphate administered to dogs with solid tumors at doses below the maximum tolerated dose. BMC Vet Res. 2013; 9:190.
26. Bernier-Latmani J, Cisarovsky C, Demir CS, Bruand M, Jaquet M, et al. DLL4 promotes continuous adult intestinal lacteal regeneration and dietary fat transport. J Clin Invest. 2015; 125(12):4572-4586.
27. Bernier-Latmani J, Petrova TV. Intestinal lymphatic vasculature: structure, mechanisms and functions. Nat Rev Gastroenterol Hepatol. 2017; 14(9):510-526.
28. Bezuidenhout AJ. The Lymphatic System. In: Evans HE, de Lahunta A, editors. Miller's Anatomy of the Dog. 4th ed. St. Louis: Elsevier Saunders; 2013. pp. 535–62.
29. Blackwood L, Murphy S, Buracco P, De Vos JP, Fornel-Thibaud P De, et al. European consensus document on mast cell tumours in dogs and cats. Vet Comp Oncol. 2012; 10(3):e1–e29.
30. Blomley MJK, Cooke JC, Unger EC, Monaghan MJ, Cosgrove DO. Science, medicine, and the future: microbubble contrast agents: a new era in ultrasound. Br Med J. 2001; 322(7296):1222–1225.
31. Blum KS, Proulx ST, Luciani P, Leroux JC, Detmar M. Dynamics of lymphatic regeneration and flow patterns after lymph node dissection. Breast Cancer Res Treat. 2013; 139(1):81-6.
32. Book AP, Fidel J, Wills T, Bryan J, Sellon R, et al. Correlation of ultrasound findings, liver and spleen cytology, and prognosis in the clinical staging of high metastatic risk canine mast cell tumors. Vet Radiol Ultrasound. 2011; 52:548-554.

33. Bookbinder PF, Butt MT, Harvey HJ. Determination of the number of mast cells in lymph node, bone marrow and buffy coat cytological specimens in dogs. J Am Vet Med Assoc. 1992; 200: 1648–1650.
34. Bordry N, Broggi MAS, de Jonge K, Schaeuble K, Gannon PO, et al. Lymphatic vessel density is associated with CD8(+) T cell infiltration and immunosuppressive factors in human melanoma. Oncoimmunology. 2018; 7(8):e1462878.
35. Borgstein PJ, Meijer S, Van Diest PJ. Are Locoregional Cutaneous Metastases in Melanoma Predictable? Ann Surg Oncol 1999; 6:315–321.
36. Bosch SL, Teerenstra S, DeWilt JH, Cunningham C, Nagtegaal ID. Predicting lymph node metastasis in pT1 colorectal cancer: A systematic review of risk factors providing rationale for therapy decisions. Endoscopy 2013; 45, 827–834.
37. Bostock D. The prognosis following surgical removal of mastocytomas in dogs. J Small Anim Pract 1973; 14: 27–40.
38. Bostock DE, Crocker J, Harris K and Smith P. Nucleolar organiser regions as indicators of post-surgical prognosis in canine spontaneous mast cell tumours. Br J Cancer 1989; 59:915–918.
39. Bradham RR, Parker EF, Barrington BA, Jr, Webb CM, Stallworth JM. The cardiac lymphatics. Ann Surg. 1970; 171(6):899-902
40. Brakenhielm E, Alitalo K. Cardiac lymphatics in health and disease. Nat Rev Cardiol. 2019; 16(1):56-68.
41. Breart B, Bousso P. S1P1 downregulation tailors CD8(+) T-cell residence time in lymph nodes to the strength of the antigenic stimulation. Eur J Immunol. 2016; 46(12):2730-2736.
42. Breslin JW, Yang Y, Scallan JP, Sweat RS, Adderley SP, et al. Lymphatic vessel network structure and physiology. Compr Physiol. 2018; 9(1):207–299.
43. Brissot HN, Edery EG. Use of indirect lymphography to identify sentinel lymph node in dogs: a pilot study in 30 tumours. Vet Comp Oncol 2017; 15:740-753.
44. Bronsert P, Enderle-Ammour K, Bader M, Timme S, Kuehs M, et al. Cancer cell invasion and EMT marker expression: A three-dimensional study of the human cancer-host interface. J Pathol 2014; 234:410–422.

45. Brown M, Assen FP, Leithner A, Abe J, Schachner H, et al. Lymph node blood vessels provide exit routes for metastatic tumor cell dissemination in mice. Science. 2018; 359(6382):1408-1411.
46. Cabanas RM. An approach for the treatment of penile carcinoma. Cancer. 1977; 39(2):456–466.
47. Cabanas RM. The concept of the sentinel lymph node. Recent Results Cancer Res 2000; 157:109-20.
48. Cabon Q, Sayag D, Texier I, Navarro F, Boisgard R, et al. Evaluation of intraoperative fluorescence imaging-guided surgery in cancer-bearing dogs: a prospective proof-of-concept phase II study in 9 cases. Transl Res. 2016; 170:73–88.
49. Cahalane AK, Payne S, Barber LG, Duda LE, Henry CJ, et al. Prognostic factors for survival of dogs with inguinal and perineal mast cell tumors treated surgically with or without adjunctive treatment: 68 cases (1994–2002) J Vet Med Sci. 2004; 225:401–408.
50. Camus MS, Priest HL, Koehler JW, Driskell EA, Rakich PM, et al. Cytologic criteria for mast cell tumor grading in dogs with valuation of clinical outcome. Vet Pathol. 2016; 53:1117–23.
51. Cartagena-Albertus JC, Moise A, Moya-García S, Cámara-Fernández N, Montoya-Alonso JA. Presumptive primary intrathoracic mast cell tumours in two dogs. BMC Vet Res. 2019; 15:204.
52. Cassali GD, Jark PC, Gamba C, Damasceno KA, Lima AE, et al. Consensus regarding the diagnosis, prognosis and treatment of canine and feline mammary tumors – 2019. Braz J Vet Pathol. 2020; 13(3):555-574.
53. Casteleyn CR, van der Steen M, Declercq J, Simoens P. The buccal lymph node (lymphonodus buccalis) in dogs: occurrence, anatomical location, histological characteristics and clinical implications. Vet J. 2008; 175(3):379-83.
54. Castells M. Mast cell mediators in allergic inflammation and mastocytosis. Immunol Allergy Clin North Am 2006; 26:465–485.
55. Chaffin K, Thrall DE. Results of radiation therapy in 19 dogs with cutaneous mast cell tumour and regional lymph node metastasis. Vet Radiol Ultrasound 2002; 43:392–395.

56. Chen J-Y, Lai Y-S, Chu P-Y, Chan S-H, Wang L-H, et al. Cancer-Derived VEGF-C Increases Chemokine Production in Lymphatic Endothelial Cells to Promote CXCR2-Dependent Cancer Invasion and MDSC Recruitment. Cancers 2019; 11:1120.
57. Chen Y, Liu ZY, Li RX, Guo Z. Structural studies of initial lymphatics adjacent to gastric and colonic malignant neoplasms. Lymphology 1999; 32:70–74.
58. Christiansen A, Detmar M. Lymphangiogenesis and cancer. Genes Cancer 2011; 2:1146-58.
59. Cochran AJ, Oshie SJ, Binder SW. Pathobiology of the sentinel node. Curr Opin Oncol 2008; 20:190–195.
60. Cochran AJ, Wen DR, Huang RR, Wang HJ, Elashoff R, et al. Prediction of metastatic melanoma in nonsentinel nodes and clinical outcome based on the primary melanoma and the sentinel node. Mod Pathol Off J US Can Acad Pathol Inc. 2004; 17(7):747-755.
61. Cohen JN, Guidi CJ, Tewalt EF, Qiao H, Rouhani SJ, et al. Lymph node-resident lymphatic endothelial cells mediate peripheral tolerance via Aire-independent direct antigen presentation. J Exp Med. 2010; 207(4):681-688.
62. Collivignarelli F, Tamburro R, Aste G, Falerno I, Del Signore F, et al. Lymphatic Drainage Mapping with Indirect Lymphography for Canine Mammary Tumors. Animals. 2021; 11(4):1115.
63. Commerford CD, Dieterich LC, He Y, Hell T, Montoya-Zegarra JA, et al. Mechanisms of tumor-induced lymphovascular niche formation in draining lymph nodes. Cell Rep. 2018; 25(13):3554-3563.
64. Conzo G, Calò PG, Sinisi AA, De Bellis A, Pasquali D, et al. Impact of prophylactic central compartment neck dissection on locoregional recurrence of differentiated thyroid cancer in clinically node-negative patients: a retrospective study of a large clinical series. Surgery. 2014; 155(6):998–1005.
65. Cousin N, Cap S, Dihr M, Tacconi C, Detmar M, et al. Lymphatic PD-L1 Expression Restricts Tumor-Specific CD8+T-cell Responses. Cancer Res 2021; 81:4133–4144.
66. Cox K, Sever A, Jones S, Weeks J, Mills P, et al. Validation of a technique using microbubbles and contrast enhanced ultrasound (CEUS) to biopsy sentinel lymph nodes (SLN) in pre-operative breast cancer patients with a

normal grey-scale axillary ultrasound. Eur J Surg Oncol. 2013; 39(7):760–765.

67. Cox TR. The matrix in cancer. Nat Rev Cancer 2021; 21:217–238.
68. Dadiani M, Kalchenko V, Yosepovich A, Margalit R, Hassid Y, et al. Real-time imaging of lymphogenic metastasis in orthotopic human breast cancer. Cancer Res. 2006;66(16):8037-8041.
69. Davies DR, Wyatt KM, Jardine JE, Robertson ID, Irwin PJ. Vinblastine and prednisolone as adjunctive therapy for canine cutaneous mast cell tumors. J Am Anim Hosp Assoc. 2004; 40(2):124-30.
70. Dieterich LC, Detmar M. Tumor lymphangiogenesis and new drug development. Adv Drug Deliv Rev 2016; 99:148–160.
71. Dieterich LC, Ikenberg K, Cetintas T, Kapaklikaya K, Hutmacher C, et al. Tumor-Associated Lymphatic Vessels Upregulate PDL1 to Inhibit T-Cell Activation. Front Immunol 2017; 8:66.
72. Dieterich LC, Kapaklikaya K, Cetintas T, Proulx ST, Commerford CD, et al. Transcriptional profiling of breast cancer-associated lymphatic vessels reveals VCAM-1 as regulator of lymphatic invasion and permeability. Int J Cancer 2019; 145:2804–2815.
73. Dihge L, Vallon-Christersson J, Hegardt C, Saal LH, Häkkinen J, et al. Prediction of lymph node metastasis in breast cancer by gene expression and clinicopathological models: development and validation within a population-based cohort. Clin Cancer Res Off J Am Assoc Cancer Res. 2019; 25(21):6368-6381.
74. Dobson JM, Scase TJ. Advances in the diagnosis and management of cutaneous mast cell tumours in dogs. J Small Anim Pract 2007; 48:424–431.
75. Donnelly L, Mullin C, Balko J, Goldschmidt M, et al. Evaluation of histological grade and histologically tumour-free margins as predictors of local recurrence in completely excised canine mast cell tumours. Vet Comp Oncol. 2015; 13(1):70-76.
76. Dubreuil P, Letard S, Ciufolini M, Gros L, Humbert M, et al. Masitinib (AB1010), a potent and selective tyrosine kinase inhibitor targeting KIT. PLoS One. 2009; 4(9):e7258.
77. Dyce KM, Sack WO, Wensing CJG. Textbook of Veterinary Anatomy. St Louis, Elsevier Health Sciences, 2009.

78. East JM, Valentine CS, Kanchev E, Blake GO. Sentinel lymph node biopsy for breast cancer using methylene blue dye manifests a short learning curve among experienced surgeons: a prospective tabular cumulative sum (CUSUM) analysis. BMC Surg. 2009; 9:2.
79. El K, Kiupel M, Durham AC, Thaiwong T, Brown DC, et al. Investigating associations between proliferation indices, C-Kit, and lymph node stage in canine mast cell tumours. J Am Anim Hosp Assoc. 2017; 53:258-264.
80. Emmett MS, Lanati S, Dunn DB, Stone OA, Bates DO. CCR7 Mediates Directed Growth of Melanomas Towards Lymphatics. Microcirculation 2011; 18:172–182.
81. Emmett MS, Lanati, S, Dunn DB, Stone OA, Bates DO. CCR7 Mediates Directed Growth of Melanomas Towards Lymphatics. Microcirculation. 2011; 18:172–182.
82. Esfehani M, Yazdankhah-Kenari A, Omranipour R, Mahmoudzadeh HA, Shahriaran S, et al. Validation of contrast enhanced ultrasound technique to wire localization of sentinel lymph node in patients with early breast cancer. Indian J Surg Oncol. 2015; 6:370-373.
83. Evans H, Lahunta AD. Miller's Anatomy of the Dog. St Louis, Elsevier Health Sciences, 2013.
84. Eward WC, Mito JK, Eward CA, Carter JE, Ferrer JM, et al. A novel imaging system permits real-time in vivo tumor bed assessment after resection of naturally occurring sarcomas in dogs. Clin Orthop Relat Res. 2013; 471(3):834–842.
85. Faries MB, Thompson JF, Cochran AJ, Andtbacka RH, Mozzillo N, et al. Completion Dissection or Observation for Sentinel-Node Metastasis in Melanoma. N Engl J Med 2017; 376:2211–2222.
86. Fejös, C, Troedson, K, Ignatenko, N, Zablotski, Y, Hirschberger, J. Extensive staging has no prognostic value in dogs with low-risk mast cell tumours. Vet Comp Oncol. 2022; 20(1):265- 275.
87. Ferrari R, Boracchi P, Chiti LE, Manfredi M, Giudice C, et al. Assessing the risk of nodal metastases in canine integumentary mast cell tumors: is sentinel lymph node biopsy always necessary? Animals. 2021; 11:2373.

88. Ferrari R, Chiti LE, Manfredi M, Ravasio G, De Zani D, et al. Biopsy of sentinel lymph nodes after injection of methylene blue and lymphoscintigraphic guidance in 30 dogs with mast cell tumors. Vet Surg. 2020; 49(6):1099-1108.
89. Ferrari R, Marconato L, Buracco P, Boracchi P, Giudice C, et al. The impact of extirpation of non-palpable/normal-sized regional lymph nodes on staging of canine cutaneous mast cell tumours: A multicentric retrospective study. Vet Comp Oncol. 2018; 16(4):505-510.
90. Fidel J, Kennedy KC, Dernell WS, Hansen S, Wiss V, et al. Preclinical validation of the utility of BLZ-100 in providing fluorescence contrast for imaging spontaneous solid tumors. Cancer Res. 2015; 75(20):4283–4291.
91. Finora K, Leibman NF, Fettman MJ, Powers BE, Hackett TA et al. Cytological comparison of fine-needle aspirates of liver and spleen of normal dogs and of dogs with cutaneous mast cell tumours and an ultrasonographically normal appearing liver and spleen. Vet Comp Oncol. 2006; 4:178–183.
92. Fisher B, Fisher ER. The interrelationship of hematogenous and lymphatic tumor cell dissemination. Surg Gynecol Obstet 1966; 122:791-8.
93. Fletcher AL, Lukacs-Kornek V, Reynoso ED, Pinner SE, Bellemare-Pelletier A, et al. Lymph node fibroblastic reticular cells directly present peripheral tissue antigen under steady-state and inflammatory conditions. J Exp Med. 2010; 207(4):689-697.
94. Follain G, Herrmann D, Harlepp S, et al. Fluids and their mechanics in tumour transit: shaping metastasis. Nat Rev Cancer. 2020;20(2):107-124.
95. Forster R, Braun A, Worbs T. Lymph node homing of T cells and dendritic cells via afferent lymphatics. Trends Immunol. 2012;33(6):271-280.
96. Fournier Q, Cazzini P, Bavcar S, Pecceu E, Ballber C, et al. Investigation of the utility of lymph node fine-needle aspiration cytology for the staging of malignant solid tumors in dogs. Vet Clin Pathol. 2018; 47(3):489-500.
97. Fournier Q, Thierry F, Longo M, Malbon A, Cazzini P, et al. Contrast enhanced ultrasound for sentinel lymph node mapping in the routine staging of canine mast cell tumours: a feasibility study. Vet Comp Oncol. 2021; 19:451–62.
98. Fox LE, Rosenthal RC, Twedt DC, Dubielzig RR, Macewen EG, et al. Plasma histamine and gastrin-concentrations in 17 dogs with mast-cell tumors. J Vet Inter Med 1990; 4(5):242–246.

99. Frimberger AE, Moore AS, LaRue SM, Gliatto JM, Bengtson AE. Radiotherapy of incompletely resected, moderately differentiated mast cel tumours in the dog: 37 cases (1989–93). J Am Anim Hosp Assoc. 1997; 33(4):320–324.

100. Fujimoto N, Dieterich L. Mechanisms and clinical significance of tumor luymphatic invasion. Cells. 2021; 10(10):2585.

101. Fujisawa Y, Nakamura Y, Kawachi Y, Otsuka F. Indocyanine green fluorescence-navigated sentinel node biopsy showed higher sensitivity than the radioisotope or blue dye method, which may help to reduce false-negative cases in skin cancer. J Surg Oncol. 2012; 106(1):41–45.

102. Fujita S, Yamamoto S, Akasu T, Moriya Y. Outcome of patients with clinical stage II or III rectal cancer treated without adjuvant radiotherapy. Int J Color Dis. 2008; 23, 1073–1079.

103. Fulcher RP, Ludwig LL, Bergman PJ, Newman SJ, Simpson AM et al. Evaluation of a two-centimeter lateral surgical margin for excision of grade I and grade II cutaneous mast cell tumours in dogs. J Am Vet Med Assoc. 2006; 228(2):210-215

104. Gambardella C, Patrone R, Di Capua F, Offi C, Mauriello C, et al. The role of prophylactic central compartment lymph node dissection in elderly patients with differentiated thyroid cancer: a multicentric study. BMC Surg. 2019; 18(Suppl 1):110–8.

105. Ganesan S, Mohindroo J, Verma P, Saini NS. Ultrasonographic features of medial iliac and jejunal lymph nodes in apparently healthy dogs. Turk J Vet Anim Sci 2016; 40:225–228.

106. Garmy-Susini B, Avraamides CJ, Schmid MC, Foubert P, Ellies LG, et al. Integrin α4β1 Signaling Is Required for Lymphangiogenesis and Tumor Metastasis. Cancer Res. 2010; 70(8):3042–3051.

107. Garrett LD. Canine mast cell tumors: diagnosis, treatment, and prognosis. Vet Med. 2014; 5:49-58.

108. Gelb HR, Freeman LJ, Rohleder JJ, Snyder PW. Feasibility of contrast-enhanced ultrasound-guided biopsy of sentinel lymph nodes in dogs. Vet Radiol Ultrasound. 2010; 51(6):628–633.

109. Gerner MY, Torabi-Parizi P, Germain RN. Strategically localized dendritic cells promote rapid T cell responses to lymph-borne particulate antigens. Immunity. 2015; 42(1):172-185.

110. Giampieri S, Manning C, Hooper S, Jones L, Hill CS, et al. Localized and reversible TGFbeta signalling switches breast cancer cells from cohesive to single cell motility. Nature Cell Biol. 2009; 11(11):1287-1296.

111. Gieger TL, Northrup NC, Wall M. Clinical management of mast cell tumors in dogs. Comp Cont Ed Pract Vet. 2005; 27:56-68.

112. Gieger TL, Thèon AP, Werner JA, McEntee MC, Rassnick KM, et al. Biological behavior and prognostic factors for mast cell tumours of the canine muzzle: 24 cases (1990-2001). J Vet Intern Med. 2003; 17:687-692.

113. Girard JP, Moussion C, Forster R. HEVs, lymphatics and homeostatic immune cell trafficking in lymph nodes. Nat Rev Immunol. 2012; 12(11):762-773.

114. Giuliano AE, Ballman KV, McCall L, Beitsch PD, Brennan MB, et al. Effect of Axillary Dissection vs No Axillary Dissection on 10-Year Overall Survival Among Women With Invasive Breast Cancer and Sentinel Node Metastasis: The ACOSOG Z0011 (Alliance) Randomized Clinical Trial. JAMA 2017; 318(10):918–926.

115. Giuliano AE, Kirgan DM, Guenther JM, Morton DL. Lymphatic mapping and sentinel lymphadenectomy for breast cancer. Ann Surg. 1994; 220:391–398

116. Giuliano AE, McCall L, Beitsch P, Whitworth PW, Blumencranz P, et al. Locoregional recurrence after sentinel lymph node dissection with or without axillary dissection in patients with sentinel lymph node metastases: the American College of Surgeons Oncology Group Z0011 randomized trial. Ann Surg 2010; 252(3):426-432.

117. Goldberg BB, Merton DA, Liu JB, Thakur M, Murphy GF, et al. Sentinel lymph nodes in a swine model with melanoma: contrast-enhanced lymphatic US. Radiology. 2004; 230(3):727–734.

118. Goldberg BB, Merton DA, Liu JB, Murphy G, Forsberg F. Contrast-enhanced sonographic imaging of lymphatic channels and sentinel lymph nodes. J Ultrasound Med. 2005; 24(7):953–965

119. Goldfarb LR, Alazraki NP, Eshima D, Eshima LA, Herda SC, et al. Lymphoscintigraphic identification of sentinel lymph nodes: clinical evaluation of 0.22-micron filtration of Tc-99m sulfur colloid. Radiology. 1998; 208:505-509.

120. Govier SM. Principles of treatment for mast cell tumors. Clin Tech Small Anim Pract. 2003; 18(2):103-106.

121. Graham JC, Myers RK. The Prognostic Significance of Angiogenesis in Canine Mammary Tumors. J Vet Intern Med. 1999; 13(5):416–418.

122. Grant J, North S, Lanore D. Clinical response of masitinib mesylate in the treatment of canine macroscopic mast cell tumours. J Small Anim Pract. 2016; 57(6):283-90.

123. Gray EE, Cyster JG. Lymph node macrophages. J Innate Immun. 2012; 4(5–6):424-436.

124. Green K, Boston SE. Bilateral removal of the mandibular and medial retropharyngeal lymph nodes through a single ventral midline incision for staging of head and neck cancers in dogs: a description of surgical technique. Vet Comp Oncol. 2017; 15(1):208-214.

125. Greene HS, Harvey EK. The Relationship between the Dissemination of Tumor Cells and the Distribution of Metastases. Cancer Res 1964; 24:799-811.

126. Grimes JA, Matz BM, Christopherson PW, Koehler JW, Cappelle KK, et al. Agreement Between Cytology and Histopathology for Regional Lymph Node Metastasis in Dogs with Melanocytic Neoplasms. Vet Pathol 2017; 54:579-587.

127. Grimes JA, Secrest SA, Northrup NC, Saba CF, Schmiedt CW. Indirect computed tomography lymphangiography with aqueous contrast for evaluation of sentinel lymph nodes in dogs with tumors of the head. Vet Radiol Ultrasound. 2017; 58(5):559–564.

128. Grimes JA, Secrest SA, Wallace ML, Laver T, Schmiedt CW. Use of indirect computed tomography lymphangiography to determine metastatic status of sentinel lymph nodes in dogs with a pre-operative diagnosis of melanoma or mast cell tumour. Vet Comp Oncol. 2020; 18(4):818–24.

129. Gundem G, Van Loo P, Kremeyer B, Alexandrov LB, Tubio JMC, et al. The evolutionary history of lethal metastatic prostate cancer. Nature. 2015; 520(7547):353-357.

130. Hadzijusufovic E, Peter B, Herrmann H, Rülicke T, Cerny-Reiterer S, et al. NI-1: a novel canine mastocytoma model for studying drug resistance and IgER-dependent mast cell activation. Allergy. 2012; 67:858–68.

131. Hahn KA, Ogilvie G, Rusk T, Devauchelle P, Leblanc A, et al. Masitinib is safe and effective for the treatment of canine mast cell tumors. J Vet Intern Med. 2008; 22(6):1301-9.

132. Halin C, Tobler NE, Vigl B, Brown LF, Detmar M. VEGF-A produced by chronically inflamed tissue induces lymphangiogenesis in draining lymph nodes. Blood. 2007; 110(9):3158-67.

133. Hay JK, Larson VS. Lomustine (CCNU) and prednisone chemotherapy for high-grade completely excised canine mast cell tumors. Can Vet J. 2019; 60(12):1326-1330.

134. Hayashi H, Tangoku A, Suga K, Shimizu K, Ueda K, et al. CT lymphography-navigated sentinel lymph node biopsy in patients with superficial esophageal cancer. Surgery. 2006; 139(2):224–235.

135. Hayes A, Adams V, Smith K, Maglennon G, Murphy S. Vinblastine and prednisolone chemotherapy for surgically excised grade III canine cutaneous mast cell tumours. Vet Comp Oncol. 2007; 5:168-176.

136. He Y, Rajantie I, Pajusola K, Jeltsch M, Holopainen T, et al. Vascular endothelial cell growth factor receptor 3-mediated activation of lymphatic endothelium is crucial for tumor cell entry and spread via lymphatic vessels. Cancer Res. 2005; 65(11):4739-46.

137. Herring ES, Smith MM, Roberston JL. Lymph node staging of oral and maxillofacial neoplasms in 31 dogs and cats. J Vet Dent 2002; 19:122–6

138. Hikasa Y, Morita T, Futaoka Y, Sato K, Shimada A, et al. Connective tissue-type mast cell leukemia in a dog. J Vet Med Sci. 2000; 62:187–90.

139. Hillman LA, Garrett LD, de Lorimier LP, Charney SC, Brost LB, et al. Biological behavior of oral and perioral mast cell tumours in dogs: 44 cases (1996-2006). J Am Vet Med Assoc. 2010; 237:936-942.

140. Hirakawa S, Kodama S, Kunstfeld R, Kajiya K, Brown LF, et al. VEGF-A induces tumor and sentinel lymph node lymphangiogenesis and promotes lymphatic metastasis. J Exp Med. 2005; 201(7):1089-99.

141. Hirche C, Murawa D, Mohr Z, Kneif S, Hunerbein M. ICG fluorescence-guided sentinel node biopsy for axillary nodal staging in breast cancer. Breast Cancer Res Treat. 2010; 121(2):373–378.

142. Holloway RW, Bravo RA, Rakowski JA, James JA, Jeppson CN, et al. Detection of sentinel lymph nodes in patients with endometrial cancer undergoing robotic-assisted staging: a comparison of colorimetric and fluorescence imaging. Gynecol Oncol. 2012; 126(1):25–29.

143. Holt D, Parthasarathy AB, Okusanya O, Keating J, Venegas O, et al. Intraoperative near-infrared fluorescence imaging and spectroscopy identifies residual tumor cells in wounds. J Biomed Opt. 2015; 20(7):76002.

144. Hornyák L, Dobos N, Koncz G, Karányi Z, Páll D, et al. The role of indoleamine-2,3-dioxygenase in cancer development, diagnostics, and therapy. Front Immunol. 2018; 9:151.

145. Horta RS, Lavalle GE, Monteiro LN, Souza MCC, Cassali GD, et al. Assessment of canine mast cell tumor mortality risk based on clinical, histologic, immunohistochemical, and molecular features. Vet Pathol. 2018; 55:212-223.

146. Hoshida T, Isaka N, Hagendoorn J, di Tomaso E, Chen YL, et al. Imaging steps of lymphatic metastasis reveals that vascular endothelial growth factor-C increases metastasis by increasing delivery of cancer cells to lymph nodes: therapeutic implications. Cancer Res. 2006; 66(16):8065-75.

147. Hottendorf GH, Nielsen SW. Pathologic survey of 300 extirpated canine mastocytomas. Zentralbl Veterinarmed A. 1967; 14(3):272–281.

148. Hume CT, Kiupel M, Rigatti L, Shofer FS, Skorupski KA, et al. Outcomes of dogs with grade 3 mast cell tumours: 43 cases (1997-2007). J Am Anim Hosp Assoc. 2011; 47(1):37-44.

149. Iida G, Asano K, Seki M, Ishigaki K, Teshima K, et al. Intraoperative identification of canine hepatocellular carcinoma with indocyanine green fluorescent imaging. J Small Anim Pract. 2013;54(11):594–600.

150. Iodence AE, Wallace ML, Grimes JA, Schmiedt CW. Dogs undergoing surgical excision of mast cell tumors are not at increased risk of incisional complications. J Am Vet Med Assoc. 2021; 260(S1):S88-S95.

151. Isotani M, Ishida N, Tominaga M, Tamura K, Yagihara H, et al. Effect of tyrosine kinase inhibition by imatinib mesylate on mast cell tumors in dogs. J Vet Intern Med. 2008; 22(4):985-8.

152. Iwasaki R, Murakami M, Kawabe M, Heishima K, Sakai H, et al. Metastatic diagnosis of canine sternal lymph nodes using computed tomography characteristics: A retrospective cross-sectional study. Vet Comp Oncol. 2018; 16(1):140–7.

153. Iwata N, Ochiai K, Kadosawa T, Takiguchi M, Umemura T. Canine extracutaneous mast-cell tumours consisting of connective tissue mast cells. J Comp Pathol. 2000; 123(4):306–310.

154. Jain RK, Fenton BT. Intratumoral lymphatic vessels: a case of mistaken identity or malfunction? J Natl Cancer Inst. 2002; 94:417-21.

155. Jalkanen S, Salmi M. Lymphatic endothelial cells of the lymph node. Nat Rev Immunol. 2020; 20(9):566-578.

156. Jewell EL, Huang JJ, Abu-Rustum NR, Gardner GJ, Brown CL, et al. Detection of sentinel lymph nodes in minimally invasive surgery using indocyanine green and near-infrared fluorescence imaging for uterine and cervical malignancies. Gynecol Oncol. 2014; 133(2):274–277.

157. Kang T, Yi M, Hunt KK, Mittendorf EA, Babiera GV, et al. Does blue dye contribute to success of sentinel node mapping for breast cancer? Ann Surg Oncol. 2010; 17(3):280–285.

158. Karaman S, Detmar M. Mechanisms of lymphatic metastasis. J Clin Invest 2014; 124(3):922-8.

159. Karnezis T, Shayan R, Caesar C, Roufail S, Harris NC, et al. VEGF-D Promotes Tumor Metastasis by Regulating Prostaglandins Produced by the Collecting Lymphatic Endothelium. Cancer Cell. 2012; 21(2):181–195.

160. Karnezis T, Shayan R, Fox S, Achen MG, Stacker SA. The connection between lymphangiogenic signalling and prostaglandin biology: a missing link in the metastatic pathway. Oncotarget. 2012b; 3(8):893-906.

161. Karpanen T, Alitalo K. Lymphatic vessels as targets of tumor therapy? J Exp Med. 2001; 194(6):F37–F42

162. Kataru RP, Ly CL, Shin J, Park HJ, Baik JE, et al. Tumor lymphatic function regulates tumor inflammatory and immunosuppressive microenvironments. Cancer Immunol Res. 2019; 7(8):1345-1358.

163. Kayanuma H, Yamada K, Maruo T, Kanai E. Computed tomography of thoracic lymph nodes in 100 dogs with no abnormalities in the dominated area. J Vet Med Sci. 2020; 82(3):279-285.

164. Kerjaschki D, Bago-Horvath Z, Rudas M, Sexl V, Schneckenleithner C, et al. Lipoxygenase mediates invasion of intrametastatic lymphatic vessels and propagates lymph node metastasis of human mammary carcinoma xenografts in mouse. J Clin Investig. 2011; 121(5):2000–2012.

165. Kim H, Lee SK, Kim YM, Lee EH, Lim SJ, et al. Fluorescent iodized emulsion for pre and intraoperative sentinel lymph node imaging: validation in a preclinical model. Radiology. 2015; 275(1):196–204

166. Kim M, Koh YJ, Kim KE, Koh BI, Nam DH, et al. CXCR4 signaling regulates metastasis of chemoresistant melanoma cells by a lymphatic metastatic niche. Cancer Res. 2010; 70(24):10411-10421.

167. Kim T, Giuliano AE, Lyman GH. Lymphatic mapping and sentinel lymph node biopsy in early-stage breast carcinoma: a meta-analysis. Cancer. 2006;106(1):4–16.

168. Kimura T, Sugaya M, Oka T, Blauvelt A, Okochi H, et al. Lymphatic dysfunction attenuates tumor immunity through impaired antigen presentation. Oncotarget. 2015; 6:18081–18093.

169. Kitagawa Y, Fujii H, Mukai M, Kubota T, Ando N, et al. Intraoperative lymphatic mapping and sentinel lymph node sampling in esophageal and gastric cancer. Surg Oncol Clin N Am. 2002: 11(2):293–304

170. Kiupel M, Camus M. Diagnosis and prognosis of canine cutaneous mast cell tumors. Vet Clin North Am Small Anim Pract. 2019; 49(5):819–36.

171. Kiupel M, Webster JD, Bailey KL, Best S, DeLay J, et al. Proposal of a 2-tier histologic grading system for canine cutaneous mast cell tumors to more accurately predict biological behaviour. Vet Pathol 2011; 48(1):147–155.

172. Kiupel M, Webster JD, Kaneene JB, Miller R, Yuzbasiyan-Gurkan V. The use of KIT and tryptase expression patterns as prognostic tools for canine cutaneous mast cell tumors. Vet Pathol. 2004; 41:371–7.

173. Knapp DW, Adams LG, Degrand AM, Niles JD, Ramos-Vara J, et al. Sentinel lymph node mapping of invasive urinary bladder cancer in animal models using invisible light. Eur Urol. 2007; 52(6):1700–1708.

174. Knoblich K, Cruz Migoni S, Siew SM, Jinks E, Kaul B, et al. The human lymph node microenvironment unilaterally regulates T-cell activation and differentiation. PLOS Biol. 2018; 16(9):e2005046.

175. Kong SH, Noh YW, Suh YS, Park HS, Lee HJ, et al. Evaluation of the novel near-infrared fluorescence tracers pullulan polymer nanogel and indocyanine green/gamma-glutamic acid complex for sentinel lymph node navigation surgery in large animal models. Gastric Cancer. 2015; 18(1):55–64.

176. Krag DN, Weaver DL, Alex JC, Fairbank JT. Surgical resection and radiolocalization of the sentinel lymph node in breast cancer using a gamma probe. Surg Oncol. 1993; 2(6):335–339;

177. Krick EL, Billings AP, Shofer FS, Watanabe S, Sorenmo KU. Cytological lymph node evaluation in dogs with mast cell tumours: association with grade and survival. Vet Comp Oncol. 2009; 7:130-138.

178. Kristal O, Rassnick KM, Gliatto JM, Northrup NC, Chretin JD, et al. Hepatotoxicity associated with CCNU (Lomustine) chemotherapy in dogs. J Vet Intern Med 2004; 18:75–80.

179. Kry KL, Boston SE. Additional local therapy with primary reexcision or radiation therapy improves survival and local control after incomplete or close surgical excision of mast cell tumors in dogs. Vet Surg. 2014; 43:182-189.

180. Ku CK, Kass PH, Christopher MM. Cytologic-histologic concordance in the diagnosis of neoplasia in canine and feline lymph nodes: a retrospective study of 367 cases. Vet Comp Oncol. 2007; 15(4):1206-1217.

181. LaDue T, Price GS, Dodge R, Page RL, Thrall DE. Radiation therapy for incompletely resected canine mast cell tumours. Vet RadiolUltrasound 1998; 39: 57–62.

182. Lane RS, Femel J, Breazeale AP, Loo CP, Thibault G, et al. IFNgamma-activated dermal lymphatic vessels inhibit cytotoxic T cells in melanoma and inflamed skin. J Exp Med. 2018; 215(12):3057-3074.

183. Lane RS, Femel J, Breazeale AP, Loo CP, Thibault G, et al. IFN-activated dermal lymphatic vessels inhibit cytotoxic T cells in melanoma and inflamed skin. J Exp Med 2018; 215;3057–3074.

184. Langenbach A, McManus PM, Hendrick MJ, Shofer FS, Sorenmo KU. Sensitivity and specificity of methods of assessing the regional lymph nodes for evidence of metastasis in dogs and cats with solid tumours. J Am Vet Med Assoc. 2001; 218:1424-1428.

185. Lapsley J, Hayes GM, Janvier V, Newman AW, Peters-Kennedy J, et al. Influence of locoregional lymph node aspiration cytology vs sentinel lymph node mapping and biopsy on disease stage assignment in dogs with integumentary mast cell tumors. Vet Surg. 2021; 50:133–41.

186. Lauweryns JM, Boussauw L. The ultrastructure of lymphatic valves in the adult rabbit lung. Z Zellforsch Mikrosk Anat.1973; 143(2):149-168.

187. Layfield DM, Agrawal A, Roche H, Cutress RI. Intraoperative assessment of sentinel lymph nodes in breast cancer. Brit J Surg. 2011; 98:4-17.

188. Le CP, Nowell CJ, Kim-Fuchs C, Botteri E, Hiller JG, et al. Chronic stress in mice remodels lymph vasculature to promote tumour cell dissemination. Nat Commun. 2016; 7:10634.

189. Leak LV, Burke JF. Ultrastructural studies on the lymphatic anchoring filaments. J Cell Biol. 1968; 36(1):129-149.

190. Lee AS, Kim DH, Lee JE, et al. Erythropoietin induces lymph node lymphangiogenesis and lymph node tumor metastasis. Cancer Res. 2011; 71(13):4506-4517.

191. Lee JH, Park DJ, Kim YH, Shin CM, Lee HS, et al. Clinical implementations of preoperative computed tomography lymphography in gastric cancer: a comparison with dual tracer methods in sentinel node navigation surgery. Ann Surg Oncol. 2013; 20(7):2296–2303.

192. Leijte JA, van der Ploeg IM, Valdés Olmos RA, Nieweg OE, Horenblas S. Visualization of tumor blockage and rerouting of lymphatic drainage in penile cancer patients by use of SPECT/CT. J Nucl Med. 2009; 50(3):364-7.

193. Leiter U, Stadler R, Mauch C, Hohenberger W, Brockmeyer N, et al. Complete lymph node dissection versus no dissection in patients with sentinel lymph node biopsy positive melanoma (DeCOG-SLT): A multicentre, randomised, phase 3 trial. Lancet Oncol 2016; 17(6):757–767.

194. Lejeune A, Skorupski K, Frazier S, Vanhaezebrouck I, Rebhun RB, et al. Aggressive local therapy combined with systemic chemotherapy provides

long-term control in grade II stage 2 canine mast cell tumour: 21 cases (1999-2012). Vet Comp Oncol 2015; 13(3):267-80.

195. Leong SP, Pissas A, Scarato M, Gallon F, Pissas MH, et al. The lymphatic system and sentinel lymph node: conduit for cancer metastasis. Clin Exp Metastasis 2022; 39(1):139-157.

196. Li S, Li Q. Cancer stem cells, lymphangiogenesis, and lymphatic metastasis. Cancer Lett. 2015; 357(2):438-447.

197. Liebner EJ. Evaluation of perfluoroctylbromide for lymphography in the dog: comparison with ethiodol. Invest Radiol. 1977; 12: 368–372.

198. Lim H, Kim J, Li L, Lee A, Jeong J, et al. Bilateral medial iliac lymph node excision by a ventral laparoscopic approach: technique description. J Vet Med Sci. 2017; 79(9):1603-1610.

199. Lim JS, Choi J, Song J, Chung YE, Lim SJ, et al. Nanoscale iodized oil emulsion: a useful tracer for pretreatment sentinel node detection using CT lymphography in a normal canine gastric model. Surg Endosc. 2012;26(8): 2267–2274.

200. Linde KJ, Stockdale SL, Mison MB, Perry JA. The effect of prednisone on histologic and gross characteristics in canine mast cell tumors. Can Vet J. 2021; 62(1):45-50.

201. Liptak JM, Boston SE. Nonselective lymph node dissection and sentinel lymph node mapping and biopsy. Vet Clin Small Anim. 2019;49:793-807.

202. Liptak JM. Histologic margins and the residual tumour classification scheme. Vet Comp Oncol. 2021; 19(1):3-4.

203. Liss MA, Stroup SP, Qin Z, Hoh CK, Hall DJ, et al. Robotic-assisted fluorescence sentinel lymph node mapping using multimodal image guidance in an animal model. Urology. 2014; 84(4):982.e9–982.14.

204. Liu J, Liu X, He J, Gou B, Deng S, et al. Percutaneous contrast-enhanced ultrasound for localization and diagnosis of sentinel lymph node in early breast cancer. Sci Rep. 2019; 9:13545.

205. Llabrés-Díaz, F. J. Ultrasonography of the medial iliac lymph nodes in the dog. Vet Radiol Ultrasound 2004; 45: 156–165.

206. London CA, Seguin B. Mast cell tumours in the dog. Vet Clin North Am Small Anim Pract. 2003; 33(3):473–489.

207. London CA, Malpas PB, Wood-Follis SL, Boucher JF, Rusk AW, et al. Multi-center, placebo-controlled, double-blind, randomized study of oral toceranib phosphate (SU11654), a receptor tyrosine kinase inhibitor, for the treatment of dogs with recurrent (either local or distant) mast cell tumor following surgical excision. Clin Cancer Res. 2009; 15(11):3856-65.

208. London CA, Thamm DH. Mast Cell Tumors. In: Vail DM, Thamm DH, Liptak JM. Withrow & MacEwen's Small Animal Clinical Oncology. 6th ed. St Louis: Elsevier. 2020.

209. Loo CP, Nelson NA, Lane RS, Booth JL, Loprinzi Hardin SC, et al. Lymphatic vessels balance viral dissemination and immune activation following cutaneous viral infection. Cell Rep. 2017; 20(13):3176–3187.

210. Lukacs-Kornek V, Malhotra D, Fletcher AL, Acton SE, Elpek KG, et al. Regulated release of nitric oxide by nonhematopoietic stroma controls expansion of the activated T cell pool in lymph nodes. Nat Immunol. 2011; 12(11):1096-1104.

211. Lund AW, Wagner M, Fankhauser M, Steinskog ES, Broggi MA, et al. Lymphatic vessels regulate immune microenvironments in human and murine melanoma. J Clin Investig. 2016; 126:3389–3402.

212. Lurie DM, Seguin B, Schneider PD, Verstraete FJ, Wisner ER. Contrast-assisted ultrasound for sentinel lymph node detection in spontaneously arising canine head and neck tumors. Invest Radiol. 2006; 41(4):415–421.

213. Lutter S, Xie S, Tatin F, Makinen T. Smooth muscle-endothelial cell communication activates Reelin signaling and regulates lymphatic vessel formation. J Cell Biol. 2012; 197(6):837-849.

214. Luzzi KJ, MacDonald IC, Schmidt EE, Kerkvliet N, Morris VL, et al. Multistep nature of metastatic inefficiency: dormancy of solitary cells after successful extravasation and limited survival of early micrometastases. Am J Pathol. 1998; 153(3):865-873.

215. Lyles SE, Milner RJ, Kow K, Salute ME. In vitro effects of the tyrosine kinase inhibitor, masitinib mesylate, on canine hemangiosarcoma cell lines. Vet Comp Oncol. 2012; 10(3):223-35.

216. Lyman GH, Somerfield MR, Bosserman LD, Perkins CL, Weaver DL, et al. Sentinel Lymph Node Biopsy for Patients With Early-Stage Breast Cancer:

American Society of Clinical Oncology Clinical Practice Guideline Update. J Clin Oncol. 2017; 35(5):561-564.

217. Ma Q, Dieterich LC, Detmar M. Multiple roles of lymphatic vessels in tumor progression. Curr Opin Immunol 2018; 53:7–12.

218. Ma Q, Dieterich LC, Ikenberg K, Bachmann SB, Mangana J, et al. Unexpected contribution of lymphatic vessels to promotion of distant metastatic tumor spread. Sci Adv. 2018; 4(8):eaat4758

219. Ma Q, Ries M, Decker Y, Müller A, Riner C, et al. Rapid lymphatic efflux limits cerebrospinal fluid flow to the brain. Acta Neuropathol. 2019; 137(1):151-165.

220. Macedo TR, de Queiroz GF, Casagrande TAC, Alexandre PA, Brandão PE, et al. Imatinib Mesylate for the Treatment of Canine Mast Cell Tumors: Assessment of the Response and Adverse Events in Comparison with the Conventional Therapy with Vinblastine and Prednisone. Cells. 2022; 11(3):571.

221. Majeski SA, Steffey MA, Fuller M, Hunt GB, Mayhew PD, et al. Indirect computed tomographic lymphography for iliosacral lymphatic mapping in a cohort of dogs with anal sac gland adenocarcinoma: technique description. Vet Radiol Ultrasound. 2017; 58: 295–303.

222. Marconato L, Bettini G, Giacoboni C, Romanelli G, Cesari A, et al. Clinicopathological features and outcome for dogs with mast cell tumours and bone marrow involvement. J Vet Intern Med. 2008b; 22: 1001–1007.

223. Marconato L, Zorzan E, Giantin M, Di Palma S, Cancedda S, et al. Concordance of c-kit mutational status in matched primary and metastatic cutaneous canine mast cell tumors at baseline. J Vet Intern Med. 2014; 28:547–53.

224. Marconato, L, Polton, G, Stefanello, D, Morello E, Ferrari R, et al. Therapeutic impact of regional lymphadenectomy in canine stage II cutaneous mast cell tumours. Vet Comp Oncol. 2018; 16:580– 589.

225. Mariani G, Moresco L, Viale G, Villa G, Bagnasco M, et al. Radioguided sentinel lymph node biopsy in breast cancer surgery. J Nucl Med. 2001; 42(8):1198–1215.

226. Masannat Y, Shenoy H, Speirs V, Hanby A, Horgan K. Properties and characteristics of the dyes injected to assist axillary sentinel node localization in breast surgery. Eur J Surg Oncol 2006; 32: 381-4.

227. Mashino K, Sadanaga N, Yamaguchi H, Tanaka F, Ohta M, et al. Expression of chemokine receptor CCR7 is associated with lymph node metastasis of gastric carcinoma. Cancer Res 2002; 62(10):2937–2941.

228. Matsuda A, Tanaka A, Amagai Y, Ohmori K, Nishikawa S, et al. Glucocorticoid sensitivity depends on expression levels of glucocorticoid receptors in canine neoplastic mast cells. Vet Immunol Immunopathol. 2011; 144(3-4):321-8.

229. Matsuda K, Sakaguchi K, Kobayashi S, Tominaga M, Hirayama K, et al. Systemic candidiasis and mesenteric mast cell tumor with multiple metastases in a dog. J Vet Med Sci. 2009; 71:229–32.

230. Matsuura N, Go T, Fujiwara A, Nakano T, Nakashima N, et al. Lymphatic invasion is a cause of local recurrence after wedge resection of primary lung cancer. Gen Thorac Cardiovasc Surg. 2019; 67:861–866.

231. Mayer MN, Kraft SL, Bucy DS, Waldner CL, Elliot KM, et al. Indirect magnetic resonance lymphography of the head and neck of dogs using Gadofluorine M and a conventional gadolinium contrast agent: a pilot study. Can Vet J. 2012; 53(10):1085–1090.

232. Mayer MN, Lawson JA, Silver TI. Sonographic characteristics of presumptively normal canine medial iliac and superficial inguinal lymph nodes. Vet Radiol Ultrasound 2010; 51:638–641.

233. Mayer MN, Silver TI, Lowe CK, Anthony JM. Radiographic lymphangiography in the dog using iodized oil. Vet Comp Oncol. 2013; 11(2): 151–161.

234. Mayer MN, Sweet KA, Patsikas MN, Sukut SL, Waldner CL. Frequency of an accessory popliteal efferent lymphatic pathways in dogs. Vet Radiol Ultrasound 2018; 59(3):365-373.

235. McCaw DL, Miller MA, Ogilvie GK, Withrow SJ, Brewer WG Jr, et al. Response of canine mast cell tumors to treatment with oral prednisone. J Vet Intern Med. 1994; 8(6):406-8.

236. McManus PM. Frequency and severity of mastocytemia in dogs with and without mast cell tumors: 120 cases (1995–97). J Am Vet Med Assoc 1999; 215:355–357.

237. McNeil EA, Prink AL, O'Brien TD. Evaluation of risk and clinical outcome of mast cell tumours in pug dogs. Vet Comp Oncol. 2006; 4(1):2–8.

238. Meier F, Will S, Ellwanger U, Schlagenhauff B, Schittek B, et al. Metastatic pathways and time courses in the orderly progression of cutaneous melanoma. Br J Dermatol. 2002; 147(1):62-70.

239. Mendez SE, Drobatz KJ, Duda LE, White P, Kubicel L, et al. Treating the locoregional lymph nodes with radiation and/or surgery significantly improves outcome in dogs with high-grade mast cell tumours. Vet Comp Oncol. 2020;18(2):239–46.

240. Merchant NB, Guillem JG, Paty PB, Enker WE, Minsky BD, et al. T3N0 rectal cancer: Results following sharp mesorectal excision and no adjuvant therapy. J Gastrointest Surg 1999; 3(6):642–647.

241. Michels GM, Knapp DW, DeNicola DB, Glickman N, Bonney P, et al. Prognosis following surgical excision of canine cutaneous mast cell tumors with histopathologically tumore-free versus nontumor-free margins: a retrospective study of 31 cases. J Am Anim Hosp Assoc. 2002; 38(5):458-466.

242. Misdorp W. Incomplete surgery, local immunostimulation, and recurrence of some tumour types in dogs and cats. Vet Q. 1987; 9(3): 279–286.

243. Misdorp W. Mast cells and canine mast cell tumours. A review. Vet Q. 2004; 26(4):156–69.

244. Mohs AM, Mancini MC, Provenzale JM, Saba CF, Cornell KK, et al. An integrated widefield imaging and spectroscopy system for contrast-enhanced, image-guided resection of tumors. IEEE Trans Biomed Eng. 2015; 62(5):1416–1424.

245. Moirano SJ, Lima SF, Hume KR, Brodsky EM. Association of prognostic features and treatment on survival time of dogs with systemic mastocytosis: a retrospective analysis of 40 dogs. Vet Comp Oncol. 2018; 16(1):E194–201.

246. Mokhtar M, Tadokoro Y, Nakagawa M, Morimoto M, Takechi H, et al. Triple assessment of sentinel lymph node metastasis in early breast cancer using

preoperative CTLG, intraoperative fluorescence navigation and OSNA. Breast Cancer. 2016; 23(2):202–210.

247. Molodtsov AK, Khatwani N, Vella JL, Lewis KA, Zhao Y, et al. Resident memory CD8+ T cells in regional lymph nodes mediate immunity to metastatic melanoma. Immunity 2021; 54:2117–2132.

248. Moore AS, Frimberger AE, Taylor D, Sullivan N. Retrospective outcome evaluation for dogs with surgically excised, solitary Kiupel high-grade, cutaneous mast cell tumours. Vet Comp Oncol. 2020; 18(3):402-408.

249. Moore JE Jr, Bertram CD. Lymphatic System Flows. Annu Rev Fluid Mech 2018; 50:459-82.

250. .

251. Morton DL, Cochran AJ, Thompson JF, Elashoff R, Essner R, et al. Sentinel node biopsy for early stage melanoma: accuracy and morbidity in MSLT-I, an international multicenter trial. Ann Surg. 2005; 242(3):302–311.

252. Morton DL, Wen DR, Wong JH, Economou JS, Cagle LA, et al. Technical details of intraoperative lymphatic mapping for early stage melanoma. Arch Surg. 1992; 127(4):392–399.

253. Morton DL. Overview and update of the phase III Multicenter Selective Lymphadenectomy Trials (MSLT-I and MSLT-II) in melanoma. Clin Exp Metastasis 2012; 29:699–706

254. Motomura K, Ishitobi M, Komoike Y, Koyama H, Noguchi A, et al. SPIO-enhanced magnetic resonance imaging for the detection of metastases in sentinel nodes localized by computed tomography lymphography in patients with breast cancer. Ann Surg Oncol. 2011;18(12):3422–3429.

255. Motomura K, Sumino H, Noguchi A, Horinouchi T, Nakanishi K. Sentinel nodes identified by computed tomography-lymphography accurately stage the axilla in patients with breast cancer. BMC Med Imaging. 2013; 13:42.

256. Mullins MN, Dernell WS, Withrow SJ, Ehrhart EJ, Thamm DH, et al. Evaluation of prognostic factors associated with outcome in dogs with multiple cutaneous mast cell tumors treated with surgery with and without adjuvant treatment: 54 cases (1998-2004). J Am Vet Med Assoc. 2006; 228(1):91-95.

257. Murphy MC, Sullivan M, Gomes BJ, Kaczmarska A, Hammond GJC. Evaluation of radiographs for the detection of sublumbar lymphadenopathy in dogs. Can Vet J. 2020; 61(7):749-756.

258. Murphy S, Sparkes AH, Blunden AS, Brearley MJ, Smith KC. Effects of stage and number of tumours on prognosis of dogs with cutaneous mast cell tumours. Vet Rec. 2006; 158:287-291.

259. Murphy S, Sparkes AH, Smith KC, Blunden AS, Brearley MJ. Relationships between the histological grade of cutaneous mast cell tumours in dogs, their survival and the efficacy of surgical resection. Vet Rec. 2004; 154(24):743-746.

260. Nadafi R, Gago de Graça C, Keuning ED, Koning JJ, Kivit S, et al. Lymph node stromal cells generate antigen-specific regulatory T cells and control autoreactive T and B cell responses. Cell Rep. 2020; 30(12):4110-4123.

261. Naganobu K, Ohigashi Y, Akiyoshi T, Hagio M, Miyamoto T, et al. Lymphography of the thoracic duct by percutaneous injection of iohexol into the popliteal lymph node of dogs: experimental study and clinical application. Vet Surg. 2006; 35(4):377–381.

262. Nakayama H, Ohuchida K, Yonenaga A, Sagara A, Ando Y, et al. S100P regulates the collective invasion of pancreatic cancer cells into the lymphatic endothelial monolayer. Int J Oncol. 2019; 55:211–222.

263. Nathanson SD, Mahan M. Sentinel lymph node pressure in breast cancer. Ann Surg Oncol. 2011; 18(13):3791-6.

264. Néčová S, Mason SL, North SM. Outcome of dogs with intermediate grade low mitotic index high Ki67 mast cell tumours treated with surgery and single agent lomustine. Aust Vet J. 2021; 99(5):146-151.

265. Newman LA. Lymphatic mapping and sentinel lymph node biopsy in breast cancer patients: a comprehensive review of variations in performance and technique. J Ame Coll Surg. 2004;199:804-16.

266. Newman SJ, Mrkonjich L, Walker KK, Rohrbach BW. Canine subcutaneous mast cell tumour: diagnosis and prognosis. J Comp Pathol. 2007; 136:231–39.

267. Niebling MG, Pleijhuis RG, Bastiaannet E, Brouwers AH, van Dam GM, et al. A systematic review and meta-analyses of sentinel lymph node

identification in breast cancer and melanoma, a plea for tracer mapping. Eur J Surg Oncol. 2016; 42(4):466–473.

268. Niedbala W, Cai B, Liu H, Pitman N, Chang L, et al. Nitric oxide induces CD4+CD25+ Foxp3 regulatory T cells from CD4+CD25 T cells via p53, IL-2, and OX40. Proc Natl Acad Sci USA. 2007; 104(39):15478-15483.

269. Moody A, Bull J, Culpan AM, Munyombwe T, Sharma N, et al. Preoperative sentinel lymph node identification, biopsy and localisation using contrast enhanced ultrasound (CEUS) in patients with breast cancer: a systematic review and meta-analysis. Clin Radiol. 2017; 72:959-971.

270. Niimi K, Yoshizawa M, Nakajima T, Saku T. Vascular invasion in squamous cell carcinomas of human oral mucosa. Oral Oncol. 2001; 37:357–364.

271. Northrup NC, Harmon BG, Gieger TL, Brown CA, Carmichael P, et al. Variation among pathologists in histologic grading of canine cutaneous mast cell tumors. J Vet Diagn Invest. 2005; 17(3):245–248.

272. Northrup NC, Howerth EW, Harmon BG, Brown CA, Carmichael, et al. Variation among pathologists in the histologic grading of canine cutaneous mast cell tumors with uniform use of a single grading reference. J Vet Diagn Invest. 2005b; 17(6):561–564.

273. Nwogu CE, Kanter PM, Anderson TM. Pulmonary lymphatic mapping in dogs: use of technetium sulfur colloid and isosulfan blue for pulmonary sentinel lymph node mapping in dogs. Cancer Invest. 2002; 20(7-8):944–947.

274. O'Keefe DA, Couto CG, Burke-Schwartz C, Jacobs RM. Systemic mastocytosis in 16 dogs. J Vet Intern Med. 1987; 1(2):75–80.

275. O'Keefe DA. Canine mast cell tumours. Vet Clin North Am Small Anim Prac. 1990; 20(4):1105–1115.

276. Ogawa F, Amano H, Eshima K, Ito Y, Matsui Y, et al. Prostanoid induces premetastatic niche in regional lymph nodes. J Clin Invest. 2014;124(11):4882-4894.

277. Oliveira MT, Campos M, Lamego L, Magalhães D, Menezes R, et al. Canine and Feline Cutaneous Mast Cell Tumor: A Comprehensive Review of Treatments and Outcomes. Top Companion Anim Med. 2020; 41:100472

278. Oliver G, Alitalo K. The lymphatic vasculature: recent progress and paradigms. Annu Rev Cell Dev Biol 2005; 21:457-83.

279. Oliver G, Kipnis J, Randolph GJ, Harvey NL. The lymphatic vasculature in the 21st century: novel functional roles in homeostasis and disease. Cell. 2020; 182(2):270-296.

280. Oliver G. Lymphatic vasculature development. Nat Rev Immunol 2004; 4:35-45.

281. Olmeda D, Cerezo-Wallis D, Riveiro-Falkenbach E, Pennacchi PC, Contreras-Alcalde M, et al. Whole-body imaging of lymphovascular niches identifies pre-metastatic roles of midkine. Nature. 2017; 546(7660):676-680.

282. Olsen JA, Thomson M, O'Connell K, Wyatt K. Combination vinblastine, prednisolone and toceranib phosphate for treatment of grade II and III mast cell tumours in dogs. Vet Med Sci. 2018; 4(3):237–51.

283. Olszewski WL, Stanczyk M, Gewartowska M, Domaszewska-Szostek A, Durlik M. Lack of functioning intratumoral lymphatics in colon and pancreas cancer tissue. Lymphat Res Biol. 2012; 10(3):112-117.

284. Owen LA. TNM Classification of Tumours in Domestic Animals. Geneva: World Health Organization, 1980. p. 53.

285. Ozaki K, Yamagami T, Nomura K, Narama I. Mast cell tumours of the gastrointestinal tract in 39 dogs. Vet Pathol. 2002; 39:557–564.

286. Padera TP, Kadambi A, di Tomaso E, Carreira CM, Brown EB, et al. Lymphatic metastasis in the absence of functional intratumor lymphatics. Science. 2002; 296(5574):1883-1886.

287. Paget S. The distribution of secondary growths in cancer of the breast. 1889. Cancer Metastasis Rev 1989; 8:98-101.

288. Palladino S, Keyerleber MA, King RG, Burgess KE. Utility of computed tomography versus abdominal ultrasound examination to identify iliosacral lymphadenomegaly in dogs with apocrine gland adenocarcinoma of the anal sac. J Vet Intern Med. 2016; 30:1858–1863.

289. Pang MF, Georgoudaki AM, Lambut L, Johansson JE, Tabor V, et al. TGF-_1-induced EMT promotes targeted migration of breast cancer cells through the lymphatic system by the activation of CCR7/CCL21-mediated chemotaxis. Oncogene. 2016; 35:748–760.

290. Papadopoulou PL, Patsikas MN, Charitanti A, Kazakos GM, Papazoglou LG, et al. The lymph drainage pattern of the mammary glands in the cat: a

lymphographic and computerized tomography lymphographic study. Anat Histol Embryol.2009;38(4):292–299.

291. Pastushenko I, Vermeulen PB, Carapeto F, Van den Eynden G, Rutten A, et al. Blood microvessel density, lymphatic microvessel density and lymphatic invasion in predicting melanoma metastases: Systematic review and meta-analysis. Br J Dermatol. 2014; 170:66–77.
292. Patnaik AK, Ehler WJ, MacEwen EG. Canine cutaneous mast cell tumour: Morphologic grading and survival time in 83 dogs. Vet Pathol. 1984; 21:469-474.
293. Patsikas MN, Dessiris A. The lymph drainage of the mammary glands in the bitch: a lymphographic study. Part I: the 1st, 2nd, 4th and 5th mammary glands. Anat Histol Embryol. 1996; 25(2):131–138.
294. Patsikas MN, Dessiris A. The lymph drainage of the mammary glands in the bitch: a lymphographic study. Part II: the 3rd mammary gland. Anat Histol Embryol. 1996b; 25(2):139–143.
295. Patsikas MN, Karayannopoulou M, Kaldrymidoy E, Papazoglou LG, Papadopoulou PL, et al. The Lymph Drainage of the Neoplastic Mammary Glands in the Bitch: A Lymphographic Study. Anat Histol Embryol. 2006; 35(4):228–34.
296. Patsikas MN, Papadopoulou PL, Charitanti A, Kazakos GM, Soultani CB, et al. Computed tomography and radiographic indirect lymphography for visualization of mammary lymphatic vessels and the sentinel lymph node in normal cats. Vet Radiol Ultrasound. 2010; 51(3):299–304.
297. Pecceu E, Serra Varela JC, Handel I, Piccineli C, Milne E, et al. Ultrasound is a poor predictor of early or overt liver or spleen metastasis in dogs with high-risk mast cell tumours. Vet Comp Oncol. 2019; 18(3):389-401
298. Pereira CT, Marques FLN, Williams J, De Martin BW, Bombonato PP. 99mTc-labeled dextran for mammary lymphoscintigraphy in dogs. Vet Radiol Ultrasound. 2008; 49(5): 487–491.
299. Pereira CT, Rahal SC, de Carvalho Balieiro JC, Ribeiro AACM. Lymphatic drainage on healthy and neoplastic mammary glands in female dogs: can it really be altered? Anat Histol Embryol. 2003; 32(5):282–290.

300. Pereira ER, Kedrin D, Seano G, Gautier O, Meijer EFJ, et al. Lymph node metastases can invade local blood vessels, exit the node, and colonize distant organs in mice. Science. 2018; 359(6382):1403-1407.

301. Petrova TV, Koh GY. Biological functions of lymphatic vessels. Science 2020; 369(6500):eaax4063.

302. Petrova TV, Koh GY. Organ-specific lymphatic vasculature: From development to pathophysiology. J Exp Med. 2018; 215:35–49.

303. Pflicke H, Sixt M. Preformed portals facilitate dendritic cell entry into afferent lymphatic vessels. J Exp Med. 2009; 206(13):2925-2935.

304. Pflug JJ, Calnan JS. Lymphatics: Normal anatomy in the dog hind leg. J Anat. 1969; 105(Pt 3):457–465.

305. Pinheiro LG, Oliveira Filho RS, Vasques PH, Filgueira PHO, Aragão DHP, et al. Hemosiderin: a new marker for sentinel lymph node identification. Acta Cir Bras. 2009;24(6):432–436.

306. Poirier VJ, Adams WM, Forrest LJ, Green EM, Dubielzig RR et al. Radiation therapy for incompletely excised grade II canine mast cell tumours. J Am Anim Hosp Assoc. 2006; 42: 430–434.

307. Pollard RE, Fuller MC, Steffey MA. Ultrasound and computed tomography of the iliosacral lymphatic centre in dogs with anal sac gland carcinoma. Vet Comp Oncol. 2017; 15:299–306.

308. Preziosi R, Morini M, Sarli G. Expression of the KIT protein (CD117) in primary cutaneous mast cell tumors of the dog. J Vet Diagn Invest. 2004; 16:554–61.

309. Proulx ST, Detmar M. Molecular mechanisms and imaging of lymphatic metastasis. Exp Cell Res. 2013b; 319(11):1611-7.

310. Proulx ST, Luciani P, Christiansen A, Karaman S, Blum KS, et al. Use of a PEG-conjugated bright near-infrared dye for functional imaging of rerouting of tumor lymphatic drainage after sentinel lymph node metastasis. Biomaterials. 2013; 34(21):5128-37.

311. Proulx ST, Luciani P, Derzsi S, Rinderknecht M, Mumprecht V, et al. Quantitative imaging of lymphatic function with liposomal indocyanine green. Cancer Res. 2010; 70(18):7053-62.

312. Pugh CR. Ultrasonographic examination of abdominal lymph nodes in the dog. Vet Radiol Ultrasound. 1994; 35:110–115.

313. Qi H, Kastenmuller W, Germain RN. Spatiotemporal basis of innate and adaptive immunity in secondary lymphoid tissue. Annu Rev Cell Dev Biol. 2014; 30:141-167.

314. Qian CN, Berghuis B, Tsarfaty G, Bruch M, Kort EJ, et al. Preparing the "soil": the primary tumor induces vasculature reorganization in the sentinel lymph node before the arrival of metastatic cancer cells. Cancer Res. 2006; 66(21):10365-10376.

315. Qiu SQ, Zhang GJ, Jansen L, Vries J, Schröder CP, et al. Evolution of sentinel lymph node biopsy in breast cancer. Crit Rev Oncol Hematol. 2018; 123:83–94.

316. Radlinsky MG, Mason DE, Biller DS, Olsen D. Thoracoscopic visualization and ligation of the thoracic duct in dogs. Vet Surg. 2002; 31(2): 138–146.

317. Randall EK, Jones MD, Kraft SL, Worley DR. The development of an indirect computed tomography lymphography protocol for sentinel lymph node detection in head and neck cancer and comparison to other sentinel lymph node mapping techniques. Vet Comp Oncol. 2020; 18:634–44.

318. Rantakari P, Auvinen K, Jäppinen N, Kapraali M, Valtonen J, et al. The endothelial protein PLVAP in lymphatics controls the entry of lymphocytes and antigens into lymph nodes. Nat Immunol. 2015; 16(4):386-396.

319. Ray A, Provenzano PP. Aligned forces: Origins and mechanisms of cancer dissemination guided by extracellular matrix architecture. Curr Opin Cell Biol. 2021; 72:63–71.

320. Reed HO, Wang L, Sonett J, Chen M, Yang J, et al. Lymphatic impairment leads to pulmonary tertiary lymphoid organ formation and alveolar damage. J Clin Invest. 2019; 129(6):2514-2526.

321. Rehnblom ER, Skinner OT, Mickelson MA, Hutcheson KD. Axillary lymphadenectomy in dogs: A description of surgical technique. Vet Comp Oncol. 2022; [in press]

322. Reynolds JS, Troy TL, Mayer RH, Thompson AB, Waters DJ, et al. Imaging of spontaneous canine mammary tumors using fluorescent contrast agents. Photochem Photobiol. 1999; 70(1):87–94.

323. Reynoso GV, Weisberg AS, Shannon JP, McManus DT, Shores L, et al. Lymph node conduits transport virions for rapid T cell activation. Nat Immunol. 2019; 20(5):602-612.

324. Rezzola, S, Sigmund, EC, Halin, C, Ronca, R. The lymphatic vasculature: An active and dynamic player in cancer progression. Med Res Rev. 2022; 42:576- 614

325. Rigby DA, Ferguson DJ, Johnson LA, Jackson DG. Neutrophils rapidly transit inflamed lymphatic vessel endothelium via integrin-dependent proteolysis and lipoxin-induced junctional retraction. J Leukoc Biol 2015; 98: 897–912.

326. Robat C, London C, Bunting L, McCartan L, Stingle N, et al. Safety evaluation of combination vinblastine and toceranib phosphate (Palladia®) in dogs: a phase I dose-finding study. Vet Comp Oncol. 2012; 10(3):174-83.

327. Rossi F, Korner M, Suarez J, Carozzi G, Meier VS, et al. Computed tomographic lymphography as a complementary technique for lymph node staging in dogs with malignant tumors of various sites. Vet Radiol Ultrasound. 2018; 59(2):155-162.

328. Rouhani SJ, Eccles JD, Riccardi P, Peske JD, Tewalt EF, et al. Roles of lymphatic endothelial cells expressing peripheral tissue antigens in CD4 T-cell tolerance induction. Nat Commun. 2015; 6:6771.

329. Saha S, Johnston G, Korant A, Shaik M, Kannan M, et al. Aberrant drainage of sentinel lymph nodes in colon cancer and its impact on staging and extent of operation. Am J Surg. 2013; 205(3):302-305.

330. Saxena K, Jolly MK, Balamurugan K. Hypoxia, partial EMT and collective migration: Emerging culprits in metastasis. Transl Oncol 2020; 13:100845.

331. Scallan JP, Zawieja SD, Castorena-Gonzalez JA, Davis MJ. Lymphatic pumping: mechanics, mechanisms and malfunction. J Physiol. 2016; 594(20):5749-5768.

332. Scarpa F, Sabattini S, Bettini G. Cytological grading of canine cutaneous mast cell tumours. Vet Comp Oncol. 2016; 14:245–51.

333. Scarpa F, Sabattini S, Marconato L, Capitani O, Morini M, et al. Use of histologic margin evaluation to predict recurrence of cutaneous malignant tumors in dogs and cats after surgical excision. J Am Vet Med Assoc. 2012; 240(10):1181-1187

334. Scase TJ, Edwards D, Miller J, Henley W, Smith K, et al. Canine mast cell tumors: correlation of apoptosis and proliferation markers with prognosis. J Vet Intern Med. 2006; 20(1):151–8.

335. Schaafsma BE, Mieog JSD, Hutteman M, Van der Vorst JR, Kuppen PJK, et al. The clinical use of indocyanine green as a near-infrared fluorescent contrast agent for image-guided oncologic surgery. J Surg Oncol. 2011; 104(3):323–332.

336. Schacher JF, Edeson JF, Sulahian A, Rizk G. An 18-month longitudinal lymphographic study of filarial diseases in dogs infected with Brugia pahangi (Buckley and Edeson, 1956). Ann Trop Med Parasitol. 1973; 67:81–94.

337. Schacher JF, Sulahian A. Lymphatic drainage patterns and experimental filariasis in dogs. Ann TropMed Parasitol. 1972; 66:209–217.

338. Schackert G, Fidler IJ. Site-specific metastasis of mouse melanomas and a fibrosarcoma in the brain or meninges of syngeneic animals. Cancer Res 1988; 48:3478-84.

339. Schineis P, Runge P, Halin C. Cellular traffic through afferent lymphatic vessels. Vascul Pharmacol. 2019; 112:31-41.

340. Schwager S, Detmar M. Inflammation and lymphatic function. Front Immunol. 2019; 10:308.

341. Scott MA and Stockham SL. Basophils and mast cells. In: Schalm's Veterinary Haematology. 5th edn., BF Feldman, JG Zinkl and NC Jain, eds., Philadelphia, LippincottWilliams &Wilkins, 2000: 308–315

342. Séguin B, Besancon MF, McCallan JL, Dewe LL, Tenwolde MC, et al. Recurrence rate, clinical outcome, and cellular proliferation indices as prognostic indicators after incomplete surgical excision of cutaneous grade II mast cell tumors: 28 dogs (1994–2002). J Vet Intern Med 2006; 20(4):933-940.

343. Séguin B, Leibman NF, Bregazzi VS, Ogilvie GK, Powers BE, et al. Clinical outcome of dogs with grade-II mast cell tumors treated with surgery alone: 55 cases (1996–1999). J Am Vet Med Assoc. 2001; 218(7):1120–3.

344. Seiler GS, Brown JC, Reetz JA, Taeymans O, Bucknoff M, et al. Safety of contrast-enhanced ultrasonography in dogs and cats: 488 cases (2002-2011). J Am Vet Med Assoc. 2013; 242:1255-1259.

345. Serra Varela JC, Pecceu E, Handel I, Lawrence J. Tolerability of a rapid-escalation vinblastine-prednisolone protocol in dogs with mast cell tumours. Vet Med Sci. 2016; 2(4):266-280

346. Sever A, Jones S, Cox K, Weeks J, Mills P, et al. Preoperative localization of sentinel lymph nodes using intradermal microbubbles and contrast-enhanced ultrasonography in patients with breast cancer. Br J Surg. 2009; 96(11):1295–1299.

347. Sever AR, Mills P, Jones SE, Cox K, Weeks J, et al. Preoperative sentinel node identification with ultrasound using microbubbles in patients with breast cancer. Am J Roentgenol. 2011;196(2):251–256.

348. Sevick-Muraca EM. Translation of near-infrared fluorescence imaging technologies: emerging clinical applications. Annu Rev Med. 2012; 63:217–231.

349. Sfiligoi G, Rassnick KM, Scarlett JM, Northrup NC, Gieger TL. Outcome of dogs with mast cell tumours in the inguinal or perineal region versus other cutaneous locations: 124 cases (1990–2001). J Am Vet Vet Med Assoc .2005; 226:1368–1374.

350. Shekell CC, Thomson MJ, Miller RI, Mackie JT. Primary tonsillar mast cell tumour in a dog. Aust Vet J. 2018; 96:184–87.

351. Shoop SJ, Marlow S, Church DB, English K, McGreevy PD, et al. Prevalence and risk factors for mast cell tumors in dogs in England. Canine Genet Epidemiol. 2015; 2(1).

352. Simpson AM, Ludwig LL, Newman SJ, Bergman PJ, Hottinger HA et al. Evaluation of surgical margins required for complete excision of cutaneous mast cell tumours in dogs. Journal of the American Veterinary Medical Association 2004; 224:236–240.

353. Sinha D, Saha P, Samanta A, Bishayee A. Emerging Concepts of Hybrid Epithelial-to-Mesenchymal Transition in Cancer Progression. Biomolecules. 2020; 10:1561.

354. Sixt M, Kanazawa N, Selg M, Samson T, Roos G, et al. The conduit system transports soluble antigens from the afferent lymph to resident dendritic cells in the T cell area of the lymph node. Immunity. 2005; 22(1):19-29.

355. Skelley JF, Price JE, Koehler R. Applications of direct lymphangiography in the dog. Am J Vet Res. 1964; 25:747–755.

356. Skinner OT, Boston SE, Souza CHM. Patterns of lymph node metastasis identified following bilateral mandibular and medial retropharyngeal

lymphadenectomy in 31 dogs with malignancies of the head. Vet Comp Oncol. 2017; 15:881-889.

357. Sledge DG, Webster J, Kiupel M. Canine cutaneous mast cell tumors: a combined clinical and pathologic approach to diagnosis, prognosis, and treatment selection. Vet J. 2016; 215:43–54.

358. Smaropoulos EC, Papazoglou LG, Patsikas MN, Vretou E, Petropoulos AS. Lymphatic regeneration following hind limb replantation: An experimental study in the dog. Eur J Pediatr Surg. 2005; 15:337–342.

359. Smiech A, Slaska B, Łopuszynski W, Jasik A, Bochyńska D, et al. Epidemiological assessment of the risk of canine mast cell tumours based on the Kiupel two-grade malignancy classification. Acta Vet Scand. 2018; 60:70.

360. Smith J, Kiupel M, Farrelly J, Cohen R, Olmsted G, et al. Recurrence rates and clinical outcome for dogs with grade II mast cell tumours with a low AgNOR count and Ki67 index treated with surgery alone. Vet Comp Oncol. 2017; 15(1):36–45.

361. Smith K, O'Brien R. Radiographic Characterization of Enlarged Sternal Lymph Nodes in 71 Dogs and 13 Cats. J Am Anim Hosp Assoc. 2012; 48(3):176–81.

362. Smith MM. Surgical approach for lymph node staging of oral and maxillofacial neoplasms in dogs. J Vet Dent 2002; 19:170–4.

363. Smith MM. Surgical approach for lymph node staging of oral and maxillofacial neoplasms in dogs. J Am Anim Hosp Assoc. 1995; 31(6):514-8.

364. Smrkovski OA, Essick L, Rohrbach BW, Legendre AM. Masitinib mesylate for metastatic and non-resectable canine cutaneous mast cell tumours. Vet Comp Oncol. 2015; 13(3):314-21.

365. Somasundaram SK, Chicken DW, Keshtgar MR. Detection of the sentinel lymph node in breast cancer. Br Med Bull 2007; 84:117-31.

366. Song E, Mao T, Dong H, Boisserand LSB, Antila S, et al. VEGF-C-driven lymphatic drainage enables immunosurveillance of brain tumours. Nature. 2020; 577(7792):689-694.

367. Soultani C, Patsikas MN, Karayannopoulou M, Jakovljevic S, Chryssogonidis I, et al. Assessment of sentinel lymph node metastasis in

canine mammary gland tumors using computed tomographic indirect lymphography. Vet Radiol Ultrasound. 2017; 58:186-196.

368. Sperveslage J, Frank S, Heneweer C, Egberts J, Schniewind B, et al. Lack of CCR7 expression is rate limiting for lymphatic spread of pancreatic ductal adenocarcinoma. Int J Cancer. 2012; 131:E371–E381.
369. Sperveslage J, Frank S, Heneweer C, Egberts, J, Schniewind, B, et al. Lack of CCR7 expression is rate limiting for lymphatic spread of pancreatic ductal adenocarcinoma. Int J Cancer. 2012; 131:E371–E381.
370. Spranger S, Gajewski TF. Impact of oncogenic pathways on evasion of antitumour immune responses. Nat Rev Cancer. 2018; 18(3):139-147.
371. Stacker SA, Williams SP, Karnezis T, Shayan R, Fox SB, et al. Lymphangiogenesis and lymphatic vessel remodelling in cancer. Nat Rev Cancer. 2014; 14(3):159-172
372. Stacker SA, Williams SP, Karnezis T, Shayan R, Fox SB, et al. Lymphangiogenesis and lymphatic vessel remodelling in cancer. Nat Rev Cancer 2014; 14:159–172.
373. Stanclift RM, Gilson SD. Evaluation of neoadjuvant prednisone administration and surgical excision in treatment of cutaneous mast cell tumors in dogs. J Am Vet Med Assoc. 2008; 232(1):53-62.
374. Stanczyk M, Olszewski WL, Gewartowska M, Domaszewska-Szostek A. Lack of functioning lymphatics and accumulation of tissue fluid/lymph in interstitial "lakes" in colon cancer tissue. Lymphology. 2010; 43(4):158-167.
375. Stefanello D, Buracco P, Sabattini S, Finotello R, Giudice C, et al. Comparison of 2- and 3-category histologic grading systems for predicting the presence of metastasis at time of initial evaluation in dogs with cutaneous mast cell tumours: 368 cases (2009-2014). J Am Vet Med Assoc. 2015; 246(7):765-769.
376. Stefanello D, Valenti P, Faverzani S, Bronzo V, Fiorbianco V, et al. Ultrasound-guided cytology of spleen and liver: a prognostic tool in canine cutaneous mast cell tumor. J Vet Intern Med. 2009; 23:1051-1057.
377. Stehlík L, Vitulová H, Simeoni F, Proks P, Vignoli M. Computed tomography measurements of presumptively normal canine sternal lymph nodes. BMC Vet Res. 2020; 16(1):269.

378. Stiborova K, Treggiari E, Amores-Fuster I, Del Busto I, Killick D, et al. Haematologic toxicity in dogs with mast cell tumours treated with vinblastine/prednisolone chemotherapy with/without radiotherapy. J Small Anim Pract. 2019; 60(9):534-542.

379. Suami H, Shin D, Chang DW. Mapping of lymphosomes in the canine forelimb: comparative anatomy between canines and humans. Plast Reconstr Surg. 2012; 129:612-620.

380. Suami H, Yamashita S, Soto-Miranda MA, Chang DW. Lymphatic territories (lymphosomes) in a canine: an animal model for investigation of postoperative lymphatic alterations. PLoS One. 2013; 8(7):1-9.

381. Suga K, Ogasawara N, Okada M, Matsunaga N. Interstitial CT lymphography-guided localization of breast sentinel lymph node: preliminary results. Surgery. 2003b; 133(2):170–179.

382. Suga K, Ogasawara N, Yuan Y, Okada M, Matsunaga N, et al. Visualization of breast lymphatic pathways with an indirect computed tomography lymphography using a nonionic monometric contrast medium iopamidol: preliminary results. Invest Radiol. 2003; 38(2):73–84.

383. Suga K, Uchisako H, Nishigauchi K, Shimizu K, Kume N, Yamada N, Nakanishi T. Technetium-99m-HMPAO as a marker of chemical and irradiation lung injury: experimental and clinical investigations. J Nucl Med. 1994; 35:1520-1527.

384. Suga K, Yuan Y, Ogasawara N, Whitman GJ. Localization of breast sentinel lymph nodes by MR lymphography with a conventional gadolinium contrast agent: preliminary observations in dogs and humans. Breast Dis. 2004; 15(1):37.

385. Suga K, Yuan Y, Ueda K, Kaneda Y, Kawakami Y, et al. Computed tomography lymphography with intrapulmonary injection of iopamidol for sentinel lymph node localization. Invest Radiol. 2004; 39(6):313–324.

386. Sugie T, Kinoshita T, Masuda N, Sawada T, Yamauchi A, et al. Evaluation of the clinical utility of the ICG fluorescence method compared with the radioisotope method for sentinel lymph node biopsy in breast cancer. Ann Surg Oncol. 2016; 23(1):44–50.

387. Sutton DR, Hernon T, Hezzell MJ, Meakin LB, Gould SM, et al. Computed tomographic staging of dogs with anal sac adenocarcinoma. J Small Anim Pract. 2022; 63(1):27-33.

388. Tacconi C, Correale C, Gandelli A, Spinelli A, Dejana E, et al. Vascular endothelial growth factor C disrupts the endothelial lymphatic barrier to promote colorectal cancer invasion. Gastroenterology. 2015; 148(7):1438-51.e8.

389. Takahashi T, Kadosawa T, Nagase M, Matsunaga S, Mochizuki M, et al. Visceral mast cell tumors in dogs: 10 cases (1982–1997). J Am Vet Med Assoc. 2000; 216:222–6.

390. Takahashi T, Kadosawa T, Nagase M, Mochizuki M, Matsunaga S, et al. Inhibitory effects of glucocorticoids on proliferation of canine mast cell tumor. J Vet Med Sci. 1997;59(11):995-1001.

391. Tanis JB, Simlett-Moss AB, Ossowksa M, Maddox TW, Guillem J, Lopez-Jimenez C, et al. Canine anal sac gland carcinoma with regional lymph node metastases treated with sacculectomy and lymphadenectomy: Outcome and possible prognostic factors. Vet Comp Oncol. 2022; 20(1):276-292.

392. Teng SP, Hsu WL, Chiu CY, Wong ML, Chang SC. Overexpression of P-glycoprotein, STAT3, phospho-STAT3 and KIT in spontaneous canine cutaneous mast cell tumours before and after prednisolone treatment. Vet J. 2012; 193(2):551-6.

393. Tewalt EF, Cohen JN, Rouhani SJ, Guidi CJ, Qiao H, et al. Lymphatic endothelial cells induce tolerance via PD-L1 and lack of costimulation leading to high-level PD-1 expression on CD8 T cells. Blood. 2012; 120(24):4772-4782.

394. Thamm DH, Avery AC, Berlato D, Bulman-Fleming J, Clifford CA, et al. Prognostic and predictive significance of KIT protein expression and c-kit gene mutation in canine cutaneous mast cell tumours: A consensus of the Oncology-Pathology Working Group. Vet Comp Oncol. 2019; 17(4):451-455.

395. Thamm DH, Mauldin EA, Vail DM. Prednisone and vinblastine chemotherapy for canine mast cell tumor - 41 cases (1992-1997). J Vet Int Med. 1999; 13:491-497.

396. Thamm DH, Turek MM, Vail DM. Outcome and prognostic factors following adjuvant prednisone/vinblastine chemotherapy for high-risk canine mast cell tumour: 61 cases. J Vet Med Sci. 2006; 68(6):581-7.

397. Thamm DH, Vail DM. Mast Cell Tumors. In: Withrow SJ, MacEwan EG, eds.Withrow & MacEwen's Small Animal Clinical Oncology. 4th ed. St. Louis, MO:Saunders Elsevier; 2007: 402–424.

398. Thamm DH, Weishaar KM, Charles JB, Ehrhart EJ 3rd. Phosphorylated KIT as a predictor of outcome in canine mast cell tumours treated with toceranib phosphate or vinblastine. Vet Comp Oncol. 2020; 18(2):169-175.

399. Thierry GR, Kuka M, De Giovanni M, Mondor I, Brouilly N, et al. The conduit system exports locally secreted IgM from lymph nodes. J Exp Med. 2018; 215(12):2972-2983.

400. Thompson JF, Uren RF, Shaw HM, McCarthy WH, Quinn MJ, et al. Location of sentinel lymph nodes in patients with cutaneous melanoma: new insights into lymphatic anatomy. J Am Coll Surg 1999; 189:195–206.

401. Thompson JJ, Pearl DL, Yager JA, Best SJ, Coomber BL, et al. Canine subcutaneous mast cell tumor: characterization and prognostic indices. Vet Pathol. 2011; 48(1):156–68.

402. Thompson JJ, Yager JA, Best SJ, Pearl DL, Coomber BL, et al. Canine subcutaneous mast cell tumors: cellular proliferation and KIT expression as prognostic indices. Vet Pathol. 2011b; 48(1):169–81.

403. Todd JE, Nguyen SM, White J, Langova V, Thomas PM, et al. Combination vinblastine and palladia for high-grade and metastatic mast cell tumors in dogs. Can Vet J. 2021; 62(12):1335-1340.

404. Troyan SL, Kianzad V, Gibbs-Strauss SL, Gioux S, Matsui A, et al. The FLARE™ intraoperative near-infrared fluorescence imaging system: a first-in-human clinical trial in breast cancer sentinel lymph node mapping. Ann Surg Oncol. 2009; 16(10):2943–2952.

405. Tucker WD, Arora Y, Mahajan K. Anatomy, Blood Vessels. In: StatPearls [Internet]. Treasure Island (FL): StatPearls Publishing; 2020.

406. Tuohy JL Milgram J, Worley DR, Dernell WS. A review of sentinel lymph node evaluation and the need for its incorporation into veterinary oncology. Vet Comp Oncol 2009; 7:81-91.

407. Tuohy JL, Worley DR. Pulmonary lymph node charting in normal dogs with blue dye and scintigraphic lymphatic mapping. Res Vet Sci. 2014; 97(1):148–155.

408. Turek MM, Forrest LJ, Adams WM, Helfand SC, Vail DM. Postoperative radiotherapy and mitoxantrone for anal sac adenocarcinoma in the dog: 15 cases (1991–2001). Vet Comp Oncol. 2003; 1:94–104.

409. Turkbey B, Hoyt RF, Agarwal HK, Bernardo M, Sankineni S, et al. Magnetic resonance sentinel lymph node imaging of the prostate with gadofosveset trisodium-albumin: preliminary results in a canine model. Acad Radiol. 2015; 22(5):646–652.

410. Turner RR, Ollila DW, Krasne DL, Giuliano AE. Histopathologic validation of the sentinel lymph node hypothesis for breast carcinoma. Ann Surg 1997; 226(3):271-6.

411. Turrel JM, Kitchell BE, Miller LM, Théon A.. Prognostic factors for radiation treatment of mast cell tumor in 85 dogs. J Am Vet Med Assoc. 1988; 193(8):936-940.

412. Ulvmar MH, Werth K, Braun A, Kelay P, Hub E, et al. The atypical chemokine receptor CCRL1 shapes functional CCL21 gradients in lymph nodes. Nat Immunol. 2014; 15(7):623-630.

413. Uren RF, Howman-Giles R, Thompson JF. Patterns of lymphatic drainage from the skin in patients with melanoma. J Nucl Med. 2003; 44(4):570-582.

414. Valent P, Akin C, Hartmann K, Nilsson G, Reiter A, et al. Advances in the classification and treatment of mastocytosis: current status and outlook toward the future. Cancer Res. 2017; 77:1261–70.

415. Van den Eynden GG, Vandenberghe MK, van Dam PJ, Colpaert CG, van Dam P, et al. Increased sentinel lymph node lymphangiogenesis is associated with nonsentinel axillary lymph node involvement in breast cancer patients with a positive sentinel node. Clin Cancer Res. 2007; 13(18 Pt 1):5391-7.

416. Van der Noordaa MEM, Vrancken Peeters MTFD, Rutgers EJT. The intraoperative assessment of sentinel nodes - Standards and controversies. Breast 2017; 34:S64-S69.

417. Vascellari M, Giantin M, Capello K, Carminato A, Morello EM, et al. Expression of Ki67, BCL-2, and COX-2 in canine cutaneous mast cell tumors: association with grading and prognosis. Vet Pathol. 2013; 50(1):110–21.

418. Veikkola T, Jussila L, Makinen T, Karpanen T, Jeltsch M, et al. Signalling via vascular endothelial growth factor receptor-3 is sufficient for lymphangiogenesis in transgenic mice. EMBO J. 2001; 20:1223-1231.

419. von der Weid PY, Zawieja DC. Lymphatic smooth muscle: the motor unit of lymph drainage. Int J Biochem Cell Biol. 2004; 36(7):1147-1153.

420. Wainberg SH, Oblak ML, Giuffrida MA. Ventral cervical versus bilateral lateral approach for extirpation of mandibular and medial retropharyngeal lymph nodes in dogs. Vet Surg. 2018; 47(5):629-633.

421. Wang Y, Cheng Z, Li J, Tang J. Gray-scale contrast-enhanced ultrasonography in detecting sentinel lymph nodes: an animal study. Eur J Radiol. 2010; 74(3):e55–e59.

422. Warland J, Amores-Fuster I, Newbury W, Brearley M, Dobson J. The utility of staging in canine mast cell tumours. Vet Comp Oncol. 2014; 12:287-98

423. Iwasaki R, Mori T, Ito Y, Kawabe M, Murakmi M, Maruo K. Computed Tomographic Evaluation of Presumptively Normal Canine Sternal Lymph Nodes. J Am Anim Hosp Assoc. 2016; 52(6):371–7.

424. Wawroschek F, Wengenmair H, Senekowitsch-Schmidtke R, Hamm M, Henke J, et al. Prostate lymphoscintigraphy for sentinel lymph node identification in canines: reproducibility, uptake, and biokinetics depending on different injection strategies. Urol Res. 2003; 31(3):152–158.

425. Weaver DL. Pathology evaluation of sentinel lymph nodes in breast cancer: protocol recommendations and rationale. Mod Pathol. 2010; 23(Suppl 2):S26–32.

426. Webster JD, Yuzbasiyan-Gurkan V, Miller RA, Kaneene JB, Kiupel M. Cellular proliferation in canine cutaneous mast cell tumors: associations with c-KIT and its role in prognostication. Vet Pathol. 2007; 44:298–308.

427. Weishaar KM, Ehrhart EJ, Avery AC, Charles JB, Elmslie RE, et al. c-Kit Mutation and Localization Status as Response Predictors in Mast Cell Tumors in Dogs Treated with Prednisone and Toceranib or Vinblastine. J Vet Intern Med. 2018; 32(1):394-405.

428. Weishaar KM, Ehrhart EJ, Avery AC, Charles JB, Elmslie RE, et al. ckit mutation and localization status as response predictors in mast cell tumors in dogs treated with prednisone and toceranib or vinblastine. J Vet Intern Med. 2018; 32:394–405.

429. Weishaar KM, Thamm DH, Worley DR, Kamstock DA. Correlation of nodal mast cells with clinical outcome in dogs with mast cell tumour and a proposed classification system for the evaluation of node metastasis. J Comp Pathol. 2014; 151:329-338.

430. Weiss L, Schmid-Schonbein GW. Biomechanical interactions of cancer cells with the microvasculature during metastasis. Cell Biophys. 1989; 14:187-215.

431. Weiss L. The pathobiology of metastasis within the lymphatic system. Surg Oncol Clin N Am. 1996; 5:15-24.

432. Weisse C, Shofer FS, Sorenmo K. Recurrence rates and sites for grade II canine cutaneous mast cell tumors following complete surgical excision. J Am Anim Hosp Assoc 2002; 38(1):71–3.

433. Welle MM, Rohrer Bley C, Howard J, Rüfenacht S. Canine mast cell tumours: a review of the pathogenesis, clinical features, pathology and treatment. Vet Dermatol. 2008; 19:321–339.

434. Wells S, Bennett A, Walsh P, Owens S, Peauroi J. Clinical usefulness of intradermal fluorescein and patent blue violet dyes for sentinel lymph node identification in dogs. Vet Comp Oncol. 2006; 4(2):114–122.

435. Wenk CH, Ponce F, Guillermet S, Tenaud C, Boturyn D, et al. Near-infrared optical guided surgery of highly infiltrative fibrosarcomas in cats using an anti-alphavss3 integrin molecular probe. Cancer Lett. 2013; 334(2):188–195.

436. Willard MD. Alimentary neoplasia in geriatric dogs and cats. Vet Clin North Am Small Anim Pract. 2012; 42:693–706.

437. Williams LE, Gliatto JM, Dodge RK, Johnson JL, Gamblin RM, et al. Carcinoma of the apocrine glands of the anal sac in dogs: 113 cases (1985−1995). J Am Vet Med Assoc 2003; 223:825–831.

438. Willmann M, Yuzbasiyan-Gurkan V, Marconato L, Dacasto M, Hadzijusufovic E, et al. Proposed diagnostic criteria and classification of

canine mast cell neoplasms: a consensus proposal. Front Vet Sci. 2021; 8:755258.

439. Wishart GC, Loh SW, Jones L, Benson JR. A feasibility study (ICG-10) of indocyanine green (ICG) fluorescence mapping for sentinel lymph node detection in early breast cancer. Eur J Surg Oncol. 2012; 38(8):651–656.

440. Wisner ER, Ferrara KW, Short RE, Ottoboni TB, Gabe JD, et al. Sentinel node detection using contrast-enhanced power Doppler ultrasound lymphography. Invest Radiol. 2003; 38(6):358–365.

441. Wisner ER, Seibert JA, Katzberg RW. Quantitative methods for indirect CT lymphography. Vet Radiol Ultrasound 1998; 39:110-116

442. Wong JH, Cagle LA,Morton DL. Lymphatic drainage of skin to a sentinel lymph node in a feline model. Ann Surg. 1991; 214:637–641.

443. Wong SY, Hynes RO. Lymphatic or hematogenous dissemination: how does a metastatic tumor cell decide? Cell Cycle. 2006; 5(8):812-817.

444. Worley DR. Incorporation of sentinel lymph node mapping in dogs with mast cell tumours: 20 consecutive procedures. Vet Comp Oncol. 2014; 12:215-226.

445. Wright T, Oblak M. Lymphadenectomy: Overview of surgical anatomy & removal of peripheral lymph nodes. Today Vet Pract. 2016; 20-29.

446. Xie F, Zhang D, Cheng L, Yu Lei, Tong F, et al. Intradermal microbubbles and contrast-enhanced ultrasound (CEUS) is a feasible approach for sentinel lymph node identification in early-stage breast cancer. World J Surg Oncol. 2015; 13:319.

447. Zengel B, Yararbas U, Sirinocak A, Ozkok G, Denecli AG, et al. Sentinel lymph node biopsy in breast cancer: review on various methodological approaches. Tumori. 2013; 99:149–153.

448. Zhang S, Zhang D, Gong M, Wen L, Liao C, et al. High lymphatic vessel density and presence of lymphovascular invasion both predict poor prognosis in breast cancer. BMC Cancer. 2017; 17:335.

CHAPTER 2

Scientific Manuscript

Running Title: Indirect lymphography of mast cell tumor

Agreement between radiographic indirect lymphography with lipiodol and patent blue for sentinel lymph node mapping of dogs with skin mast cell tumor[1]

Vinicius G. P. Albernaz[a,b], Natália N. Kano[b], Giovanna L. Bonatto[b], William da S. Prieto[b], Renato Silva de Sousa [b], and Juliany G. Quitzan[a,*]

[a]Department of Veterinary Surgery and Reproduction, School of Veterinary Medicine and Animal Science, São Paulo State University (Unesp), Botucatu, São Paulo, Brazil; [b]Department of Veterinary Medicine, Federal University of Paraná, Curitiba, Paraná, Brazil.

* Corresponding author at: Department of Veterinary Surgery and Reproduction, School of Veterinary Medicine and Animal Science, São Paulo State University (Unesp), Distrito de Rubião Jr. s/n, 18618-683, Botucatu São Paulo Brazil.

E-mail address: j.quitzan@unesp.br (J.G. Quitzan).

Abstract

Metastasis to sentinel lymph nodes (SLN) is the main route to systemic dissemination of cutaneous mast cell tumor (cMCT), one of the most common skin cancers in dogs. Early detection of lymph node metastasis is crucial to correctly stage and treat dogs with cMCT. However, the SLN is widely variable among individuals and anatomic sites. The objective of the study was to evaluate the role of iodized oil (IO) indirect lymphography (IL) combined with patent blue (PB) colorimetric method in detecting SLN in dogs with naturally occurring cMCT. Twenty-three dogs were enrolled in the prospective study. IO IL detected 29

[1]The following manuscript was written in accordance with the Author Guideline for submission to the Veterinary Comparative Oncology journal (John Wiley & Sons Ltd). Full instructions can be found at: https://onlinelibrary.wiley.com/page/journal/14765829/homepage/forauthors.html.

contrasted SLN in 19 dogs while PB detected 26 SLN in 19 dogs. In each method, 4 dogs have no lymph node detected. Thirty-one lymph nodes were resected in 20 dogs, of which 10 were metastatic. Laparotomy was necessary to remove opacified iliac lymph nodes in 26% of the dogs. The rate of agreement between IO IL and patent blue with regional lymph nodes was 82.6%. The rate was 78.2% when comparing IL and patent blue. Only one dog had a draining SLN different from the regional lymph node as detected by IL. In a clinical setting, IO IL was responsible to increase the number of resected lymph nodes by 41% (29% of the resected SLN). There was no difference in detected SLN by PB and IO IL in the base scenario (p=0.1855), however, in a clinical scenario, there was a significant difference favoring IL (p=0.0081). Unequally opacified SLN could not be significatively associated with metastasis (p=.2264). The same occurred with light-blue color SLN (p=.6673). However, tumor size was significative higher in dogs with lymph node metastasis (p=.0456). Enlarged lymph nodes had a 4.6-fold more risk of being metastatic than non-palpable/normal-sized nodes (p=.0374). The SLN mapping was responsible for 62.5% of the postoperative indications of adjuvant chemotherapy, however, only one case was indicated solely by the IL. However, 60% of dogs with metastatic disease had an intracavitary metastatic SLN that could only be detected preoperatively by IL. Preoperative IO IL associated with patent blue is an efficient method to detect SLN in cMCT undergoing curative surgery. IL increases the rate of SLN detected in a clinical setting. The pattern of SLN opacification should not be used to predict metastasis.

Keywords: Surgical Oncology; Lymphatic Metastasis; Lymphadenectomy; Mastocytoma; Oncologic Staging

1. INTRODUCTION

The cutaneous mast cell tumor (cMCT) is the most diagnosed skin tumor in dogs (Sledge et al., 2016; Kiupel et al., 2019; Willmann et al., 2021). The lymphatic system is the main pathway for cMCT to spread, which makes lymph nodes (LN) evaluation an essential aspect of MCT staging (Kiupel et al., 2019). LN metastasis is a well-established predictor of negative prognosis in cMCT, as

it highly increases the risk of distant metastasis (Cahalane et al., 2004; Murphy et al., 2006; Thamm et al., 2006; Hayes et al., 2007; Krick et al., 2009; Hillman et al., 2010; Hume et al., 2011; Blackwood et al., 2012; Warland et al., 2014). Also, dogs with LN metastasis must receive adjuvant chemotherapy after surgical resection of the primary tumor (Blackwood et al., 2012; Warland et al., 2014; Oliveira et al., 2020).

LN staging and removal are crucial steps in establishing the prognosis and treatment of cMCT (Krick et al., 2009; Ferrari et al., 2018; Lapsley et al., 2020) LN resection is so important for cMCT treatment that even prophylactic lymphadenectomy in low-grade cMCT seems to be associated with a lower risk for disease progression (Sabattini et al., 2021). However, relying only on clinical examination to detect LN at risk of metastasis is not reasonable as a retrospective study found a 65% rate of pre-metastatic or metastatic disease in non-palpable or normal-sized LNs (Ferrari et al., 2018). Some authors recommend that early detection of LN metastasis should be performed in all dogs with cMCT, regardless of grade (Blackwood et al., 2012; Ferrari et al., 2018; Kiupel et al., 2019; Willimann et al., 2021).

A remarkable consideration that is usually underrated in most situations is the possible metastatic drainage to unusual LN. Metastasis of cMCT has been described to drain to colic, medial iliac, and accessory axillary LN (Fournier et al., 2020). Thus, detecting which LN should be sampled or removed is often challenging, as the locoregional node close to the tumor site may not be the draining one (Kiupel et al., 2019; Liptak et al., 2019). A non-selective dissection of the LN is the practice of removing the locoregional node that normally drains the tumor site (Liptak et al., 2019). However, a study found that about 40% of the draining nodes would be missed considering only non-selective resection (Worley et al., 2014). On the other hand, removing the regional LN with evidence of metastatic cMCT was associated with a better prognosis (Marconato et al., 2018).

The concept of sentinel lymph node (SLN) aroused with the promise of aiding the surgeon in the decision-making process of which LN should be removed (Liptak et al., 2019). SLN is the first draining LN to drain a tumor in a specific region (Liptak et al., 2019). The SLN theory relies on the fact that is extremely rare to find metastasis on LN further on the basin if the first draining

node were negative (Liptak et al., 2019). In human patients with malignant thyroid and breast cancer, the rate of distant metastasis simultaneously with negative SLN was less than 0.1% (Turner et al., 1997; Balasubramanian et al., 2011). The orderly progress of the lymphatic metastasis from one LN to another makes the SLN a physical barrier to the dissemination of neoplastic cells for secondary nodes and, ultimately, to distant organs (Wong et al., 1991; Giuliano et al., 1994; Morton et al., 2005; Somasundaram et al., 2007; Cochran et al., 2008; Balasubramanian et al., 2011). Once SLN were free of metastasis, it was not necessary to pursue other basins LN, reducing surgical time and postoperative morbidity ((Wong et al., 1991; Morton et al., 2005; Cochran et al., 2008; Morton et al., 2012; Liptak et al., 2019).

Detection of the SLN is not a straightforward procedure, as lymphatic drainage is naturally variable among individuals and even more unpredictable in the presence of a neoplasm (Thompson et al., 1999; Herring et al., 2002; Smith, 2002; Lurie et al., 2006; Gelb et al., 2010; Suami et al., 2013; Worley, 2014; Liptak et al., 2019). The use of lymphoscintigraphy in a study of cMCT found that 42% of the dogs had a SLN different from that expected to drain the tumor region (Worley et al., 2014). Several techniques have been evaluated for SLN mapping in both humans and animals. The injection of blue dyes, such as patent blue (PB), methylene blue, or isosulfan blue is the simplest and most widely used SLN mapping technique, as it is a colorimetric method that allows intraoperative visualization of both afferent lymphatic vessels and the draining LN (Worley et al., 2014; Beer et al., 2018; Liptak et al., 2019). Despite being essential during surgery, colorimetric methods fail to inform the surgeon of how many, and which LNs must be accessed as it depends exclusively on intraoperative visualization (Somasundaram et al., 2007). This fact led to a rate of false-negative as high as 86% when using only blue dyes as the SLN mapping technique (Qiu et al., 2018).

The combination of the colorimetric method with preoperative or intraoperative lymphoscintigraphy or near-infrared imaging arose as the gold-standard SLN mapping technique in humans (Balogh et al., 2002; Kim et al., 2006; Niebling et al., 2016). However, special facilities, equipment, and nuclear waste management preclude their wide use in animals (Beer et al., 2018; Liptak et al., 2019). Radiographic and CT indirect lymphography (IL) emerged as

adequate alternatives for preoperative SLN mapping (Patsikas et al., 2010; Mayer et al., 2013; Brissot et al., 2017; Beer et al., 2018; Liptak et al., 2019; Lapsley et al., 2020). IL uses a peritumoral injection of iodized oil (IO) or hydrosoluble contrast agents to detect SLN through simple radiographic or CT-scan, respectively (Brissot et al., 2017; Soultani et al., 2017; Majeski et al., 2017; Grimes et al., 2017; Beer et al., 2018; Liptak et al., 2019; Lapsley et al., 2020). IO IL can also be associated with blue dyes to allow both preoperative and intraoperative SLN mapping simultaneously (Brissot et al., 2017; Liptak et al., 2019).

IL has been recently evaluated for SLN mapping in canine cMCTs and other tumors (Mayer et al., 2013; Worley et al., 2014; Brissot et al., 2017), but the retrospective nature of the studies and inclusion of other tumor types impaired draw cMCT specific conclusions. The primary objective of this study is to determine the agreement between radiographs IL with lipiodol, and intraoperative SLN mapping with PB in dogs with cMCT. We hypothesize that IL would detect more SLN than intraoperative PB. The secondary objective included the following hypothesis: (1) indirect lymphography would detect intracavitary LNs that are not usually investigated or accessed through superficial surgery for skin tumors; (2) Pattern of IO and PB drainage would be associated with metastatic LN disease; (3) Clinicopathological variables would be associated with locoregional metastatic disease.

2. METHODS

2.1. Pilot Study

To base the following research, a pilot study was conducted on a dog with cMCT using the same methodology described further. Radiographs were taken 10 minutes after peritumoral injection of IO. In this dog, the afferent lymphatic vessels could be seen draining from the tumor site (scrotum) toward both inguinal SLN that were unequally opacified (Figure 21A). Twenty-four hours after IO injection, the afferent lymphatic vessels could not be seen, and both right and left inguinal were uniformly contrasted. In addition to the SLN detected initially, the right medial iliac LN was also uniformly opacified after 24 hours (Figure 21B).

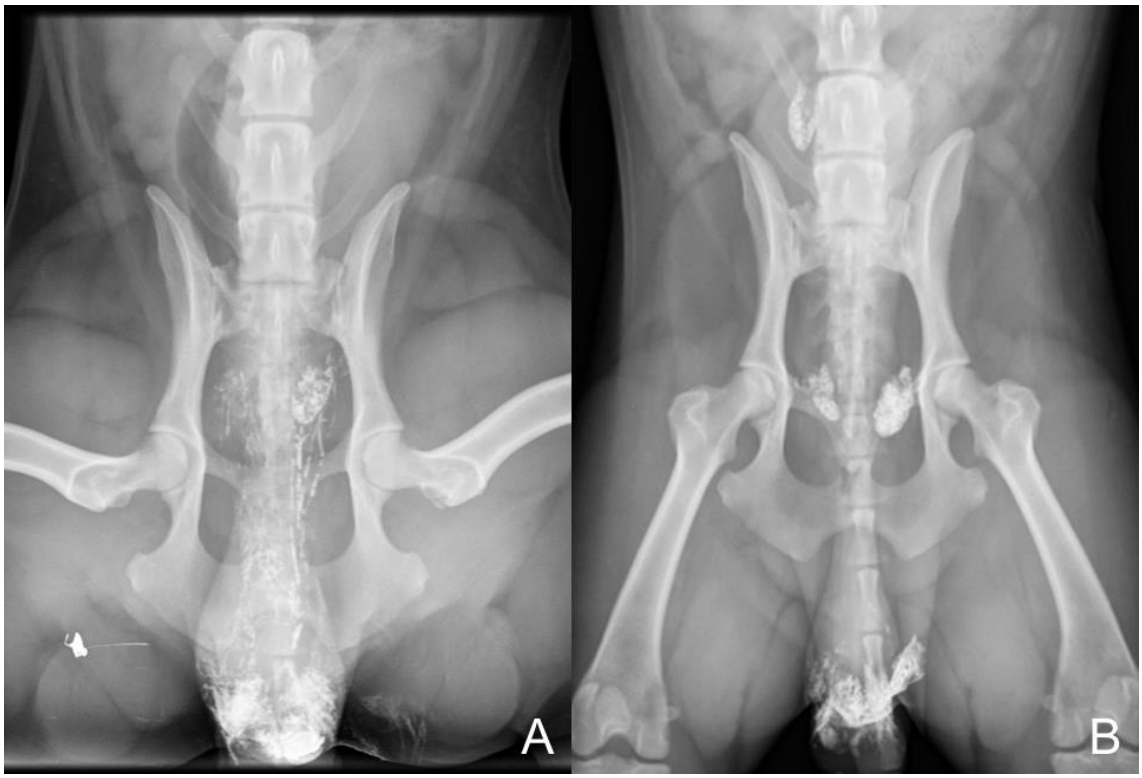

Figure 21. (A) A pilot radiographic study (Ventral pelvic view) of Case #6 was performed 10 minutes after peritumoral injection (Scrotum) of iodized oil. Afferent lymphatic vessels can be seen draining the tumor site toward both inguinal lymph nodes. The contrasted signal at the left bottom side is a plate artifact. (B) Radiographic study 24 hours after peritumoral injection of iodized oil. Afferent lymphatic vessels cannot be seen, but both inguinal and right iliac lymph nodes exhibit a uniform opacification.

2.2. Study Design and Patient Selections

This study was approved by the Ethics Committee on Animal Use (CEUA/FMVZ-UNESP – Protocol n. 0195/2020 and CEUA/SCA-UFPR – Protocol n. 057/2020) according to the Brazilian Law decree 11,794/2008, 6,899/2009. and by rules of the Conselho Nacional de Controle da Experimentação Animal (CONCEA). The study was conducted at the Veterinary Teaching Hospitals of the Universidade Federal do Paraná (Curitiba - Brazil) and Universidade Estadual Paulista (Botucatu – Brazil).

This was a prospective clinical study of a cohort of client-owned adult dogs with the diagnosis of primary naturally occurring cMCT. Dogs bearing cytologically confirmed cMCT amenable to curative-intent surgical resection and

no clinical or imaging evidence of distant metastasis were enrolled between March 2021 and January 2022.

Each dog underwent routine staging procedures, including an oncological clinical evaluation, a complete physical examination, fine needle aspirate biopsy and cytology for tumor triage, complete blood count, serum biochemical profile, abdominal ultrasound, and 3-view thoracic radiographs. Those dogs with a known sensibility to contrast agents or renal disease, previous surgery close to the tumor site, recurrence or bearing subcutaneous, mucosal, mucocutaneous, extracutaneous/extramucosal MCT, mast cell leukemia (according to Willmann et al., 2021) or other tumor type were excluded. All clients signed informed consent before dogs were enrolled in the study.

Collected clinical variables included: (1) Longest diameter, in centimeters and subclassified in > 3cm or < 3 cm; (2) primary tumor location, subdivided into High risk (i.e., head and neck, inguinal, scrotal, perivulvar, or perineal) or low risk (i.e., thorax, abdomen, and limbs, except for digits) sites; (3) Presence of ulceration; (4) presence of Darier's sign; (5) Locoregional LN with the highest probability to be the SLN according to Suami et al., (2013); (6) Subjective superficial LN sizes as determined by palpation, subclassified in increased, normal or non-palpable;

2.3. Indirect Lymphography

An Iodized Oil (IO; Lipiodol® Ultra-Fluid, iodized ethyl-esters of the fatty acids of poppy seed oil, iodine 480mg/ml; Guerbet Ltda, Brazil) was used for IL. Intradermal injection of 2 ml of IO was performed with a 24 G needle attached to a 1 ml syringe into four quadrants (0.5 ml per quadrant), around the tumor. Injections were performed 0.5 to 1 cm away from the tumor to avoid penetration of the tumor capsule. Also, all injection sites were double-checked before application to avoid inadvertent intravascular injection. The injection sites were carefully massaged to stimulate IO absorption into lymphatic vessels. In cases where physical restrain was insufficient for intradermal injection, sedation was provided. For dogs with multiple tumors, the largest one was considered the object of interest for SLN mapping.

Dogs were evaluated by a clinician for immediately post-injection reaction during the first 10 minutes and by the owner thereafter. Any owner-reported side effect was noted.

Two or three-view radiographs of the tumor site and adjacent regions were performed 24 hours after IO injection and immediately before surgery to identify the location and number of contrasted-enhanced LNs. LN contrast-uptake (opacification) was classified as uniform (well-defined edges and homogeneous opacification), unequal (poorly defined edges and uneven opacification), or absent (no contrast uptake) as described previously (Mayer et al., 2013).

2.4. Intraoperative SLN Mapping

Immediately after radiographs, the dogs underwent general anesthesia for surgical procedures. Patent blue (PB; 25mg/ml; Guerbet, Brazil) was injected around the tumor using the same criteria for lipiodol injection, 15 minutes before the first incision, totalizing 1 ml per dog. All contrasted and/or blue-colored SLN were accessed with intention of lymphadenectomy. When no additional incision was required (e.g., iliac, aortic, inguinal LN), the contralateral local LN that did not contrast was visualized during surgery to ensure it was not blue-colored. In the absence of both SLN mapping contrast and color, a non-selective dissection of the RLN was performed based on the previous description of normal dog lymphatic territories (Suami et al., 2013). A subjective visual scale (Dark Blue, Light Blue, or absent) was used to rate the degree of PB uptake as a previous description (Brissot et al., 2017).

2.5. Surgical Resection and Histological Evaluation

All dogs received appropriate anesthetic and analgesic protocols as determined by the responsible anesthesiologist. All surgical procedures were performed under general anesthesia and in a single step. Surgical resection of the primary cMCT included 1 to 3 cm of healthy tissue around the palpable tumor for lateral margins and 1 fascial plane for deep margins. Clean instruments and gloves were used when LN resection was performed after surgical resection of primary cMCT to avoid seeding neoplastic cells to LN sites. In cases where

abdominal lymphadenectomy was required, laparotomy was performed before cMCT resection.

Lymphadenectomy was performed through a midline or over the node incision and using sharp and blunt dissection. The blood vessels were ligated using 3-0 or 4-0 PDS or coagulated using an electrosurgical device. Intraabdominal LN was accessed through an abdominal ventral midline approach and dissected using blunt and digital dissection and bleeding was controlled using digital compression. Wound closure was performed routinely.

All tissue samples were fixed in 10% neutral-buffered formalin and paraffin-embedded following routine histological processing, tumor, and margin examination. All samples were stained with hematoxylin-eosin and toluidine blue. The cutaneous nature of MCT was confirmed on histology and primary cMCT was graded according to 3-tier Patnaik (Patnaik et al., 1984) and 2-tier Kiupel (Kiupel et al., 2011) grade systems. Margins were classified as incomplete when there were neoplastic mast cells at the cutting edge of the sample and complete when there were no neoplastic cells at the border (histologic tumor-free margin >0mm). The LN were histologically evaluated for MCT metastasis graded according to Weishaar et al. (2014) HN0-3 system. Locoregional metastasis was defined as HN ≥1 (i.e., pre-metastatic, early, and overt metastasis).

Dogs were evaluated 24h, 48h, and 14 days after surgery for lymphedema, suture dehiscence, and any postoperative complication. Once the dogs were fully recovered from surgery, they were free to pursue further therapy as decided by the clinical oncologist and owner. Adjuvant therapies were indicated in cases of grade III/high-grade MCT and locoregional metastasis. Scar revision surgery was indicated in incompletely resected tumors. The percentage of dogs whose adjuvant treatment indication changed because of SLN mapping with IO IL or PB colorimetric method was recorded.

2.6. Sample Size and Statistical Analysis

A sample size of 17 animals was estimated to detect a difference of 42% considering a null hypothesis of 0%. The 42% disagree rate between locoregional and SLN on canine cutaneous MCT using scintigraphy was used to base the

sample size (Worley et al., 2014). The calculation was performed for a power of 0.95 and resulted in an actual α of 0.0245. Considering 15% of friction, the minimum sample size was increased to at least 20 dogs. The sample size was calculated using an a priori test of proportion for a difference of constants (Binominal, one sample case) in the software G*Power 3.1.9.7 (Universität Düsseldorf).

To adjust the results of the study from a clinical perspective, an analysis that excluded the deep-located SLN from the PB group was performed, considering that if they colored by PB, they could only be detected as SLN by the IO LN. This group of results was named "Clinical Scenario", to differentiate from the results of the "Experimental Scenario".

Continuous variables were described by mean ± standard-deviation (SD) or median (range), as appropriate; categorical variables were represented by count and percentage. Normality was evaluated by the Shapiro-Wilk test. The difference between the number of SLN detected by IO IL and PB was compared using a paired T-test. Differences between SLN IO opacification and pattern of PB drainage as well as the association between clinicopathological variables (i.e., cMCT site, 3-cm size cut-off, presence of deep invasion, Darier sign, and LN size) and LN metastasis were tested by Fisher exact test. Also, sensitivity, specificity, positive predictive value, and negative predictive value on the prediction of locoregional metastasis were calculated. cMCT size as a continuous variable was compared between normal and metastatic dogs using an unpaired t-test. The 95% confidence interval (CI) was calculated by the Koopman asymptotic score method for relative risk and the Wilson-Brown method for sensitivity and specificity. Two-tailed value of $p<0.05$ was considered statistically significant. GraphPad Prism software version 8.0.1 (GraphPad Software Inc.) was used for data analysis.

3. RESULTS

3.1. Patient and MCT Characteristics

Twenty-three dogs met the inclusion criteria and comprised the study population. Table 1 summarizes the demographic data of the cohort. All cMCTs could be diagnosed by cytology following fine needle aspirate biopsy. Solitary

cMCT occurred in 21 dogs and 2 dogs had one more concurrent cMCT in a different body area. For these 2 dogs, the largest tumor was considered the main MCT for SLN evaluation. The additional cMCT (n=2) were located at the contralateral hindlimb (case #3) and abdominal flank (case #11). Except for one dog with III-high-grade MCT (Case #23), all other cMCTs (n=22) were II-low grade as determined by histology after surgical resection.

Table 5. Demographic informations and tumor characteristics of 23 dogs with cutaneous mast cell tumor that underwent sentinel lymph node mapping with preoperative indirect lymphography using iodized oil and intraoperative patent blue colorimetric method.

Parameter	Value
Age	7.6 ± 2.5 years (range, 2 – 11 years)
Bodyweight	19.5 ± 8.8 kg (range, 5 – 35 kg)
Sex	
Female	12 (52.2%) – 9 spayed
Male	11 (47.8%) – 5 neutered
Breed	
Mixed Breed	10 (43.5%)
Pittbull	4 (17.4%)
Labrador Retriever	2 (8.7%)
Boxer	2 (8.7%)
Lhasa Apso	1 (4.3%)
Maltese	1 (4.3%)
Shih Tzu	1 (4.3%)
Pug	1 (4.3%)
French Bulldog	1 (4.3%)
MCT Location	
Hindlimb	12 (52.1%)
Forelimb	5 (21.7%)
Thorax	3 (13%)
Scrotum	2 (8.7%)
Abdomen	1 (4.3%)
MCT Size	
Long Axis	2.84 ± 1.96 cm (range, 0.8 – 9.8)
Short Axis	2.37 ± 1.58 cm (range, 1 – 8.5)
Height	1.52 ± 0.93 cm (range, 0.3 – 4.5)
Volume	27.16 ± 76.91 cm^3 (range, 0.43 – 374.9)
Macroscopic Aspects	
Darrier's Sign	4 (17.4%)
Deep Tissue Invasion	6 (26.1%)
Ulceration	0 (0%)
Clinical Signs	
Symptomatic	0 (0%)
Asymptomatic	23 (100%)

Twelve dogs had the superficial inguinal as the RLN (52.2%), 5 had the ventral superficial cervical (21.7%), 4 the axillary (17.4%), and 2 the popliteal (8.7%). Clinical examination detected 26.1% (n=6) of the RLNs were enlarged, 21.7% (n=5) were normal size and 52.2% (n=12) could not be palpated. Four dogs that had tumors located at the midline, both sides LNs were considered the draining LN. All bilateral RLNs in these cases had the same pared status on clinical examination (i.e., Case #6 with bilaterally enlarged LNs and Case #11, #13, and #20 whose both LN could not be palpated). There was no evidence of distant metastasis after survey image examinations in all dogs.

3.2. Indirect Lymphography Mapping

IO injection and indirect radiographic lymphography mapping were performed in solitary MCT (n=21) or the main MCT (n=2) in dogs with multiple lesions. No dog had an immediate reaction to the peritumoral injection of lipiodol. There was no systemic sign of MCT degranulation; however, 2 dogs (8.7%) had mild hyperemia around the injection sites (Figure 21). These local reactions did not cause any disturbance and were resected along with the tumor margins 24 hours after injection.

Figure 22. Local mild hyperemia was seen 24 hours after peritumoral intradermal injection of iodized oil (Case #1).

IL identified 29 contrasted SLN in 19 dogs. No contrasted SLN was found in 4 (17.4%) dogs. The mean and median contrasted SLN was 1.2 ± 0.81 and 1 (range, 0 – 3) per dog, respectively. Among the dogs that had contrasted LNs, 52.6% (n=10) dogs had only one opacified SLN, 42.1% (n=8) had two, and 5.2% (n=1) had three. Regarding the contrast-uptake pattern, 41.3% (n=12) of the SLN were uniformly opacified and 58.6% (n=17) uniquely opacified.

Superposition of the contrasted inguinal LN to the femur (lateral-lateral views), or pelvis (dorsal-ventral view) occurred in 7/14 (50%) of the contrasted inguinal LN (Figure 23A and B). Also, there was a superposition of the contrasted iliac LNs to the vertebrae in 4/6 (66.6%) dogs. When a discrete uniquely SLN contrast occurred in association with superposition to osseous structures careful attention to the radiographs was necessary as demarcation could be easily missed (Figure 23C and D). Lateral radiographs confirmed SLN opacification, but attention was still required to not miss unequally contrasted nodes (Figure 23E).

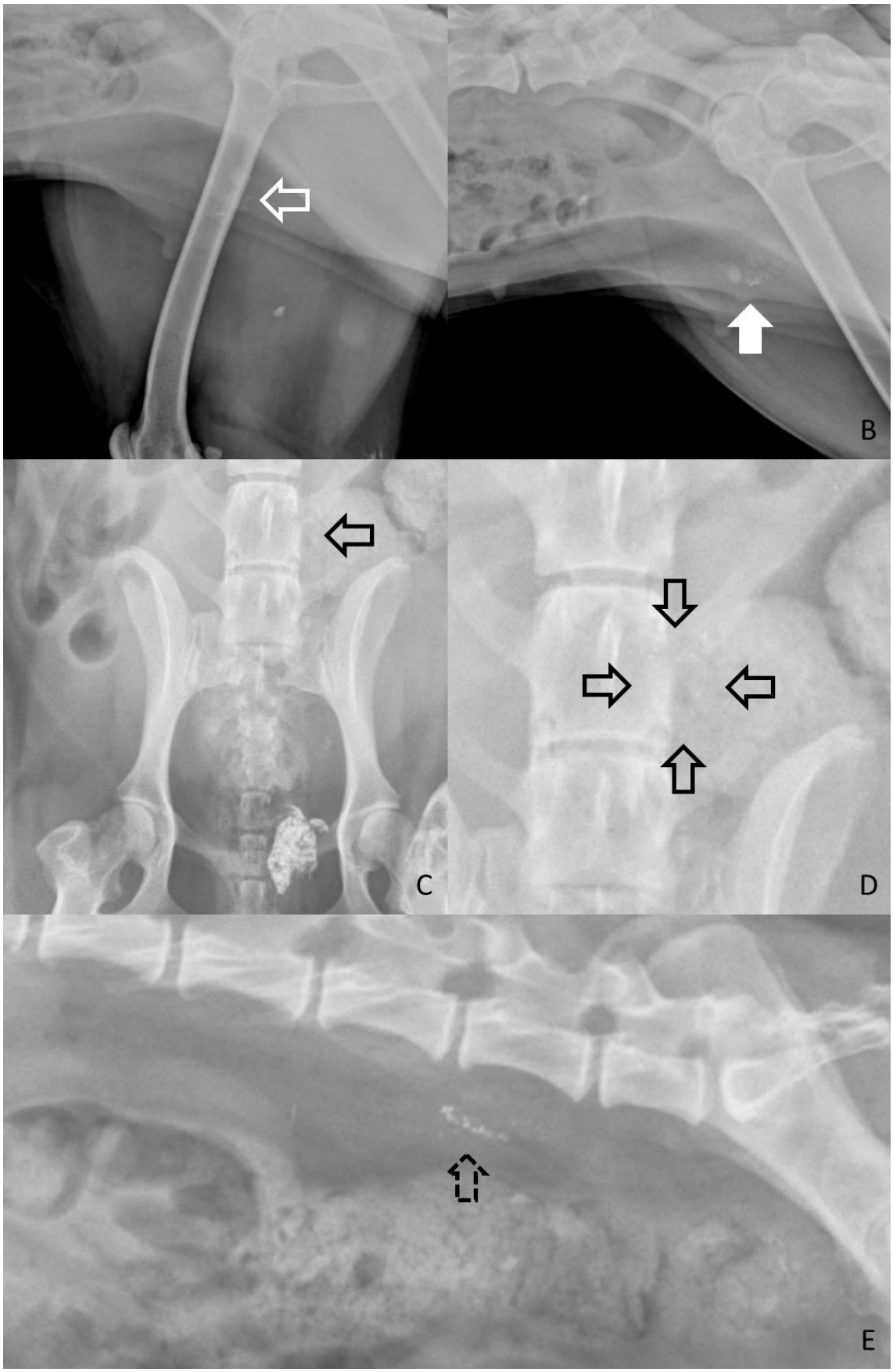

Figure 23. Radiographic images of SLN superposition to osseous structures and gastrointestinal viscera. (A and B) Lateral view of an unequally opacified inguinal lymph node (Case #3) superposed to the femur middle shaft (White blank arrow)

and after a caudal extension of the forelimbs (White solid arrow). (C and D) Ventral view of an unequally opacified iliac lymph node (Case #13) superposed to the left lateral aspect of L6 and colon fecal content (Black blank arrow). (E) Lateral view of the same iliac lymph node exhibiting a patchy opacification (Black dashed arrow).

3.3. Intraoperative Patent Blue Colorimetric Mapping

Intraoperative SLN mapping with PB detected 26 LN in 19 dogs. A mean of 1.1 ± 0.69 and a median of 1 (range, 0 – 2) per dog. Intraoperative PB drainage also demarcated afferent lymphatic vessels that aided the surgeon in locating the SLN (Figure 24A and B), even when an intracavitary search was conducted due to IO IL contrast uptake (Figure 24C and D). Seven dogs (36.8%) had two blue-colored SLN, while the remaining (n=12; 63.2%) had only one SLN. Among the blue-colored LNs, 18 (69.2%) were dark blue (Figure 24E) and 8 (30.8%) light blue. There was no LN PB uptake in 4 dogs (17.4%) (Figure 24F).

When considering a clinical scenario that excluded PB-colored deep located LN, only 21 LN in 19 dogs could be detected by the PB method. A mean and median of 0.9 ± 0.5 and 1 (range, 0 – 2) per dog.

There was no PB-associated adverse event detected. A dog that had systemic absorption of blue dye developed blue-colored mucosa and skin that resolved spontaneously in 36 hours (Case #7). Except for interfering with the evaluation of pulse oximetry measurements in this dog, PB injection did not cause any concern or require treatment. All dogs had blue-colored urine during the first 24-48 hours after surgery, but it was also self-limiting and did not cause any disturbance.

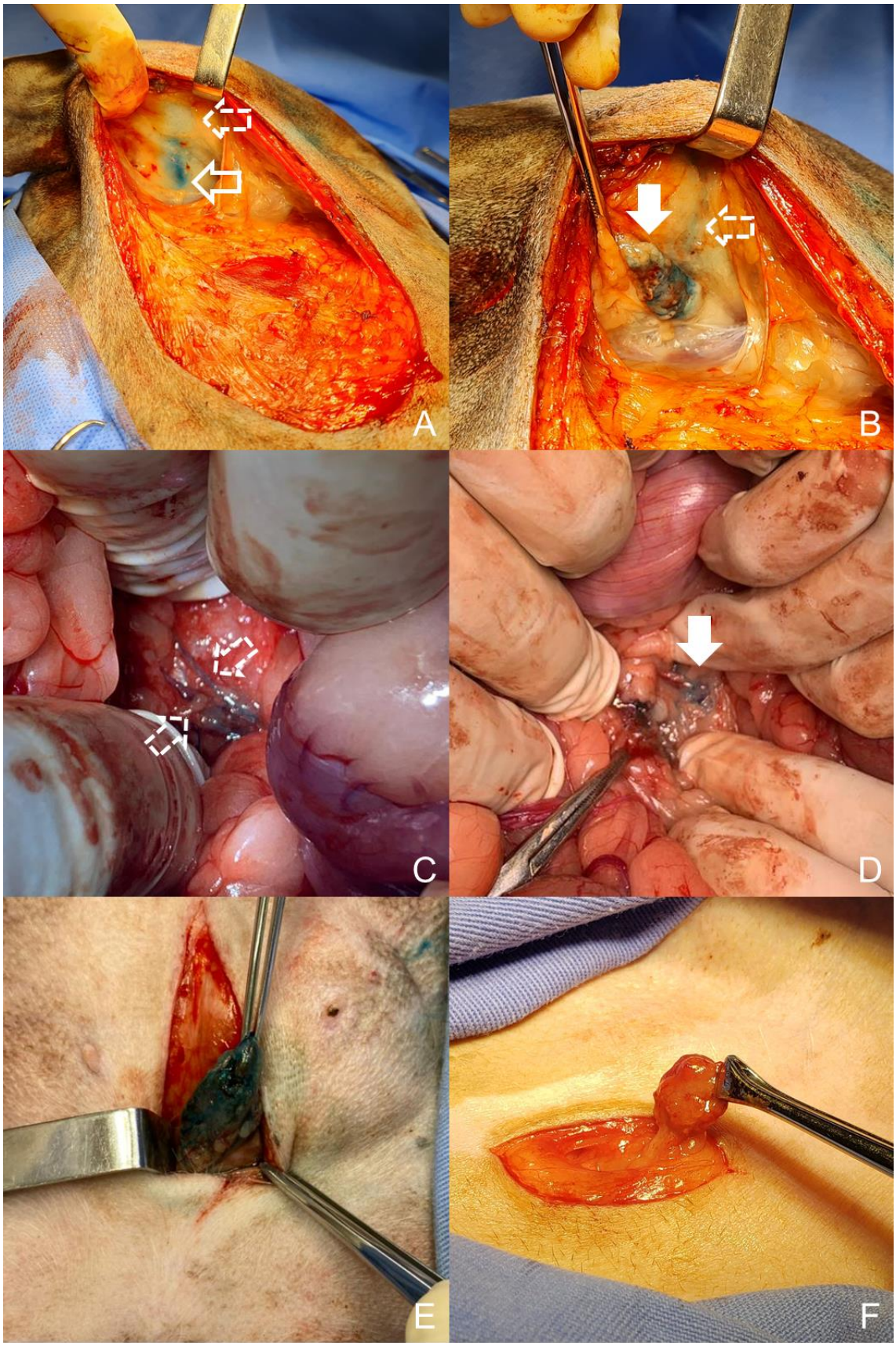

Figure 24. Intraoperative patent blue colorimetric method for sentinel lymph node mapping. (A and B) Axilar dissection through the incision was previously performed for tumor resection (Case #4). Afferent lymphatic vessels (dashed white arrow) and the axillary lymph node site (blank white arrow before dissection

and solid white arrow after dissection) with dark blue color can be seen. Spillage of patent blue can be seen on the tissues around the lymph node. (C) Median laparotomy view of Intraabdominal blue-stained afferent lymphatic vessels draining toward the iliac lymph node (Case #5). (D) Dark-colored iliac lymph node before dissection of perinodal fat. (E) Dark-colored inguinal lymph node (Case #6) (F) No patent blue uptake by an inguinal lymph node

3.4. Surgical Procedures

MCT resection and lymphadenectomy were attempted in all 23 dogs. However, surgeons could not locate and consequently resect the SLN in 3 out of 23 of the dogs (13%). All unresected SLN were the axillary LN. The inability to find and resect the axillary LNs were caused by its non-palpable size associated with the absence of PB uptake (Cases #13, #19, and #20). In two of these dogs, IO IL also failed to contrast the SLN (Case #13 and #20). On the other hand, the inguinal and popliteal LN could be resected in two dogs (Case #1 and #3) even when both methods failed.

A total of 31 LNs were removed in 20 dogs, with a mean and median of 1.34 ± 0.77 and 1 (range 0 – 3) per dog, respectively. In 2 dogs (10%), LN resection was bilateral, with both right and left inguinal LN removed simultaneously (Cases #6 and #11). In other 9 dogs (34.7%; Cases #1, #5, #6, #7, #9 #10, #11, #12, #14) surgeons were able to visualize the contralateral LN (inguinal [n=9] and iliac [n=8]) through the same surgical access to guarantee there were not bilaterally blue-dyed. The resected LNs were as follows: 16 (51.6%) inguinal LN, 6 (19.3%) medial iliac LN, 5 (16.1%) ventral superficial cervical LN, 2 (6.4% axillary, and 2 (6.4%) popliteal LN. Six dogs (26%) required a laparotomy to have one medial iliac LN resected. Intracavitary lymphadenectomy occurred uneventfully as there was no LN adhered to vascular structures. The addition of a laparotomy incision to access abdominal LN required changing of recumbency and increased the intraoperative time (not measured). However, it did not result in increased morbidity as no dog experienced adverse events related to the procedure.

Suture dehiscence of the tumor resection incision (n=5/23; 21.7%), lymphedema (n=2/20) of the hindlimb (n=1/12) and forelimb (n=1/5), edema of lymphadenectomy incision site (n=1/20), and seroma (n=1/23) occurred. Except

for suture dehiscence that required second-intention healing, all other complications were mild and self-limiting.

3.5. Agreement of IL, PB and expected SLN

The IO IL SLN mapping agreed with the expected SLN based on lymphatic territories (RLN) in 19 out of 23 dogs (82.6%). Of the 4 dogs in which IL disagree with the expected SLN, 3 of them had no LN contrasted. The remaining dog (Case #3) had a tumor caudolateral to the tibia draining to the right inguinal LN rather than the right popliteal LN. Moreover, IL could detect more than one SLN in 8 out of 23 dogs (34.7%). These additional SLN were the medial iliac (n=6) in dogs whose cMCT should drain to the inguinal LN (i.e., lateral thigh [n=2], knee [n=1], flank fold [n=2], and scrotum [n=1]), and the inguinal in a dog with a tumor at the dorsal tarsus, expected to drain to the popliteal LN (Case #17), and the axillary in a tumor at the dorsal carpus, that should drain to the ventral superficial LN (Case #15).

The rate of agreement of PB colorimetric method and locoregional expectation of SLN was 82.6% (n= 19/23) dogs. All four cases in which PB disagreed with the expected SLN were caused by the absence of PB uptake by the LNs. It is important to note that 6 out of 23 dogs (26.1%) had two SLN draining PB from the tumor. However, in 5 of these 6 dogs, the additional SLN was iliac, which could only be found because of previous contrast uptake seen during IL and, otherwise, would not be visualized. A cMCT (Case #17) had simultaneous drainage of PB to the popliteal (expected) and inguinal LN (extra SLN). In a dog (Case #11) in which bilateral drainage was expected, PB drained only to the left inguinal LN.

Table 6. Summary of lymph nodes detected by each method and the corresponding rate of agreement. RLN = Regional Lymph Node; PB Method =Patent Blue Colorimetric Method; IO IL = Iodized Oil Indirect Lymphography; LN = Lymph node; SLN = Sentinel Lymph Node; VSC = Ventral Superficial Cervical Lymph node; n = Number; * = Excluding all medial iliac lymph nodes

	RLN	PB Method	IO IL	Resected LN
n of LN Detected				
Base Scenario	27 (100%)	26 (100%)	29 (100%)	31 (100%)

Clinical Scenario	27(100%)	21* (-19.2%)	29 (100%)	31(100%)
LN Detected				
Inguinal	14 (51.8%)	14 (53.8%)	14 (48.2%)	16 (51.6%)
Medial Iliac	0 (0%)	5 (19.2%)	6 (20.6%)	6 (19.3%)
VSC	5 (18.5%)	5 (19.2%)	5 (17.2%)	5 (16.1%)
Axillary	6 (22.2%)	1 (3.8%)	3 (10.3%)	2 (6.4%)
Popliteal	2 (7.4%)	1 (3.8%)	1 (3.4%)	2 (6.4%)
LN Status				
HN0	16 (59.3%)	18 (69.3%)	18 (62.1%)	21 (67.7%)
HN≥1	6 (22.2%)	8 (30.7%)	10 (34.4%)	10 (32.2%)
Not resected	5 (18.5%)	0 (0%)	1 (3.4%)	-
Unexpected SLN		6	9	-
Rate of Agreement				
With RLN		82.6%	82.6%	
With PB			78.2%	

When comparing the IL SLN with PB mapping, there was an agreement in 18 out of 23 dogs (78.2%). Three dogs (Cases #1, #13, and #20) that simultaneously failed to opacify and blue color were considered an agreement. In the five dogs in which IL and PB disagreed, four (20%) favored the IO IL, as there was no PB uptake or IL detected an additional SLN (Case #6, #11, #15, and #19). The other favored PB as there was no contrast uptake (Case #8).

In summary (Table 5), of the total LN resected (n=31), 80.6% (n=25) were identified as SLN by both IL and PB, 12.9% (n=4) by IL only, and 3.2% by PB only (n=1). There was no statistical difference between both techniques in the number of detected SLN (P=.1855). However, when considering a clinical setting in which intracavitary LN would not be surgically accessed to confirm PB uptake (Case #5, #6, #7, #9, #10, #11, and #12) and cases of PB failure (Case #15 and #19), IO IL mapping was responsible for 29% (n=9 of 31) of the SNL resected, a 41% increase when comparing to PB colored superficial LN only. In this clinical scenario, the IO IL significative detected more SLN than the PB technique (P=.0081).

3.6. Drainage Patterns and Metastasis

In 3 of the 23 dogs, the SLN could not be found or resected, and histology could not be carried out. SLNs were metastatic (HN ≥1) in 6 out of 20 dogs (30%) or 10 out of 31 SLN resected (32.2%) Seven (70%) of these were classified as

overt metastasis (HN3), two (20%) as early metastasis (HN2) and only one (10%) as a pre-metastatic stage (HN1). In the remaining cases (n=21), LN was free of metastatic disease (i.e., HN0 and/or reactive). Among the intracavitary LN resected (n=6), half of them (n=3) were HN≥1, and the other half were considered non-metastatic (HN0).

In a dog with cMCT at the dorsal tarsus (Case #17), the popliteal LN was metastatic (HN2) while the ipsilateral inguinal LN was reactive. Both LN contrasted on IL and colored on blue dye mapping but diverged in histological status. Another dog with a caudal thigh cMCT (Case #7) had both inguinal and iliac LN contrasted and blue-dyed, but only the iliac was metastatic (HN1). Except for these two dogs, all other cases in which multiple SLNs were detected and resected had the same paired histologic status (3 metastatic [HN3] and 8 normal [HN0])

Among the HN≥1 LN (n=10), 8 (80%) were unequally contrasted on indirect lymphography and only two (20%) were uniformly contrasted. Considering the normal SLN (HN0) that contrasted on IL (n=18), 50% (n=9) and 50% (n=9) were unequally and uniformly contrasted, respectively. Three normal SLN (9.6%) did not contrast. There was no significant difference between metastatic and normal SLN considering the contrasting pattern (p=.2264). Using unequally contrasted SLN to predict locoregional metastasis had an 80% sensitivity (95% CI, 49 to 96.4%) and 50% specificity (95% CI, 29 to 71%). Positive predict value and negative predictive value were 47% (95% CI, 26.1 to 69%) and 81.8% (95% CI, 52.3 to 96.7%), respectively. There was a 2.6-fold (95% CI, 0.81 to 9.8) increased risk for metastasis if the SLN were unequally contrasted.

A similar result occurred when comparing light and dark blue colored SLN. There was no difference between both colors and locoregional metastasis (p=.9999). A sensitivity of 70% (95% CI, 39.6 to 89.22%) and specificity of 27.7% (95% CI, 12.5 to 50.8%) was found. Positive predict value was 35% (95% CI, 18.1 to 56.7%) and negative predictive value was 62.5% (95% CI, 30.5% to 86.3%). Among the blue colored SLN (n=26), 18 were dark blue with 7 (27.7%) metastatic and 13 (72.2%) normal/reactive. Light blue SLN occurred in 8 cases, with 5 (62.5%) normal and 3 (37.5%) metastatic.

Table 7 summarizes all patients and their respective results.

There were no association between opacification pattern and color (p=.9999), since there were 4 unequal-light (14.8%), 13 unequal-dark (48.1%), 3 uniform-light (11.1%), and 7 uniform-dark LN (26%).

There was a significant difference in tumor size between dogs with normal and metastatic SLN (p=.0456). However, there was no difference when size was categorized as >3 cm and <3 cm (p=.3359). Enlarged superficial SLN were significantly associated with the diagnosis of locoregional metastasis (p=.0374). The main clinical variables and association with metastatic SLN are summarized in table 8.

3.7. Impact on Treatment Decision

Eight out of 23 dogs (34.8%) were indicated for adjuvant or additional treatment after curative-intent surgical resection. The main reason that led to requirement of additional treatment was incomplete surgical resection (87.5%, n=7), locoregional metastatic disease (75%, n=6) and histological degree (12.5%, n=1). If LN were not histologically staged, 5 out of 8 dogs (62.5%) would receive scar revision surgery because of incomplete resection, but not adjuvant chemotherapy. SLN mapping changed treatment recommendations toward adding adjuvant chemotherapy in 5 dogs with LN metastasis. A dog with III-high grade cMCT would receive chemotherapy regardless of nodal status. The addition of radiographic IL, LN resection, and histology of more than just RLN or blue-colored SLN was not responsible for improving the rate of adjuvant chemotherapy recommendation, except for case #7 which had a metastatic iliac, but not on inguinal LN. On the other hand, 4 out of 6 dogs (Cases #5, #6, #7, and #11) had at least one metastatic LN detected on IL that would not be resected in a clinical setting.

Table 7. Summary of 23 dogs with cutaneous mast cell tumor submitted to iodized oil indirect lymphography (IO IL) and patent blue (PB) sentinel lymph node mapping, respective findings, and results of the histological evaluation.

Dog	Tumor Location	RLN	LN Size	IO IL	Opacification Pattern	PB Mapping	PB Staining	SLN Status	Grade
#1	L Gluteal	L Inguinal	Normal	No Contrast	No Contrast	No Color	No color	HN0	II/Low
#2	L Carpo	L VSC	NP	L VSC	Unequal	L VSC	Light	HN0	II/Low
#3	R Lateral Tibia	R Popliteal	Normal	No Contrast R Inguinal	No Contrast Unequal	No color R Inguinal	No color Dark	HN0 HN0	II/Low
#4	L Thorax Flank	L Axillary	NP	L Axillary	Uniform	L Axillary	Light	HN0	II/Low
#5	L Thigh	L Inguinal	Normal	L Inguinal L Iliac	Unequal Unequal	L Inguinal L Iliac	Light Dark	HN3 HN3	II/Low
#6	Scrotum	R + L Inguinal	Increased	R + L Inguinal R Iliac	Unequal Unequal	R + L Inguinal No Color	Dark + Light No Color	HN3 HN3	II/Low
#7	R Thigh	R Inguinal	Normal	R Inguinal R Iliac	Uniform Unequal	R Inguinal R Iliac	Dark Dark	HN0 HN1	II/Low
#8	L Flank Fold	L Inguinal	Normal	No Contrast	No Contrast	L Inguinal	Light	HN0	II/Low
#9	L Knee	L Inguinal	Increased	L Inguinal L Iliac	Uniform Unequal	L Inguinal L Iliac	Dark Light	HN0 HN0	II/Low
#10	L Flank Fold	L Inguinal	NP	L Inguinal L Iliac	Unequal Unequal	L Inguinal L Iliac	Dark Dark	HN0 HN0	I/Low
#11	Scrotum	R + L Inguinal	NP	R + L Inguinal	Unequal	L Inguinal	Dark	HN3/HN2	II/Low
#12	L Flank Fold	L Inguinal	NP	L Inguinal L Iliac	Unequal Unequal	L inguinal L Iliac	Dark Dark	HN0 HN0	II/Low
#13	Ventral Thorax	R + L Axillary	NP	No Contrast	No Contrast	No Color	No Color	NR	II/Low
#14	L Thigh	L Inguinal	NP	L Inguinal	Unequal	L Inguinal	Dark	HN0	II/Low
#15	R Dorsal Carpus	R VSC	NP	R VSC R Axillary	Uniform Uniform	R VSC No Color	Dark No Color	HN0 HN0	II/Low
#16	R Medial Thigh	R Inguinal	Normal	R Inguinal	Unequal	R Inguinal	Dark	HN0	II/Low
#17	R Dorsal Tarsus	R Popliteal	Increased Normal	R Popliteal R Inguinal	Uniform Uniform	R Popliteal R Inguinal	Dark Dark	HN2 HN0	II/Low
#18	L Thigh	L Inguinal	NP	L Inguinal	Uniform	L Inguinal	Light	HN0	II/Low

#19	R Abdomen	R Axillary	NP	R Axillary	Uniform	No color	No color	NR	II/Low
#20	Ventral Thorax	R + L Axillary	NP	No Contrast	No Contrast	No color	No color	NR	II/Low
#21	R Interdigital	R VSC	NP	R VSC	Uniform	R VSC	Dark	HN0	II/Low
#22	R Carpus	R VSC	NP	R VSC	Uniform	R VSC	Dark	HN0	I/Low
#23	R Digit	R VSC	Increased	R VSC	Uniform	R VSC	Light	HN3	III/High

Legend: LN = Lymph node; RLN = Regional Lymph Node; IO IL = Iodized oil Indirect Lymphography; PB = Patent Blue; SLN = Sentinel Lymph Node; R = Right; L = Left; VSC = Superficial Cervical Ventral; NR = Not Resected.

Table 8. Association between cutaneous mast cell tumor clinical variables and metastatic status of sentinel lymph nodes, respective relative risk (RR), and 95% confidence interval (95% CI).

Clinical Variables	Total (n=23)	Normal (n=14)	Metastasis (n=6)	P	RR	95% CI
Site						
Low-risk site	19	12 (7.7%)	3 (50%)	.0709	3.75	1.09 – 11.53
High-risk site	4	1 (92.3%)	3 (50%)			
Tumor Size						
Mean ± SD	20	2.32 ± 1.21	4.31 ± 3.02	.0456		
3 cm cut-off						
<3cm	13	5 (33.3%)	2 (35.7%)	.3359	2.44	0.65 – 9.84
>3cm	10	9 (66.7%)	4 (64.3%)			
Deep Invasion						
Yes	6	3 (21.4%)	3 (50%)	.3027	3.33	0.64 – 7.83
No	17	11 (78.6%)	3 (50%)			
Darier's Sign						
Yes	4	1 (7.1%)	2 (23.5%	.2018	2.83	0.75 – 8.10
No	19	13 (76.5%)	4 (66.7%)			
LN Size						
Non-palpable /normal	17	12 (85.7%)	2 (33.3%)	.0374	4.66	1.25 – 17.91
Enlarged	6	2 (14.3%)	4 (66.7%)			

4. DISCUSSION

In this cohort of dogs with cMCT, IO IL had a high rate of agreement with both RLN (82.6%) and PB colorimetric method (82.6%). A study with 26 dogs with various cancers had an 84.6% (22 dogs) rate of agreement between IO IL and the intraoperative blue dye method (Brissot et al., 2017). However, the simple agreement between SLN mapping techniques may not be the most important rate to be considered. In our study a difference between RLN and SLN only occurred in one dog, but, about 30% of the dogs had at least one additional SLN other than the RLN. A study evaluating lymphoscintigraphy found that about 42% of the dogs with cMCT had a SLN different from the RLN (Worley et al., 2014). Almost 20% of the dogs had an additional SLN detected only by IO IL in our study, which seems to be more beneficial as IL is a preoperative technique aiming to aid surgeons on which SLN must be approached. The possible spillage of contrast agent to second echelon LNs was a concern because increases surgical morbidity without a clear benefit. However, as most additional LNs were also blue-colored and PB mapping is considered the standard of care in both humans and animals (Brissot et al., 2017; Liptak et al., 2019), we considered that all

additional LNs were most probably SLN as well. Furthermore, half of the detected medial iliac LN were metastatic, confirming they were correctly identified as SLN.

It is important to note that, despite most medial iliac LNs being correctly identified as SLN by both methods, there was no external or superficial mark (i.e., blue-colored lymphatics) that indicate the iliac as the SLN. In other words, IO IL was responsible to guide the surgeon toward an abdominal surgical approach in approximately 26% of the dogs. The importance of preoperative SLN mapping was clear when half of the dogs with locoregional metastasis had an intracavitary metastatic SLN that once left unresected, would probably progress to severe lymphadenopathy and require further lymphadenectomy or bring additional morbidity. The same occurred in cases when drainage was not obvious, such as forelimb tumors and ventral thorax. Despite being no difference between the SLN number detected on IL and PB, when considering that the abovementioned conditions simulate a clinical scenario, IO IL increased SLN detection by 41% and significatively detected more SLN than the PB technique ($P<0.05$) due to its preoperative nature. This fact improved both staging and treatment of metastatic disease. However, it remains unclear whether the resection of additional SLN also reflects in a better long-term progression-free survival or overall survival time.

A recent retrospective study found that even prophylactic resection of LN is associated with a better prognosis, but no SLN mapping technique was described (Sabattini et al., 2021). Despite LN resection being highly recommended for suspected or known metastatic LN, the role of prophylactic lymphadenectomy is controversial and there is no standard evidence-based approach. Despite detecting metastasis in intracavitary SLN detected by IO IL, half of the dogs (n=3) were submitted to a laparotomy to remove medial iliac LN that resulted in non-metastatic. A randomized clinical trial is still necessary to make clear the real benefit of prophylactic resection of multiple and intracavitary SLN. The possibility of increased morbidity, costs, and surgical time must be well-balanced with other still theoretical factors (Sabattini et al., 2021).

There is a hypothesis that histological normal LN can bear isolated malignant mast cells that once left in place can cause tumor recurrence, further metastatic spread, and worsening the outcome (Marconato et al., 2018.; Sabattini

et al., 2021). This hypothesis has been confirmed in human melanoma and prophylactic lymphadenectomy was recommended in some patients (Balch et al., 1996; Balch et al., 2000). Also, the HN1 (Weishaar et al., 2014) is usually considered non-metastatic, but the presence of an increased number of reactive mast cells at the LN may represent micrometastasis rather than a mere proliferation (Marconato et al., 2008; Weishaar et al., 2014; Sabattini et al., 2021). In this context, a SLN mapping technique, such as IO IL, that allow early detection of multiple LN containing reactive, pre-metastatic, or micrometastasis of MCT may benefit these patients by allowing prophylactic resection. Despite we did not quantify the additional intraoperative time required for single or multiple SLN resections mostly requiring a laparotomy and changing the recumbency, there was no major complication associated with the procedures. Other authors found an average addition of 40 minutes to the procedure but also does not report complications or increased hospitalization length related to the intervention (Lapsley et al., 2020; Sabattini et al., 2021).

While the benefit of prophylactic LN resection remains unclear, a significantly better outcome was reported in grade II cMCT when metastatic LN was resected compared to metastasis found on cytology that was not resected (Baginski et al., 2014). A resection of LN containing metastatic mast cells decreases the local tumor burden on proliferation which may be responsible for a better outcome (Baginski et al., 2014).

We followed the IO IL and PB mapping protocol previously described for peritumoral injection in dogs (Mayer et al., 2012; Worley et al., 2014; Brissot et al., 2017). However, IO failed to opacify SLN in about 17% of the dog, almost 2 failures for every 10 dogs injected. Other studies reported a higher success rate, with at least one SLN opacified in 96.6% (Brissot et al., 2017) and 100% (Patsikas et al., 2006). In healthy dogs, failure to contrast LN occurred in 4 out of 25 dogs, which ultimately had a second IO injection that finally contrasted at least one LN (Mayer et al., 2012). A second IO injection was not performed on the dogs of our study as it would require postponing the surgical procedure. Lymphosonography also failed to detect SLN initially in some patients, requiring a second contrast injection in 3 out of 5 cases (Fournier et al., 2020).

The reason for SLN contrast failures remains unknown, but we hypothesize it may be caused by an inadvertent subcutaneous (rather than intradermal) injection or an idiosyncrasy that might be related to a low density of afferent lymphatic vessels on the tumor periphery. It is not possible to rule out the possibility of contrasted SLN being overlapped by bone structures or too unequally contrasted to be seen, however, these possibilities seem unlikely as the radiographs were extensively reviewed by multiple experienced professionals. Increasing the IO dose or reinjecting individuals that failed to contrast could be an alternative. Moreover, cases of IO drainage failure should be investigated as the absence of contrast uptake by the SLN does not mean there is no SLN or no metastatic disease in progress. Furthermore, a cluster of metastatic tumor cells clotting the lymphatic vessels cannot be ruled out. Two out of 33 dogs in a CT IL study had no contrasted SLN, but afferent lymphatic vessels were contrasted and both LNs were histologically metastatic. It was hypothesized that a metastatic disease caused the interruption of continuous lymph flow (Soultani et al., 2016). In another study with CT IL, 17% of the SLN were identified solely by the direction of contrasted lymphatic pathways rather than LN contrast uptake (Lapsley et al., 2020). The inability to visualize afferent lymphatic vessels on radiographic IL precludes the SLN indirect identification in these situations.

The hypothesis that an unequally contrasted SLN had a higher chance of being metastatic could not be confirmed in this study. This was based on the mechanistic idea that neoplastic tissue growing inside the LN would block the contrast agent to spread throughout all entire lymphatic tissue leading to a patchy opacification (Wisner et al., 1996; Soultani et al., 2016). A study evaluating CT IL found an association between a heterogeneous contrasted LN with metastasis (Soultani et al., 2016). Most of the metastatic SLN were unequally opacified in our study, but half of the normal SLN also exhibit an unequal opacification leading to a high rate of false-positive if the pattern were used as the sole criteria. Furthermore, PB and IO doses certainly can affect the degree of blue staining and intensity of LN opacification, respectively. Finally, we do not recommend using the pattern of IO uptake on radiographic IL to predict metastatic disease until further studies; however, unequally contrasted LN must be sampled or removed as they are SLN, and about half of them were metastatic in this study.

IO IL did not significatively alter the decision to pursue adjuvant chemotherapy when compared to the non-selective dissection and PB colorimetric method in our study. However, if LN were not resected and histologically evaluated, about 25% of the dogs would not receive any type of additional therapy as most were II-low grade. A recent prospective study had 50% of the dogs change postoperative treatment recommendations toward chemotherapy when indirect lymphography using CT scans was used in addition to RLN cytology (Lapsley et al., 2020). A retrospective study evaluating normal-sized LNs in predominantly low-grade cMCT, found that about 49.5% of the dogs would not receive adjuvant chemotherapy if LN were not excised (Ferrari et al., 2018). However, a non-selective dissection of the locoregional LN was used in the study. The authors hypothesized that non-selective dissection of the RLN matches well with SLN mapping due to the high rate of locoregional metastasis detected in their study (Ferrari et al., 2018), which was supported by our findings. However, surgeons not performing a SLN mapping technique may miss important metastatic SLN that once removed could approximate the dog of a macroscopic disease-free condition.

In dogs with multiple MCTs, both were resected in the same surgical procedure, but we choose to inject IO only in the largest tumor to precisely reflect the SLN of that region. The addition of IO injections on all tumors would certainly approximate the study of a clinical setting, however, it would bring a confounding factor while interpreting radiographs as we would not be able to determine from which tumor the contrast drained. A study evaluating IO injection and IL of multiple tumors is necessary to ensure there are advantages in staging.

Most of the dogs in our cohort had II-low grade MCTs and a low rate of locoregional metastatic disease was expected. However, 30% of the dogs had local metastasis, twice higher than the 16.2% and 16.5% of grade II and low-grade MCTs of a large retrospective study (Stefanello et al., 2015). On the other hand, a wide variable rate of LN metastasis ranging from 5 to 62% has been reported for grade II cMCT (Séguin et al., 2001; Weisse et al., 2002; Séguin et al., 2006; Baginski et al., 2014; Fournier et al., 2020). Other studies reported variable rates of LN metastasis depending on whether SLN mapping strategies were used or not. SLN metastasis of various grade cMCT ranges from 25 to 60% when SLN mapping was performed (Worley et al., 2014; Ferrari et al., 2020;

Fournier et al., 2020; Lapsley et al., 2020) and 42% to 46% when non-selective dissection was done (Ferrari et al., 2018; Fournier et al., 2018). A multicentric retrospective study found a 65% rate of metastasis in non-palpable or normal LN of dogs bearing cMCT (Ferrari et al., 2018). Oncologists and surgeons must be aware of the possibility of LN metastasis in all cases of cMCT and consider full staging even in well-differentiated or low-grade cMCT (Fournier et al., 2020). Considering the above-mentioned rate of metastatic disease on additional SLN, we also recommend SLN mapping for low-grade cMCT until further studies evaluate the long-term benefit of this practice. Despite our findings, a recent study suggested that MCTs without negative prognostic factors may not need extensive staging (Fejös et al., 2022). However, it should be considered that the histopathological result after surgery is the gold-standard to confirm the tumor grade, and, in a clinical scenario, it is not possible to determine whether the tumor is low grade based on cytological preoperative examination only. Also, cMCT can assume the low-high form, in which a low-grade MCT exhibit a high-grade biological behavior (Bae et al., 2020). A recent consensus proposal on canines recommended SLN evaluation for all dogs with cMCT but did not indicate full staging for low-grade cMCT unless organomegaly or signs of metastasis were present (Willmann et al., 2021).

Only mild complications occurred after IO injection, however, none of these carried important disturbance. Furthermore, peritumoral tissues were resected along with the MCT 24 hours after injection preventing long-term evaluation of possible local tissue reaction, but also removing the hyperemic sites.

Uniquely contrasted LNs were sometimes challenged to identify on simple radiographs as they were often superposed to bone structures, especially on pelvic, abdominal, or hindlimb radiographs. Multiple radiographs with the limbs extended and flexed were required to assure correct identification of the LN and determine its side. Medial iliac LN identification was also a challenge and required special attention to detect contrast due to the superposition of the vertebral column, colon, and normal abdominal opacity. Altering the brightness and contrast of the digital images was necessary in a few cases.

The owners were not instructed to perform any gastrointestinal preparation before radiographic for SLN mapping with IL. However, further studies should consider indicating gastrointestinal preparation before radiographic survey as gas or fecal content inside the colon or intestinal loops makes it harder to detect uniquely contrasted iliac LNs.

Three dogs with suspected axillary SLN could not be located intraoperatively. The main reason that prevented SLN resection was the absence of blue dye uptake associated with the complexity of the surgical approach and limited vision. Also, surgeons reported that in at least one case a diffuse blue discoloration of the surrounding fat and muscle difficulted LN identification. Other authors also reported difficulties to locate the axillary LN (Lapsley et al., 2020) and other non-colored LN (Fournier et al., 2020). These findings support the importance of an intraoperative maker in association with preoperative mapping. Alternative techniques to aid intraoperative localization of LNs were recently proposed. A pilot study suggested the use of an ultrasound-guided hook-wire device for intraoperative localization of superficial inguinal LNs that could be extrapolated to other superficial nodes (Pierini et al., 2020). A retrospective study found a slightly better lymphadenectomy success rate using an ultrasound-guided anchor wire to guide the surgeon during intraoperative localization of peripheral nodes when compared to methylene blue and no technique (Rossanese et al., 2022). Surprisingly and despite complex anatomy, intracavitary LN could be easily identified and dissected without complications.

Limitations of this study include the heterogenicity and the small number of dogs in the cohort, the variability of anatomic sites, the presence of dogs with more than one cMCT, and the non-randomized/non-blinded nature of the study. The absence of a control group and long-term follow-up after surgery preclude establishing the disease-free intervals or survival time of dogs with cMCT submitted to IO IL. Further studies should evaluate if adding a radiographic IL as a preoperative technique for SLN mapping and the resulting increased number of SLN resected also improve the outcome of these dogs before an evidence-based recommendation can be made. However, as complications of lymphadenectomy seem to be uncommon or mild in dogs (Sabattini et al., 2021), the clinician that chooses to approach multiple LN may not be concerned about

additional or unnecessary harm. Furthermore, there is currently weak evidence that early lymphadenectomy decreased the risk of tumor progression in low-grade MCT (Sabattini et al., 2021).

A recent consensus proposed FNA cytology for RLN and SLN as a triage method of detecting LN metastasis (Willmann et al., 2021). Although feasible, we did not include LN cytology because we intended to submit all suspect nodes to histopathological examination, and due to the high rate of nondiagnostic samples or false-negative of FNA (Langenbach et al., 2001; Ku et al., 2017; Ferrari et al., 2018; Lapsley et al., 2020; Sabattini et al., 2021). The usability of FNA cytology to guide treatment decision remains highly controversial (Fournier et al., 2018; Lapsley et al., 2020; Willmann et al., 2021). A direct comparison of FNA cytology of the RLN and SLN mapping was beyond the scope of this study.

We have indicated postoperative adjuvant chemotherapy for dogs with metastatic LN due to the risk of disease dissemination (Blackwood et al., 2012). However, a recent retrospective study evaluating high-grade and low-grade cMCT with SLN metastasis suggested that grade rather than the stage is a determinant for the prognosis (Guerra et al., 2022).

A pilot study of radiographic IL taken 10 minutes after contrast injection was performed before the beginning of the study. Despite the single case, we strongly recommend the clinician to wait for the optimal time for the radiographic survey due to the risk of missing contrasted SLN. The time until radiographs may be lower if a hydrosoluble contrast agent is used, as occurs with CT IL in which the patient can be scanned 10 minutes after injection (Lapsley et al., 2020).

Dogs with node metastasis had significantly larger primary cMCT lesions (mean of 4.3 ± 3.0 vs 2.3 ± 1.2). Other studies evaluating SLN mapping techniques also found an increased rate of metastasis in larger cMCT (>2.6cm; Fournier et al., 2020). Enlarged SLN were 4.6-fold more likely at risk of being metastatic. Palpably enlarged LN were more likely to bear metastatic disease in another study, with a sensitivity and specificity of 71% and 54% respectively (Baginski et al., 2014).

Preoperative IO IL associated with PB colorimetric technique is a reliable and efficient method to stage dogs with cMCTs undergoing curative-intent

surgical resection. Despite not significantly altering the number of SLN detected, when in a clinical scenario IO IL detected more SLN than PB, mainly intraabdominal LN in which PB does not allow visualization without additional surgery. The association of IO IL with intraoperative PB seems to be essential due to the difficulty in locating some SLN when not colored. Until further studies, the pattern of SLN opacification should not be used to predict metastasis. Finally, the IO IL seems to be useful, accessible, and easy to incorporate into the routine of most veterinary facilities.

ACKNOWLEDGMENTS

The authors would like to thank all residents and veterinary doctors of the Veterinary Hospital, Federal University of Paraná, Curitiba, Paraná, Brazil for their contribution to case selection and patient management. This study was financed in part by the Coordenação de Aperfeiçoamento de Pessoal de Nível Superior - Brasil (CAPES) - Finance Code 001

CONFLICT OF INTEREST STATEMENT

The authors declare that there were no conflicts of interest.

FUNDING

This research did not receive any specific grant from funding agencies in the public, commercial, or not-for-profit sectors.

AUTHORS CONTRIBUTION

JGQ and VGPA conceived the study design and executed data analysis. VGPA, NNK, GLB, WSP, and JGQ contributed to patients' selection, data acquisition, contrast injection, radiographic and ultrasonographic studies and interpretation, surgical procedures, and post-operative management. All authors wrote, revised, and approved the final version of this original article.

REFERENCES

1. Bae S, Milovancev M, Bartels C, et al. Histologically low-grade, yet biologically high-grade, canine cutaneous mast cell tumours: A systematic

review and meta-analysis of individual participant data. Vet Comp Oncol. 2020; 18: 580– 589

2. Baginski H, Davis G, Bastian RP, The prognostic value of lymph node metastasis with grade 2 MCTs in dogs: 55 cases (2001-2010). J Am Vet Hosp Assoc 2014; 50(2): 89-95.
3. Balasubramanian SP, Harrison BJ. Systematic review and meta-analysis of sentinel node biopsy in thyroid cancer. Br J Surg 2011;98:344–444.
4. Balch CM, Soong S, Ross MI, et al. Long-term results of a multi-institutional randomized trial comparing prognostic factors and surgical results for intermediate thickness melanomas (1.0 to 4.0 mm). Ann Surg Oncol. 2000;7(2):87–97.
5. Balch CM, Soong S-J, Bartolucci AA, et al. Efficacy of an elective regional lymph node dissection of 1 to 4 mm thick melanomas for patients 60 years of age and younger. Ann Surg. 1996;224(3):255–66.
6. Balogh L, Thuróczy J, Andócs G, et al. Sentinel lymph node detection in canine oncological patients. Nucl Med Rev. 2002;5(2):139–144.
7. Beer P, Pozzi A, Rohrer Bley C, Bacon N, Pfammatter NS, Venzin C. The role of sentinel lymph node mapping in small animal veterinary medicine: A comparison with current approaches in human medicine. Vet Comp Oncol 2018; 16:178-187.
8. Blackwood L, Murphy S, Buracco P, et al. European consensus document on mast cell tumours in dogs and cats. Vet Comp Oncol. 2012; 10(3):e1–e29.
9. Brissot HN, Edery EG. Use of indirect lymphography to identify sentinel lymph node in dogs: a pilot study in 30 tumors. *Vet Comp Oncol*. 2016;15:740-753.
10. Cahalane AK, Payne S, Barber LG, et al. Prognostic factors for survival of dogs with inguinal and perineal mast cell tumours treated surgically with or without adjunctive treatment: 68 cases (1994-2002). J Am Vet Med Assoc. 2004;225:401-408.
11. Cochran AJ, Oshie SJ and Binder SW. Pathobiology of the sentinel node. Curr Opin Oncol 2008; 20:190–195.
12. Fejös, C, Troedson, K, Ignatenko, N, Zablotski, Y, Hirschberger, J. Extensive staging has no prognostic value in dogs with low-risk mast cell tumours. Vet Comp Oncol. 2022; 20(1): 265- 275.

13. Fejös, C, Troedson, K, Ignatenko, N, Zablotski, Y, Hirschberger, J. Extensive staging has no prognostic value in dogs with low-risk mast cell tumours. Vet Comp Oncol. 2022; 20(1):265- 275.
14. Ferrari R, Marconato L, Buracco P, et al. The impact of extirpation of non-palpable/normal-sized regional lymph nodes on staging of canine cutaneous mast cell tumours: A multicentric retrospective study. *Vet Comp Oncol.* 2018;1–6.
15. Fournier Q, Cazzini P, Bavcar S, et al. Investigation of the utility of lymph node fine-needle aspiration cytology for the staging of malignant solid tumors in dogs. Vet Clin Pathol. 2018; 47(3):489-500.
16. Fournier Q, Thierry F, Longo M, et al. Contrast-enhanced ultrasound for sentinel lymph node mapping in the routine staging of canine mast cell tumours: A feasibility study. Vet Comp Oncol. 2020; 19(3):451-462.
17. Gelb HR, Freeman LJ, Rohleder JJ, Snyder PW. Feasibility of contrast-enhanced ultrasound-guided biopsy of sentinel lymph nodes in dogs. Vet Radiol Ultrasound. 2010;51(6):628–633.
18. Giuliano AE, Kirgan DM, Guenther JM and Morton DL. Lymphatic mapping and sentinel lymphadenectomy for breast cancer. Ann Surg 1994; 220:391–398
19. Grimes JA, Secrest SA, Northrup NC, Saba CF, Schmiedt CW. Indirect computed tomography lymphangiography with aqueous contrast for evaluation of sentinel lymph nodes in dogs with tumors of the head. Vet Radiol Ultrasound. 2017;58:559–564.
20. Hayes A, Adams V, Smith K, Maglennon G, Murphy S. Vinblastine and prednisolone chemotherapy for surgically excised grade III canine cutaneous mast cell tumours. Vet Comp Oncol. 2007;5:168-176.
21. Herring ES, Smith MM, Roberston JL. Lymph node staging of oral and maxillofacial neoplasms in 31 dogs and cats. J Vet Dent 2002;19:122–6
22. Hillman LA, Garrett LD, de Lorimier LP, Charney SC, Brost LB, Fan TM. Biological behavior of oral and perioral mast cell tumours in dogs: 44 cases (1996-2006). J Am Vet Med Assoc. 2010;237:936-942.
23. Hume CT, Kiupel M, Rigatti L, Shofer FS, Skorupski KA, Sorenmo KU. Outcomes of dogs with grade 3 mast cell tumours: 43 cases (1997-2007). J Am Anim Hosp Assoc. 2011;47:37-44.

24. Kim T, Giuliano AE, Lyman GH. Lymphatic mapping and sentinel lymph node biopsy in early-stage breast carcinoma: a meta-analysis. Cancer. 2006;106(1):4–16.
25. Kiupel M, Camus M. Diagnosis and prognosis of canine cutaneous mast cell tumors. Vet Clin North Am Small Anim Pract. 2019;49:819–36.
26. Kiupel M, Webster JD, Bailey KL, Best S, DeLay J, Detrisac CJ, Fitzgerald SD, Gamble D, Ginn PE, Goldschmidt MH, Hendrick MJ, Howerth EW, Janovitz EB, Langohr I, Lenz SD, Lipscomb TP, Miller MA, Misdorp W, Moroff S, Mullaney TP, Neyens I, O'Toole D, Ramos-Vara J, Scase TJ, Schulman FY, Sledge D, Smedley RC, Smith K, W Snyder P, Southorn E, Stedman NL, Steficek BA, Stromberg PC, Valli VE, Weisbrode SE, Yager J, Heller J, Miller R. Proposal of a 2-tier histologic grading system for canine cutaneous mast cell tumors to more accurately predict biological behaviour. Vet Pathol 2011; 48:147–155.
27. Krick EL, Billings AP, Shofer FS, Watanabe S, Sorenmo KU. Cytological lymph node evaluation in dogs with mast cell tumours: association with grade and survival. Vet Comp Oncol. 2009;7:130-138.
28. Lapsley J, Hayes GM, Janvier V, et al. Influence of locoregional lymph node aspiration cytology vs sentinel lymph node mapping and biopsy on disease stage assignment in dogs with integumentary mast cell tumors. Vet Surg. 2021; 50(1):133-141.
29. Liptak JM, Boston SE. Nonselective lymph node dissection and sentinel lymph node mapping and biopsy. Vet Clin Small Anim. 2019;49:793-807.
30. Lurie DM, Seguin B, Schneider PD, Verstraete FJ, Wisner ER. Contrast-assisted ultrasound for sentinel lymph node detection in spontaneously arising canine head and neck tumors. Invest Radiol. 2006;41(4):415–421.
31. Majeski SA, Steffey MA, Fuller M, Hunt GB, Mayhew PD, Pollard RE. Indirect computed tomographic lymphography for iliosacral lymphatic mapping in a cohort of dogs with anal sac gland adenocarcinoma: technique description. Vet Radiol Ultrasound. 2017;58: 295–303.
32. Marconato L, Marchetti V, Francione D, et al. Morphometrical approach for predicting regional lymph node micrometastatic load in canine mast cell tumours: preliminary results. Vet Comp Oncol. 2008;6(3):162–70.
33. Marconato L, Polton G, Stefanello D, et al. Therapeutic impact of regional

lymphadenectomy in canine stage II cutaneous mast cell tumours. Vet Comp Oncol. 2018;16(4):580–9.

34. Marconato, L, Polton, G, Stefanello, D, et al. Therapeutic impact of regional lymphadenectomy in canine stage II cutaneous mast cell tumours. Vet Comp Oncol. 2018; 16: 580– 589.
35. Marconato, L, Polton, G, Stefanello, D, et al. Therapeutic impact of regional lymphadenectomy in canine stage II cutaneous mast cell tumours. Vet Comp Oncol. 2018; 16:580– 589.
36. Mayer MN, Kraft SL, Bucy DS, Waldner CL, Elliot KM, Wiebe S. Indirect magnetic resonance lymphography of the head and neck of dogs using Gadofluorine M and a conventional gadolinium contrast agent: a pilot study. Can Vet J. 2012;53(10):1085–1090.
37. Mayer MN, Silver TI, Lowe CK, Anthony JM. Radiographic lymphangiography in the dog using iodized oil. Vet Comp Oncol. 2013;11(2): 151–161.
38. Morton DL, Cochran AJ,Thompson JF, et al. Sentinel node biopsy for early stage melanoma: accuracy and morbidity in MSLT-I, an international multicenter trial. Ann Surg. 2005; 242:302–311.
39. Murphy S, Sparkes AH, Blunden AS, Brearley MJ, Smith KC. Effects of stage and number of tumours on prognosis of dogs with cutaneous mast cell tumours. Vet Rec. 2006;158:287-291.
40. Niebling MG, Pleijhuis RG, Bastiaannet E, Brouwers AH, van Dam GM, Hoekstra HJ. A systematic review and meta-analyses of sentinel lymph node identification in breast cancer and melanoma, a plea for tracer mapping. Eur J Surg Oncol. 2016;42(4):466–473.
41. Oliveira MT, Campos M, Lamego L, Magalhães D, Menezes R, Oliveira R, Patanita F, Ferreira DA. Canine and Feline Cutaneous Mast Cell Tumor: A Comprehensive Review of Treatments and Outcomes. Top Companion Anim Med. 2020; 41:100472
42. Patnaik AK, Ehler WJ, MacEwen EG. Canine cutaneous mast cell tumour: Morphologic grading and survival time in 83 dogs. Vet Pathol 1984; 21:469-474.
43. Pierini A, Marchetti V, Rossanese M, et al. Ultrasound-guided hook-wire localization for surgical excision of non-palpable superficial inguinal lymph nodes in dogs: A pilot study. Animals. 2020; 10:2314.

44. Qiu SQ, Zhang GJ, Jansen L, et al. Evolution of sentinel lymph node biopsy in breast cancer. Crit Rev Oncol Hematol 2018;123:83–94.
45. Rossanese M, Pierini A, Pisani G, Freeman A, Burrow R, et al. Ultrasound-guided placement of an anchor wire or injection of methylene blue to aid in the intraoperative localization and excision of peripheral lymph nodes in dogs and cats. J Am Vet Med Assoc 2022; 260(S1): S75-S82.
46. Séguin B, Besancon MF, McCallan JL, et al. Recurrence rate, clinical outcome, and cellular proliferation indices as prognostic indicators after incomplete surgical excision of cutaneous grade II mast cell tumors: 28 dogs (1994–2002). J Vet Intern Med 2006; 20(4):933-40.
47. Séguin B, Leibman NF, Bregazzi VS, et al. Clinical outcome of dogs with grade-II mast cell tumors treated with surgery alone: 55 cases (1996–1999). J Am Vet Med Assoc 2001;218(7): 1120–3.
48. Sledge DG, Webster J, Kiupel M. Canine cutaneous mast cell tumors: a combined clinical and pathologic approach to diagnosis, prognosis, and treatment selection. Vet J. 2016; 215:43–54.
49. Smith MM. Surgical approach for lymph node staging of oral and maxillofacial neoplasms in dogs. J Vet Dent 2002;19:170–4.
50. Somasundaram SK, Chicken DW, Keshtgar MRS. Detection of sentinel lymph node in breast cancer. Br Med Bull 2007;84:117–31.
51. Soultani C, Patsikas MN, Karayannopoulou M, et al. Assessment of sentinel lymph node metastasis in canine mammary gland tumors using computed tomographic indirect lymphography. Vet Radiol Ultrasound. 2016;58:186–196
52. Stefanello D, Buracco P, Sabattini S, et al. Comparison of 2- and 3-category histologic grading systems for predicting the presence of metastasis at the time of initial evaluation in dogs with cutaneous mast cell tumors: 386 cases (2009-2014). J Am Vet Med Assoc. 2015; 246:765-769.
53. Suami H, Yamashita S, Soto-Miranda MA, Chang DW. Lymphatic territories (lymphosomes) in a canine: an animal model for investigation of postoperative lymphatic alterations. PLoS One. 2013;8:1-9.
54. Thamm DH, Turek MM, Vail DM. Outcome and prognostic factors following adjuvant prednisone/vinblastine chemotherapy for high-risk canine mast cell tumour: 61 cases. J Vet Med Sci. 2006;68:581-587.

55. Thompson JF, Uren RF, Shaw HM, et al. Location of sentinel lymph nodes in patients with cutaneous melanoma: new insights into lymphatic anatomy. J Am Coll Surg 1999;189:195–206.
56. Turner RR, Ollila DW, Krasne DL, et al. Histopathologic validation of the sentinel lymph node hypothesis for breast carcinoma. Ann Surg 1997;226:271-6.
57. Wang Y, Cheng Z, Li J, Tang J. Gray-scale contrast-enhanced ultrasonography in detecting sentinel lymph nodes: an animal study. Eur J Radiol. 2010;74(3):e55–e59.
58. Warland J, Amores-Fuster I, Newbury W, Brearley M, Dobson J. The utility of staging in canine mast cell tumours. Vet Comp Oncol. 2014; 12:287-29.
59. Weisse C, Shofer FS, Sorenmo K. Recurrence rates and sites for grade II canine cutaneous mast cell tumors following complete surgical excision. J Am Anim Hosp Assoc 2002;38(1):71–3.
60. Willmann M, Gurkan-Yuzbasiyan V, Marconato L, et al. Proposed diagnostic criteria and classification of canine mast cell neoplasms: A Consensus Proposal. Front Vet Sci 2021; 8:1-10.
61. Wisner ER, Seibert JA, Katzberg RW. Quantitative methods for indirect CT lymphography. Vet Radiol Ultrasound. 1998; 39:110-116
62. Worley DR. Incorporation of sentinel lymph node mapping in dogs with mast cell tumours: 20 consecutive procedures. Vet Comp Oncol. 2014; 12:215-226.

CHAPTER 3

SUPPLEMENTARY FILE 1

Experimental Design of the Study

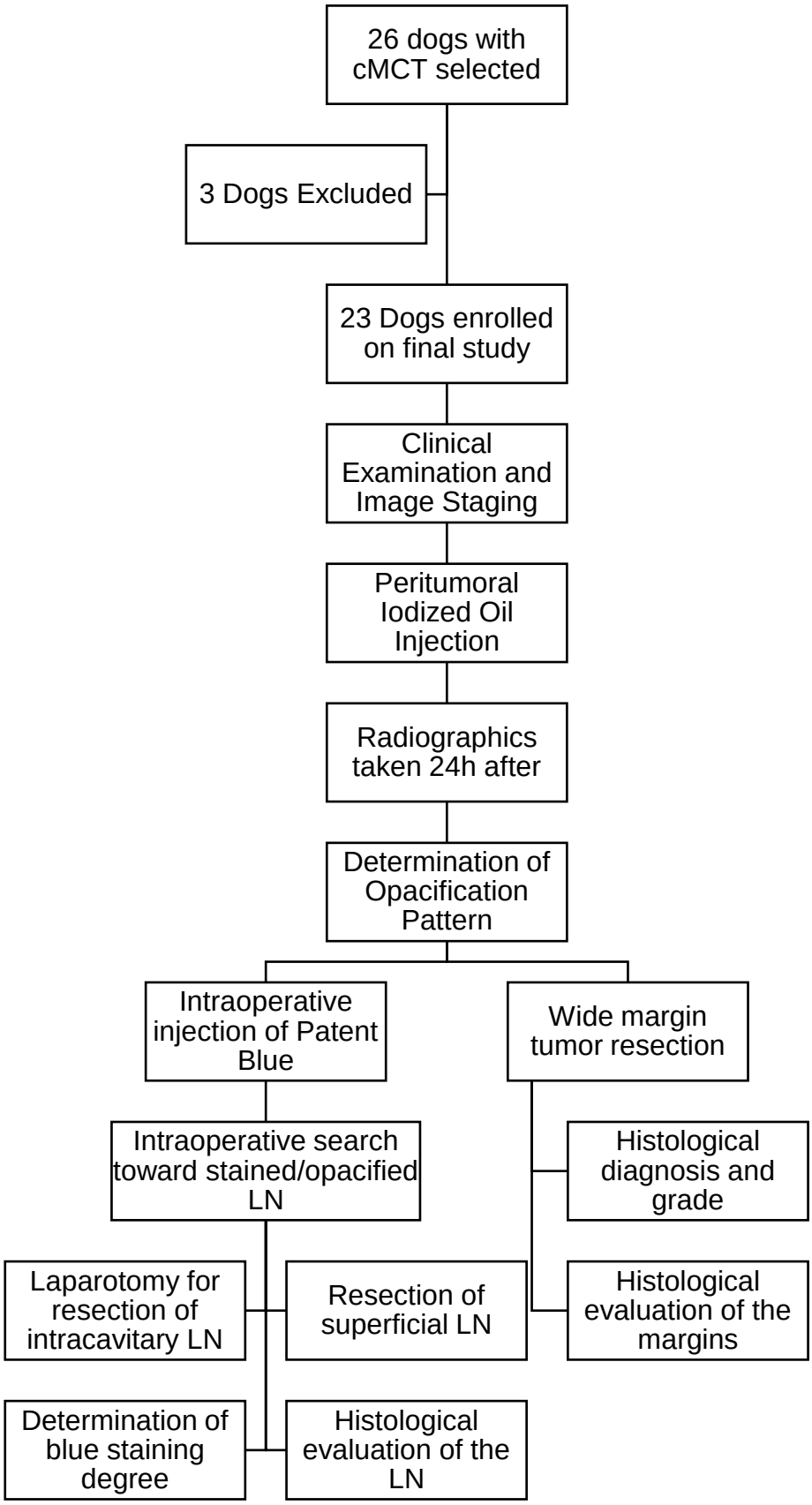

SUPPLEMENTARY FILE 2

Summary of all Patients enrolled in the study

#	Sex	Breed	Age (years)	Weight (kg)	Number Tumors	Tumor Size (cm)	Tumor Location	RLN	LN Size	Number Colored SLN	Number Opacified SLN	LN Status
#1	Male	Pittbull	4	30	1	1.2	Gluteal	Inguinal	N	0	0	HN0
#2	Male	Pug	10	10	1	1.5	Carpus	VSC	N	1	1	HN0
#3	Female	Mixed	8	20	3	1.4	Tibia	Popliteal	N	1	1	HN0
#4	Male	Lhasa	8	10	1	4	Thorax	Axillary	N	1	1	HN0
#5	Female	Mixed	10	18	1	9.8	Thigh	Inguinal	↑	2	2	HN3
#6	Male	Mixed	9	11	1	3	Scrotum	Bilateral Inguinal	↑	2	3	HN3
#7	Male	Maltese	7	5	1	1.2	Thigh	Inguinal	N	2	2	HN1
#8	Female	Mixed	8	19	1	1.7	Flank Fold	Inguinal	N	1	0	HN0
#9	Female	Mixed	6	25	1	1.9	Knee	Inguinal	↑	2	2	HN0
#10	Female	Mixed	10	20	1	0.8	Flank Fold	Inguinal	N	2	2	HN0
#11	Male	Pittbull	9	31	2	4.5	Scrotum	Inguinal	N	1	2	HN3/2
#12	Female	Mixed	11	11	1	3.6	Flank Fold	Inguinal	N	2	2	HN0
#13	Male	Mixed	8	9	1	3.4	Thorax	Bilateral Axillary	N	0	0	HNX
#14	Male	Pittbull	10	34	1	2.1	Thigh	Inguinal	↑	1	1	HN0
#15	Male	Mixed	8	27	1	4	Carpus	VSC	N	1	2	HN0

#16	Female	Boxer	11	25	1	4	Thigh	Inguinal	N	1	1	HN0
#17	Male	Mixed	8	21	1	5	Tarsus	Popliteal	↑	2	2	HN2
#18	Female	Pittbull	3	24	1	1.9	Thigh	Inguinal	N	1	1	HN0
#19	Male	French Bulldog	4	17	1	2.2	Abdomen	Axillary	N	0	1	HNX
#20	Female	Labrador	9	26	1	1.2	Thorax	Bilateral Axillary	N	0	0	HNX
#21	Female	Shih Tzu	7	10	1	1	Digit	VSC	N	1	1	HN0
#22	Female	Boxer	2	30	1	3.5	Carpus	VSC	N	1	1	HN0
#23	Female	Labrador	6	35	1	2.4	Digit	VSC	N	1	1	HN3

SUPPLEMENTARY FILE 3

Summary of draining Sentinel Lymph Nodes based on tumor locations

This table summarizes the SLNs according to the tumor location of the Cohort of dogs with cutaneous mast cell tumor.

Regions	RLN	Possible SLN
Ventral and Flank Thorax		
	Axillary	Uni- or Bilateral Axillary
Ventral Abdomen		
	Axillary Inguinal	Axillary
Scrotum		
	Inguinal	Uni- or Bilateral Inguinal Medial Iliac
Carpus		
	VSC	VSC Axillary
Digit		
	VSC	VSC
Tarsus		
	Popliteal	Popliteal Inguinal
Lateral Tibia and Knee		
	Popliteal	Inguinal Popliteal Medial Iliac
Thigh, Gluteal and Flank Fold		
	Inguinal	Inguinal Medial Iliac

Legend: RLN = Regional Lymph Node; SLN = Sentinel Lymph Nodes; VSC = Ventral Superficial Cervical

SUPPLEMENTARY FILE 4

Universidade Federal do Paraná Animal Ethics Committees Approval

UNIVERSIDADE FEDERAL DO PARANÁ
SETOR DE CIÊNCIAS AGRÁRIAS
COMISSÃO DE ÉTICA NO USO DE ANIMAIS

CERTIFICADO

Certificamos que o protocolo número 057/2020, referente ao projeto de pesquisa **"Mapeamento dos linfonodos sentinelas por meio de linfografia indireta com contraste lipossolúvel em cães com mastocitoma cutâneo",** sob a responsabilidade de **Vinicius Gonzalez Peres Albernaz** – que envolve a produção, manutenção e/ou utilização de animais pertencentes ao filo Chordata, subfilo Vertebrata (exceto o homem), para fins de pesquisa científica ou ensino – encontra-se de acordo com os preceitos da Lei nº 11.794, de 8 de Outubro de 2008, do Decreto nº 6.899, de 15 de julho de 2009, e com as normas editadas pelo Conselho Nacional de Controle da Experimentação Animal (CONCEA), e foi aprovado pela COMISSÃO DE ÉTICA NO USO DE ANIMAIS (CEUA) DO SETOR DE CIÊNCIAS AGRÁRIAS DA UNIVERSIDADE FEDERAL DO PARANÁ - BRASIL, com grau 2 de invasividade, em 01/02/2021.

Finalidade	Pesquisa
Vigência da autorização	Janeiro/2021 até Junho/2021
Espécie/Linhagem	*Canis lupus familiaris* (canino)
Número de animais	20
Peso/Idade	Variável
Sexo	Machos e fêmeas
Origem	Hospital Veterinário da Universidade Federal do Paraná, Curitiba/PR, Brasil.

*A autorização para início da pesquisa se torna válida a partir da data de emissão deste certificado.

CERTIFICATE

We certify that the protocol number 057/2020, regarding the research project **"Sentinel lumph node mapping by indirect lumphography using liposoluble contrast in dogs with cutaneous mast cell tumor"** under **Vinicius Gonzalez Peres Albernaz** – which includes the production, maintenance and/or utilization of animals from Chordata phylum, Vertebrata subphylum (except Humans), for scientific or teaching purposes – is in accordance with the precepts of Law nº 11.794, of 8 October 2008, of Decree nº 6.899, of 15 July 2009, and with the edited rules from Conselho Nacional de Controle da Experimentação Animal (CONCEA), and it was approved by the ANIMAL USE ETHICS COMMITTEE OF THE AGRICULTURAL SCIENCES CAMPUS OF THE UNIVERSIDADE FEDERAL DO PARANÁ (Federal University of Paraná, Brazil), with degree 2 of invasiveness, on 2021, February 1st.

Purpose	Research
Validity	January/2021 until June/2021
Specie/Line	*Canis lupus familiaris* (canine)
Number of animals	20
Weight/Age	Various
Sex	Male/Female
Origin	Veterinary Hospital of the Federal University of Paraná, Curitiba/PR, Brazil.

*The authorization to start the research becomes valid from the date of issue of this certificate.

Curitiba, 01 de fevereiro de 2021

Simone Tostes de Oliveira Stedile
Coordenadora CEUA-SCA

SUPPLEMENTARY FILE 5

São Paulo State University Animal Ethics Committees Approval

unesp UNIVERSIDADE ESTADUAL PAULISTA "JÚLIO DE MESQUITA FILHO"

fmvz - unesp
Faculdade de Medicina Veterinária e Zootecnia
Campus de Botucatu

ATESTADO

Atesto que o Projeto "Mapeamento dos linfonodos sentinelas por meio de linfografia indireta com contraste lipossolúvel em cães com mastocitoma cutâneo " **Protocolo CEUA 0195/2020** , a ser conduzido por Vinicius Gonzales Peres Albernaz, responsável/orientador Juliany Gomes Quitzan, para fins de pesquisa científica/ensino - encontra-se de acordo com os preceitos da Lei nº 11.794, de 08 de outubro de 2008, do Decreto nº 6.899, de 15 de julho de 2009, e com as normas editadas pelo Conselho Nacional de Controle de Experimentação Animal - CONCEA.

Finalidade	PESQUISA CIENTÍFICA
Vigência do projeto	04/01/2021 a 31/08/2021
Nome Comum / Espécie / Linhagem	CANINA / CANIS LUPUS FAMILIARIS /
Raça	Diversas
Nº de animais machos	0
Nº de animais fêmeas	0
Nº de animais sexo indefinido	20
Peso médio de animais machos	0
Peso médio de animais fêmeas	0
Peso médio de animais sexo indefinido	0
Idade	2 ano(s) e 0 mes(es) e 0 dia(s).
Procedência	Animais oriundos do atendimento hospitalar

Projeto de Pesquisa aprovado em reunião da CEUA em 16/12/2020

JOSÉ NICOLAU PRÓSPERO PUOLI FILHO
Presidente da CEUA da FMVZ, UNESP - Campus de Botucatu

Faculdade de Medicina Veterinária e Zootecnia
Seção Técnica Acadêmica
Rua Prof. Dr. Walter Mauricio Corrêa, s/n
UNESP - Campus de Botucatu/SP - Cep 18618-681
(14) 3880-2176 - patrizia@fmvz.unesp.br - www.fmvz.unesp.br

CHAPTER 4

General Discussion and Future Perspectives

cMCT and techniques to evaluate lymphatic metastasis are “hot topics” in veterinary oncology literature. In the last year, several papers have been published on this theme evaluating dozens of different aspects. However, most studies carry evident bias or limitations that limit their conclusion or extrapolation to routinely day-by-day use. Furthermore, even considering that cMCT is one of the most studied cancers in veterinary oncology, knowledge, and the evidence available to support some interventions are far behind those available for humans.

1. CRITICAL APPRAISAL OF THE STUDY

Based on the hypothesis that intraoperative blue dye injection may not detect all SLN that drain a specific region, we designed this prospective cohort study to fill the knowledge gap over indirect radiographic lymphography for SLN mapping. Prospective clinical trials are hard to conduct and besides the efforts to minimize bias, a couple of factors may have skewed the results. It is important to describe some questions that could not be answered with this research and must be addressed with criticism.

Does radiographic indirect lymphography with lipiodol cost beneficial? Despite x-ray equipment being widely available in most veterinary facilities, lipiodol contrast cannot be easily found and has a high cost, which can prevent its routine use in a clinical setting. Also, the detection of an increased number of SLN, mostly deep on the abdomen requiring laparotomy, raised a concern about increasing morbidity associated with the additional incision/surgical approach. All patients in the study recovered uneventfully, but the lack of long-term evaluation and a control group prevented a throughout evaluation of outcomes. Finally, a question remains to be answered: Dogs with mast cell tumors submitted to multiple SLN resections experience long-term benefits on the outcome that justify evidence-based indication of indirect lymphography with lipiodol? A randomized controlled clinical trial is still necessary to find an answer.

How to proceed to indirect lymphography with lipiodol in dogs with more than one MCT? Considering that dogs bearing multiple cMCT lesions

simultaneously, the practice of injecting lipiodol in the largest tumor may not be the best approach when aiming for better outcomes in clinical practice. We did not evaluate whether the administration of lipiodol is useful for patients with multiple cMCTs and if there is simultaneous drainage from multiple tumors to a single or multiple SLN. These questions may not be answered by IO IL mapping, as it is not able to opacify the lymphatic vessels adequately and, therefore, demarcate to which LN the afferent lymphatic pathway is running toward.

LNs detected on radiographic indirect lymphography are SLNs? When conducting the research, this question raised our attention, and we hypothesized that during the 24 hours interval between injection and radiographs, the contrast may drain from the SLN to second echelon LNs, thus making some contrasted LNs falsely positive to be a sentinel. Unfortunately, it is impossible to answer this question with the proposed methodology. Serial radiographs taken <24 hours may evidence the lymphatic vessels' source and direction and detect whether multiple contrasted LNs drain from the SLN or the primary tumors. This is an important question to be answered as some surgeons advocate removing only one LN when there are multiple contrasted LNs on radiographs.

How could we bring IO IL close to the routine practice? Patients enrolled in the study were selected from the oncologic clinic of a veterinary teaching hospital. We found it difficult to convince some clients of the importance of RLN staging. Some patients meeting the inclusion criteria cannot be enrolled in the study due to the owner’s concern about allergic reactions and additional surgical incisions. However, most clients were pleased to contribute to the study and collaborate towards easing the process. Outside the experimental environment, the clinician may argue that IO IL reduces the requirement of extensive dissection as it brings better precision in detecting SLN before surgery and improves preoperative planning.

2. FUTURE PERSPECTIVES ON SENTINEL LYMPH NODE MAPPING

In addition to the questions that remain to be answered described in the previous section, new techniques have been proposed to better map SLN. These techniques deserve to be cited here to encourage further studies.

A recent study used iohexol (Omnipaque®), a hydrosoluble contrast agent, for radiographic indirect LN mapping. The use of iohexol decreases the cost of acquisition of the contrast, thus encouraging wider use of SLN mapping through indirect lymphography in a clinical setting. It is important to assume that before iohexol is used routinely, it is necessary to study whether the results of iohexol are equivalent to lipiodol on radiographs. Also, it is necessary to establish a standard technique and the ideal time between contrast agent injection and radiographic to prevent incomplete mapping and false-negative results.

The advent of near-infrared technologies applied to the detection of SLN through the injection of indocyanine green brings together the best of both worlds. Despite still requiring a deep study of its equivalence or superiority to other methods, the Infrared detection of indocyanine green enables the surgeon to preoperatively know which LN is the sentinel while simultaneously guiding it during the procedure. Limitations regard the low penetration of the infrared at the live tissues may prevent its use to detect intracavitary SLN when performing superficial skin surgery. In this scenario, lymphography techniques may still be used to bring additional information on SLN mapping. As lymphoscintigraphy seems to be difficult to be widely included in most veterinary facilities due to the nuclear disposal concern, the infrared seems more suitable for most veterinary hospitals despite being expensive.

3. LACK OF BASIC SCIENCE STUDIES OF LYMPHATIC METASTASIS IN DOGS

While extensively studied in humans, the biology of cancer specific to animals is much less addressed. However, even in humans, the pathophysiology of metastasis is mainly studied in a vascular system due to a lack of lymphatic-specific markers, which was only recently demonstrated.

The role of the lymphatic system on cancer progression is a frequent theme in clinical studies published in reputable journals, however, little is known about the molecular and pathophysiological aspects of cancer spread from a primary site to LNs and beyond in cMCT and other animal tumors. Most studies addressing the lymphatic systems and cancer in dogs are clinical retrospective or, less commonly, prospective that provide some evidence of how the lymphatic

system behavior clinically in the presence of a malignancy. However, pure basic science research is equally necessary, as oncologists studying metastasis almost always rely on human literature to speculate or hypothesize about phenomena seen in animals.

For example, the occurrence of “in transit” metastasis and clusters of cell “clotting” lymphatic vessels causing a diversion of the normal lymph flow to other lymphatic basins are a theoretical phenomenon somewhat described in some human studies, but a mere hypothesis in dogs. The veterinary oncologist also does not know if distant metastasis is caused by tumor cells that invade LN blood vessels and/or completed all the pathways through multiple LN until been debouched at the thoracic duct and finally to the cranial vena cava. Despite initially it does not seem to correlate with important clinical circumstances, knowing how distant metastasis progress from LN metastasis may be an important piece to the puzzle of whether an extensive LN dissection is really necessary.

The knowledge of lymphatic metastasis is crucial to the progression of veterinary oncology to understand the mechanisms involved and possible clinical implications. Furthermore, finding molecular markers and key receptors on lymphatic metastasis can be an effective target for future drugs.

4. THE FALSE-NEGATIVE LYMPH NODE PROBLEM

There is currently no standard approach to histological criteria to establish whether an LN is metastatic. Classifications such as that proposed by Weishaar aid on translate what is seen on a histology slide to the clinical application, however, this is not standard of care as studies of validations are still necessary. Several questions on whether each classification means clinically to treatment and prognosis are still to be answered.

Furthermore, a gold-standard pattern LN cutting during histological processing is absent. Most studies describe different methods of preparing and cutting the tissue and the lack of standardization may be a reason for the wide variability between studies.

This factor raises a concern that non-metastatic LN may harbor metastatic niches that were missed during tissue processing at the laboratory resulting in a false-negative and negatively affecting decision-making. Those patients in a clinical setting that are early affected by metastatic disease or recurrence of cMCT in the absence of risk factors may be experiencing a false-negative diagnosis. To our knowledge, there is no verified method described to mitigate this effect to date.

5. LESSONS LEARNED WITH THIS STUDY

1. IO IL detected more LN than relying only upon the RLN or PB mapping, especially when considering a clinical scenario. However, this does not mean that IO IL should take the place of PB mapping as both techniques are complementary and the rate of resected SLN would probably decrease in the absence of PB mapping.
2. Intracavitary or deep-located LN are often SLN of skin tumors and must be considered when dealing with tumors located at the abdomen and hindlimb.
3. Conducting an abdominal exploration for SLN increases intraoperative time but it is easily performed and does not increase surgical morbidity. However, the additional cost involved in private practice may be a concern when adopting this procedure. The clinician that chooses to perform IO IL must be willing to discuss all the implications with the owner.
4. Except by size at palpation, the pattern of LN opacification and other clinical variables are not useful to predict metastasis and should not be used routinely. Veterinary oncology still lacks a minimally invasive metastasis assessment technique to predict metastasis previously to a surgical procedure.